Environmental Radioactivity: Methodological Approaches and Applications in Earth and Environmental Physics, and Homeland Security

Wolfango Plastino

Department of Physics - University of Roma Tre
National Institute of Nuclear Physics - Section of Roma Tre and Gran Sasso National Laboratory

plastino@fis.uniroma3.it

ROMA TRE UNIVERSITÀ DEGLI STUDI

ERMES Environmental Radioactivity Monitoring for Earth Sciences

INFN Istituto Nazionale di Fisica Nucleare

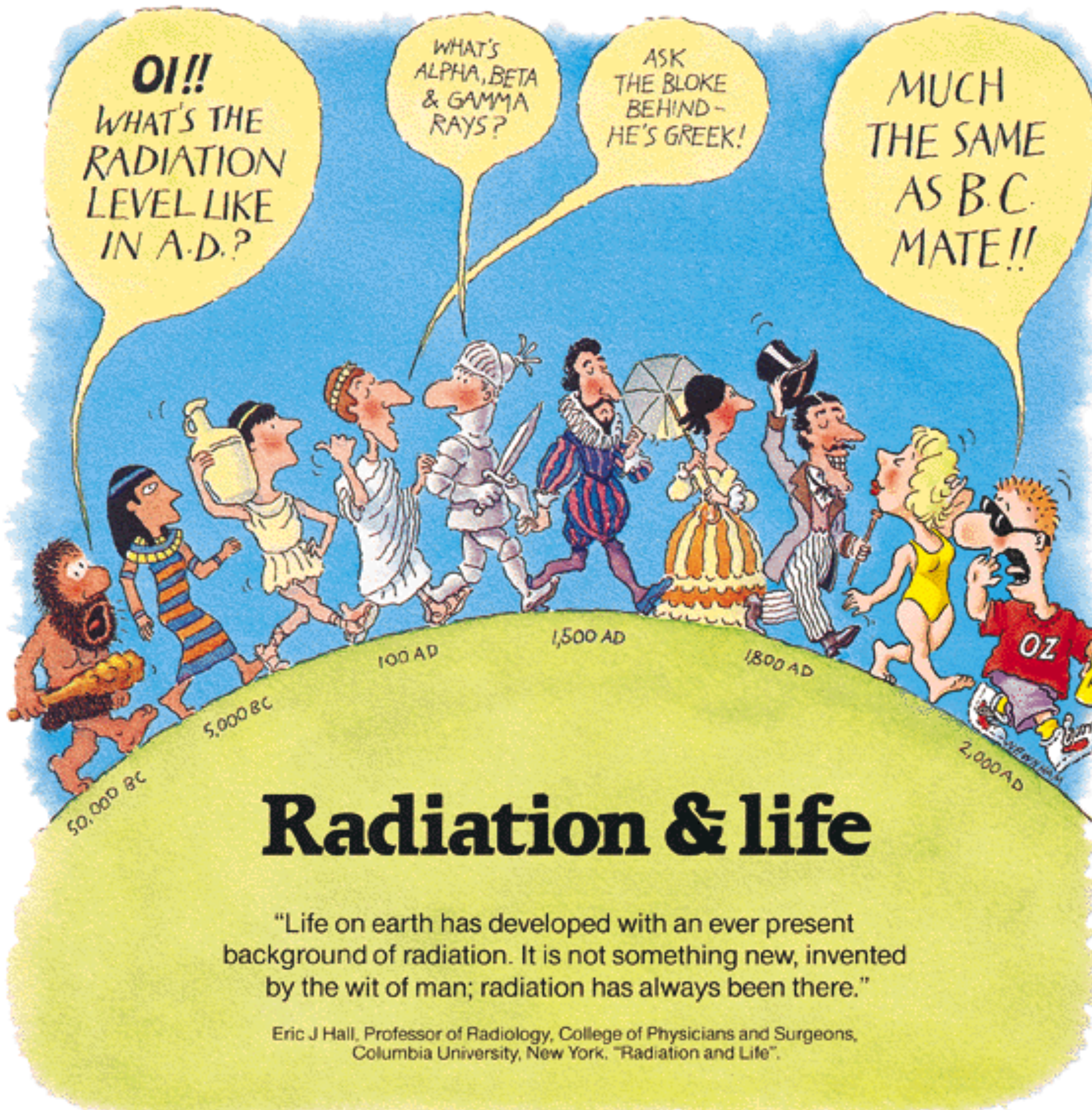
OI!! WHAT'S THE RADIATION LEVEL LIKE IN A.D.?
WHAT'S ALPHA, BETA & GAMMA RAYS?
ASK THE BLOKE BEHIND - HE'S GREEK!
MUCH THE SAME AS B.C. MATE!!
50,000 BC
5,000 BC
100 AD
1,500 AD
1800 AD
2,000 AD
OZ
Radiation & life
"Life on earth has developed with an ever present background of radiation. It is not something new, invented by the wit of man; radiation has always been there."
Eric J Hall, Professor of Radiology, College of Physicians and Surgeons, Columbia University, New York. "Radiation and Life".

Atmosphere	Cosmogenic and anthropogenic radionuclides in the atmosphere ($^{3}H(t_{1/2} = 12.3$ a), $^{3}\underline{H}$, ^{7}Be (53 d), ^{10}Be ($1.5x10^{6}$ a), ^{14}C (5730 a), $^{14}\underline{C}$, ^{26}Al ($7.1x10^{5}$ a), ^{32}Si (140 a), ^{36}Cl ($3.01x10^{5}$ a), $^{36}\underline{Cl}$, ^{39}Ar (269 a), ^{81}Kr ($2.3x10^{5}$ a), $^{85}\underline{Kr}$ (10.8 a), ^{129}I ($1.7x10^{7}$a), $^{129}\underline{I}$) Study of trace gases: CO_2, CO, OH, O_3, CH_4 (^{14}C) Transport and origin of carbonacous aerosols (^{14}C, $^{14}\underline{C}$) and loess (^{10}Be) Exchange of stratospheric and tropospheric air (^{7}Be, ^{10}Be)
Biosphere	Dating in archaeology and other fields (^{14}C, ^{41}Ca ($1.04x10^{5}$ a)) Calibration with tree rings, corals, lake & ocean sediments, spaleothems (^{14}C) Studies in forensic medicine through bomb-peak dating ($^{14}\underline{C}$) In-vivo tracer studies in plants, animals, and humans ($^{14}\underline{C}$, $^{26}\underline{Al}$, $^{41}\underline{Ca}$, $^{79}\underline{Se}$ ($3.0x10^{5}$ a), $^{99}\underline{Tc}$ ($2.11x10^{5}$ a), $^{129}\underline{I}$)
Hydrosphere	Dating of groundwater (^{14}C, ^{36}Cl, ^{39}Ar, ^{81}Kr, ^{129}I) Global ocean circulation pattern (^{14}C, $^{14}\underline{C}$ ^{39}Ar, ^{99}Tc, $^{129}\underline{I}$) Paleoclimatic studies in lake and ocean sediments (^{14}C)
Cryosphere	Paleoclimatic studies in ice cores from glaciers and polar ice sheets (^{10}Be, ^{14}C, ^{26}Al, ^{32}Si, ^{36}Cl, ^{39}Ar, ^{81}Kr) Variation of cosmic ray intensity with time (^{10}Be, ^{14}C, ^{36}Cl) Bomb-peak identification ($^{36}\underline{Cl}$, $^{41}\underline{Ca}$, $^{129}\underline{I}$)

Kutschera, W., 2005. The role of isotopes in environmental and climate studies, Nuclear Physics A, 645-648.

Contents

- **Solid Earth Physics**: Is daughter better than parent? A case study: Radon vs Uranium

- **Fluid Earth Physics**: From water vapor to the Benthic Boundary Layer

- **Anthropogenic Isotopes and Forcing**: Nuclear Power Plants and Nuclear Test

Geodynamic Processes in the Earth's Lithosphere and Mantle

More attention should be devoted to the pre-earthquake and volcanic eruption studies of geodynamic processes, especially on characteristics of fluids filling the fractures before the main shock and eruption. Uranium in groundwater has been tested as a potential indicator of pre-earthquake processes as it may be associated with geodynamics of preparation phases of earthquakes.

Another possible physical process during the pre- and post-phases of the earthquake could be investigated: the first stage seems to be characterized by U variations in groundwater that can modulate the radon concentration, the second one (after the main shock) do not show any U anomalies, justifying the different radon patterns before and after the main shock.

^{238}U-Series ^{235}U-Series ^{232}Th-Series

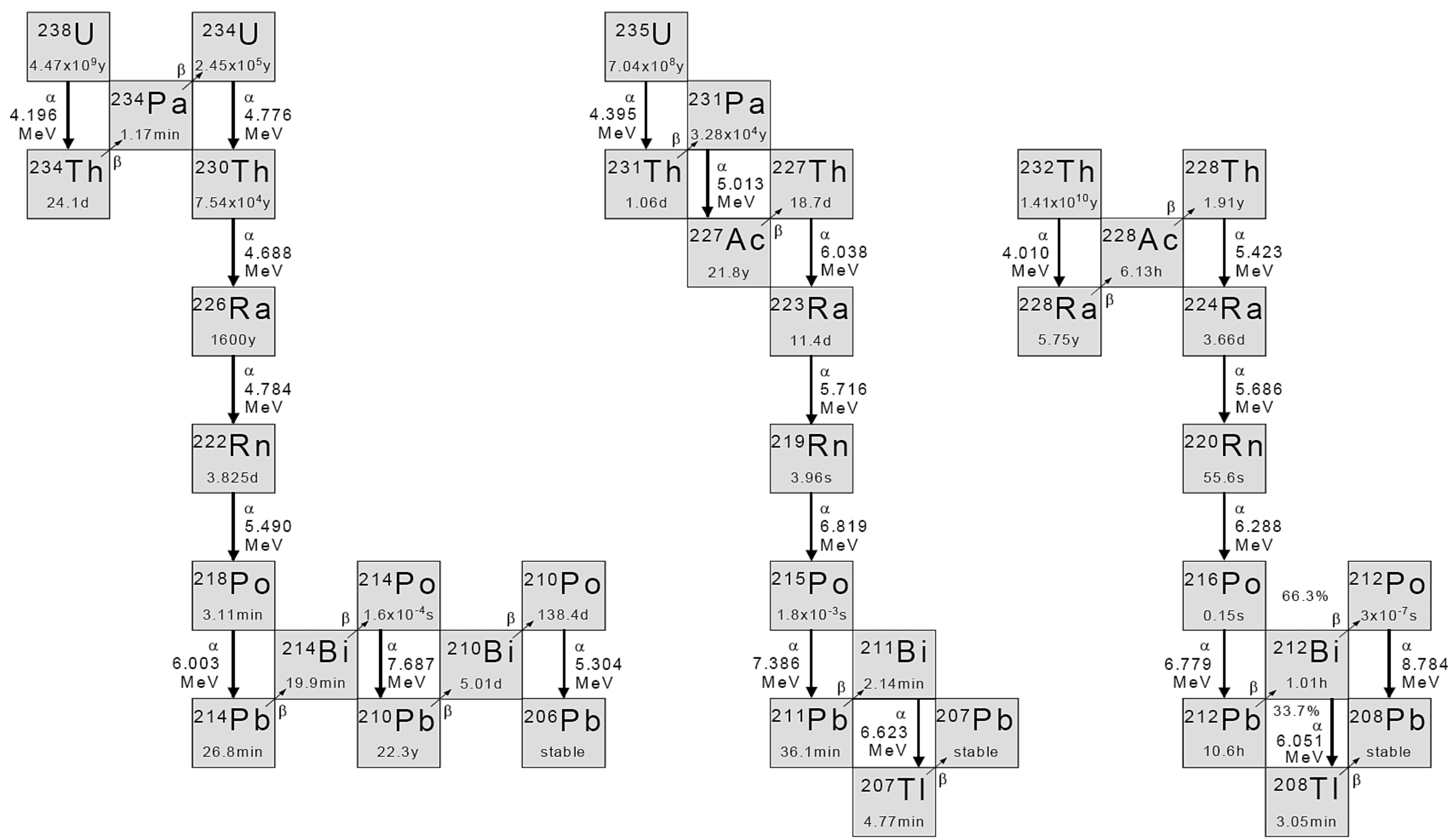

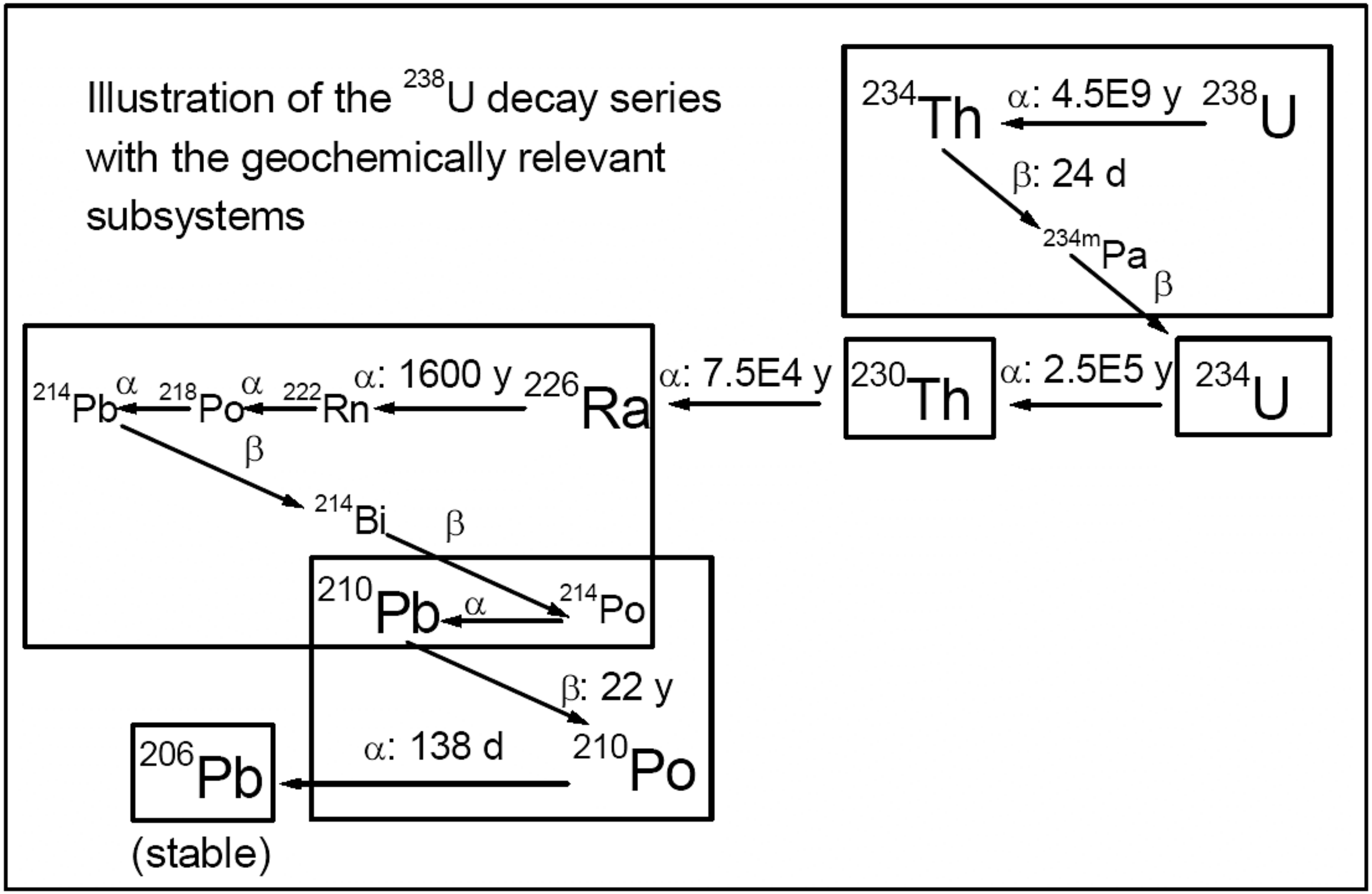

© J. Eikenberg, Paul Scherrer Institute

type of sample		^{238}U		^{232}Th		^{226}Ra (1)	
		[ppm]	[mBq/g]	[ppm]	[mBq/g]	[ppt]	[mBq/g]
igneous	granite	2 - 10	25 - 120	5 - 30	20 - 120	0.5 - 4	25 - 120
	Gabbro	0.5 - 2	5 - 25	2 - 6	5 - 25	0.1 - 0.5	5 - 25
	Basalt	0.1 - 1	1 - 10	0.3 - 4	1 - 15	0.02 - 0.2	1 - 10
	Ultramafics	< 0.02	< 0.2	< 0.05	< 0.2	< 0.01	< 0.2
sedimentary	Shales	2 - 4	25 - 50	5 - 15	20 - 120	0.5 - 1	25 - 50
	Limestone	1 - 3	10 - 40	0 - 3	0 - 10	0.2 - 1	10 - 40
	Speleothem	1 - 3	10 - 40	0 - 3	0 - 10	0.2 - 1	10 - 40
	Coral	2 - 4	25 - 50	< 0.01	<0.04	0.5 - 1	25 - 50
	Clay	1 - 4	10 - 50	1 - 15	5 - 60	0.2 - 1	10 - 50
water (2)	sea water (3)	3 - 4	40 - 50	< 0.01	< 0.05	0.01 - 0.1	0.5 – 5
	river water (4)	0.1 - 1	1 - 10	< 0.01	< 0.05	0.01 - 0.1	0.5 – 5

© J. Eikenberg, Paul Scherrer Institute

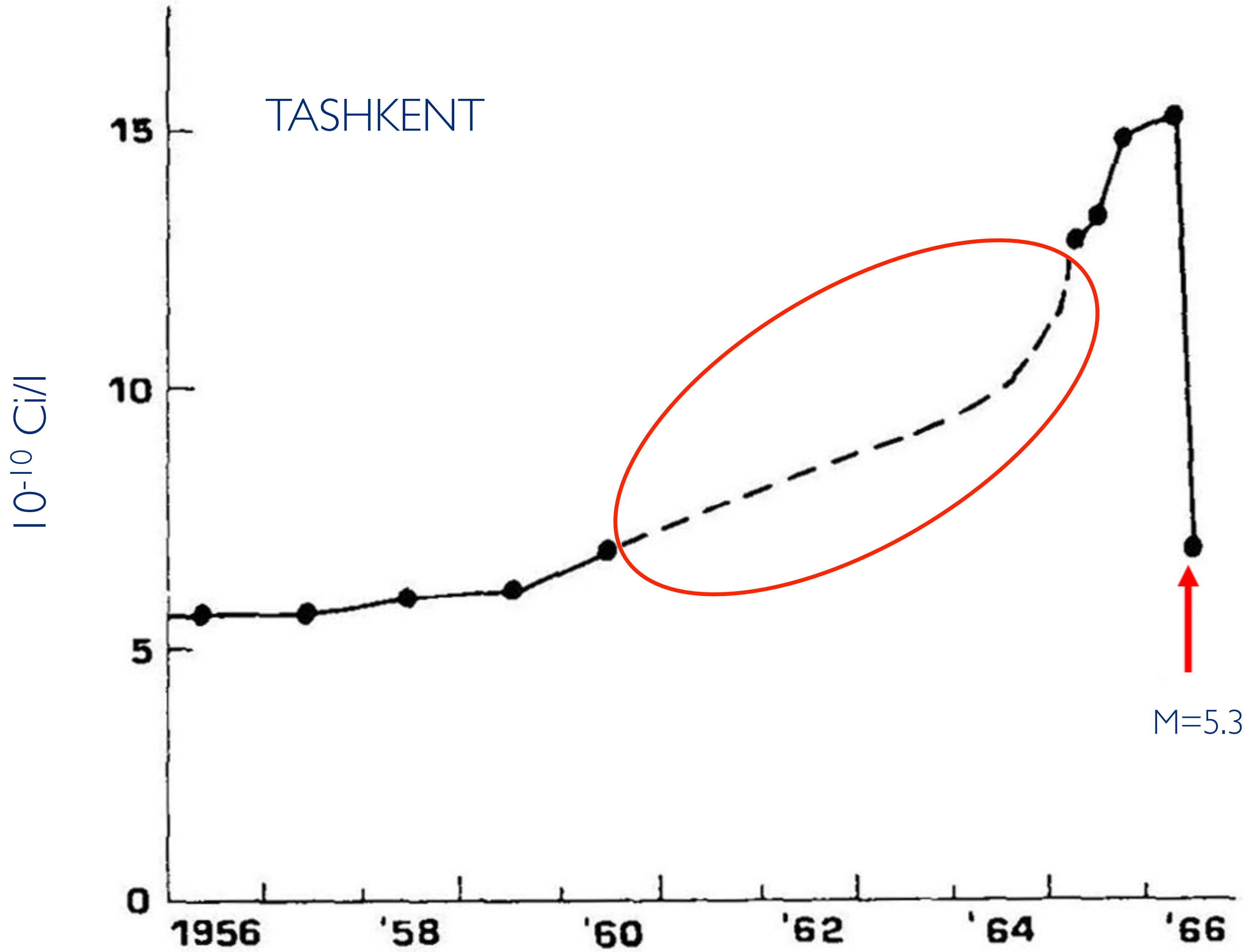

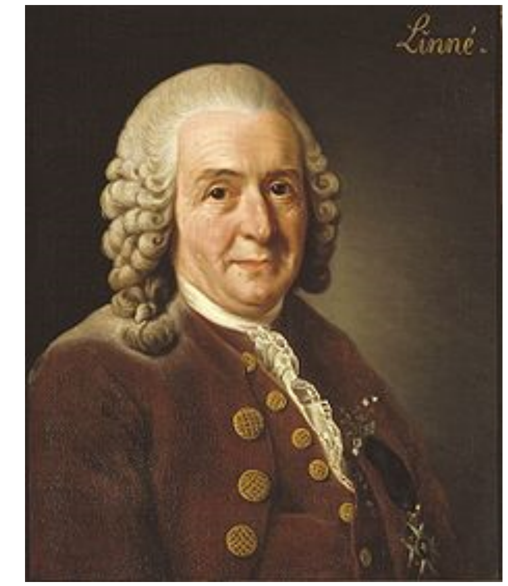

Natura non facit saltus

Ulomov, V.I., Mavashev, B.Z., 1967. A precursor of a strong tectonic earthquake. Doklady Akademii Sciences SSSR, Earth Sciences Sections 176, 9–11.

$$^{226}_{88}\text{Ra} \rightarrow \, ^{222}_{86}\text{Rn} + \, ^{4}_{2}\text{He}$$

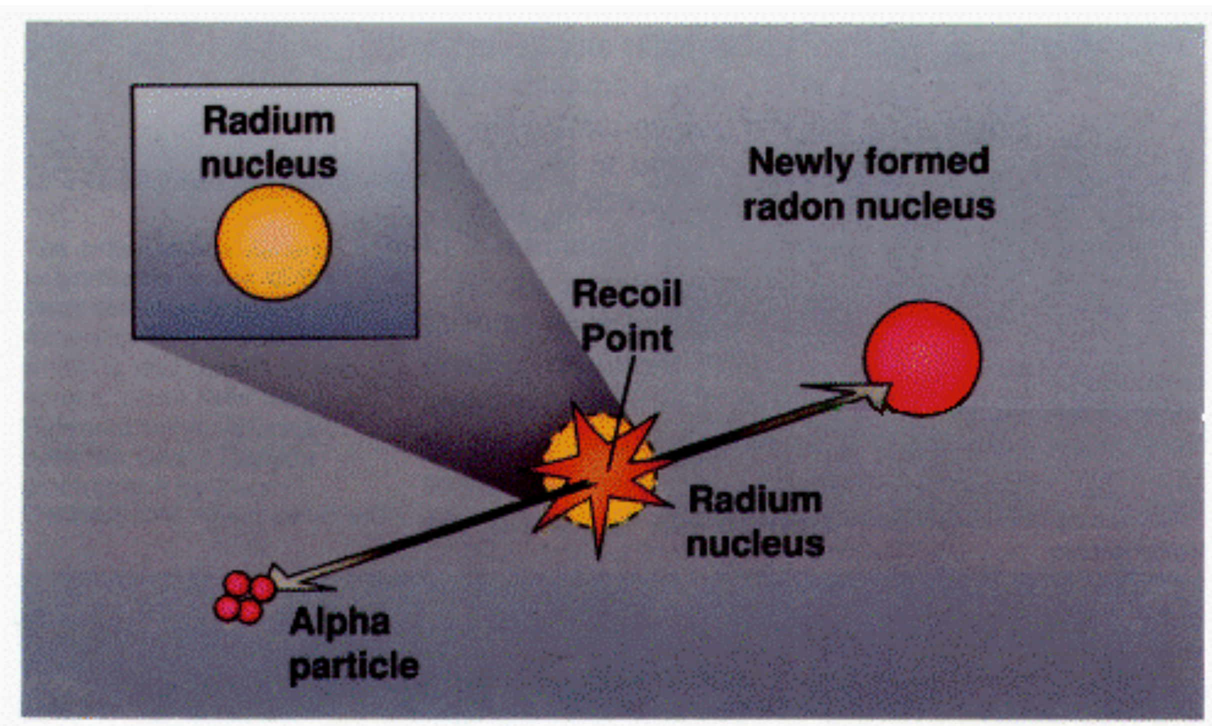

Radium decay involves the release of the excess energy which is shared between the α particle which forms (98.1%), and the new radon atom

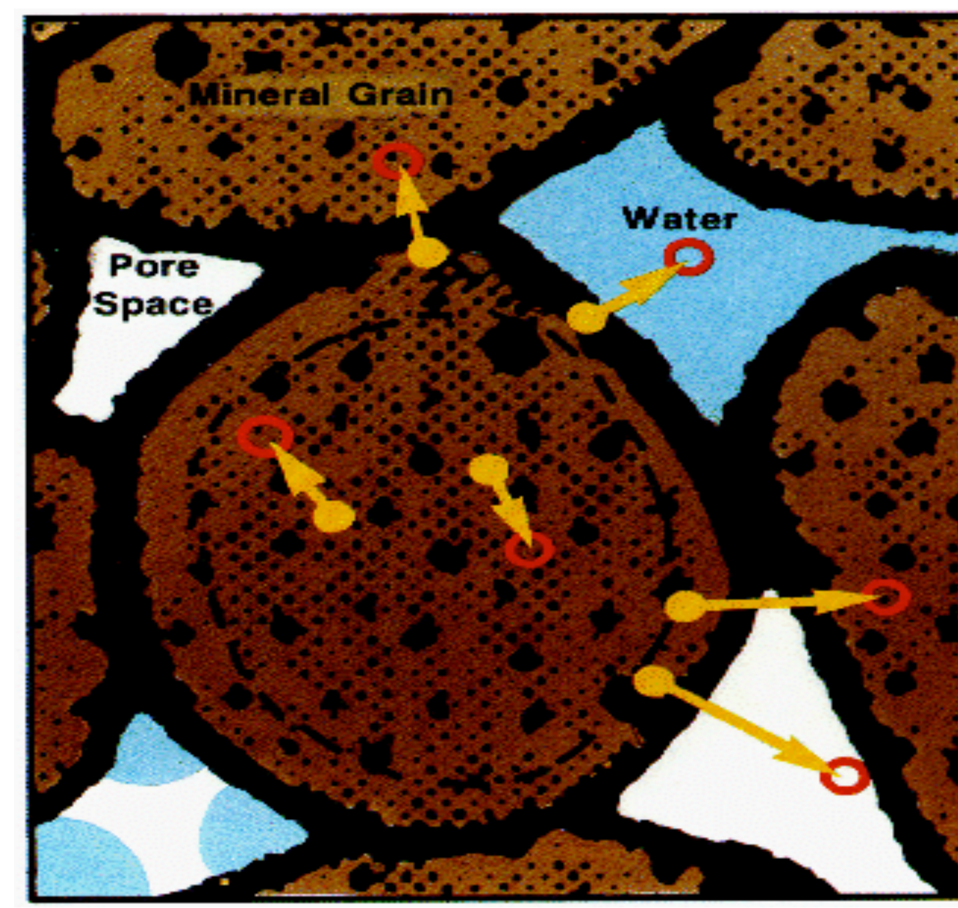

The emanating power of rocks is defined as the ratio between the amount of radon escaping from the solid matrix and that produced by radioactive decay

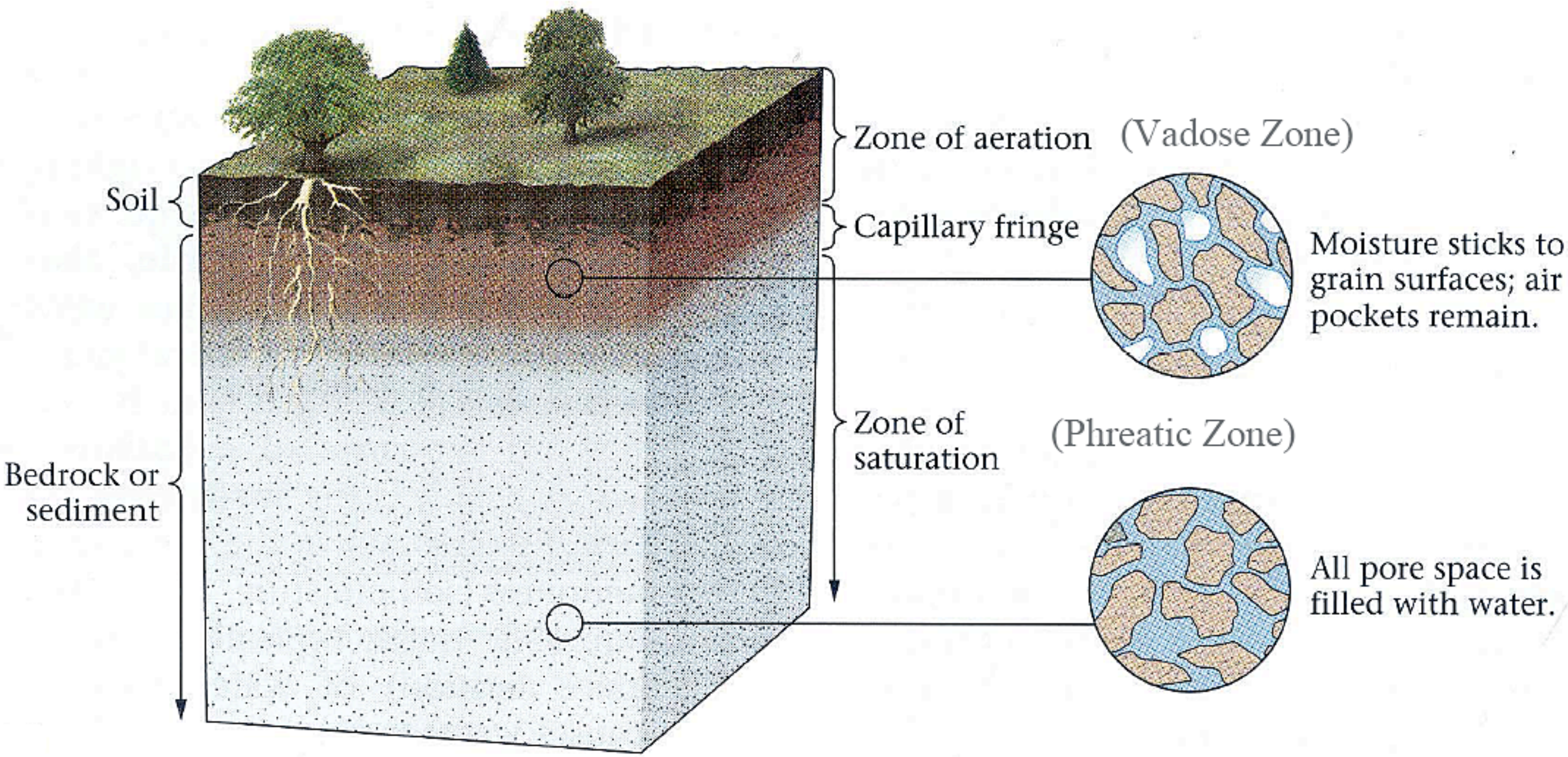
Zone of aeration
(Vadose Zone)
Soil
Capillary fringe
Moisture sticks to grain surfaces; air pockets remain.
Zone of saturation
(Phreatic Zone)
Bedrock or sediment
All pore space is filled with water.

Galileo Galilei	Isaac Newton	Aneesur Rahman	Paul A. M. Dirac
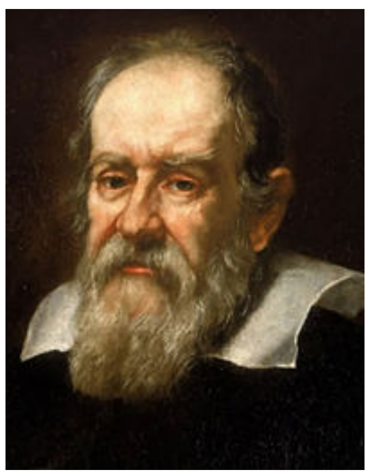	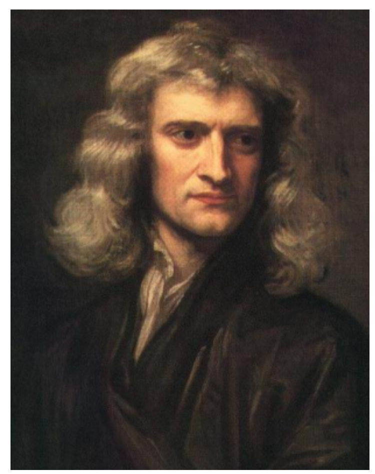		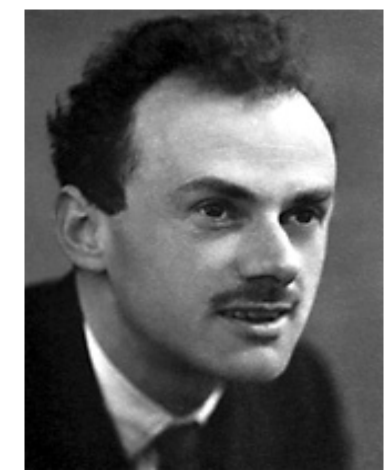
Measurement	Calculus	Simulation	Forecast

Gran Sasso National Laboratory

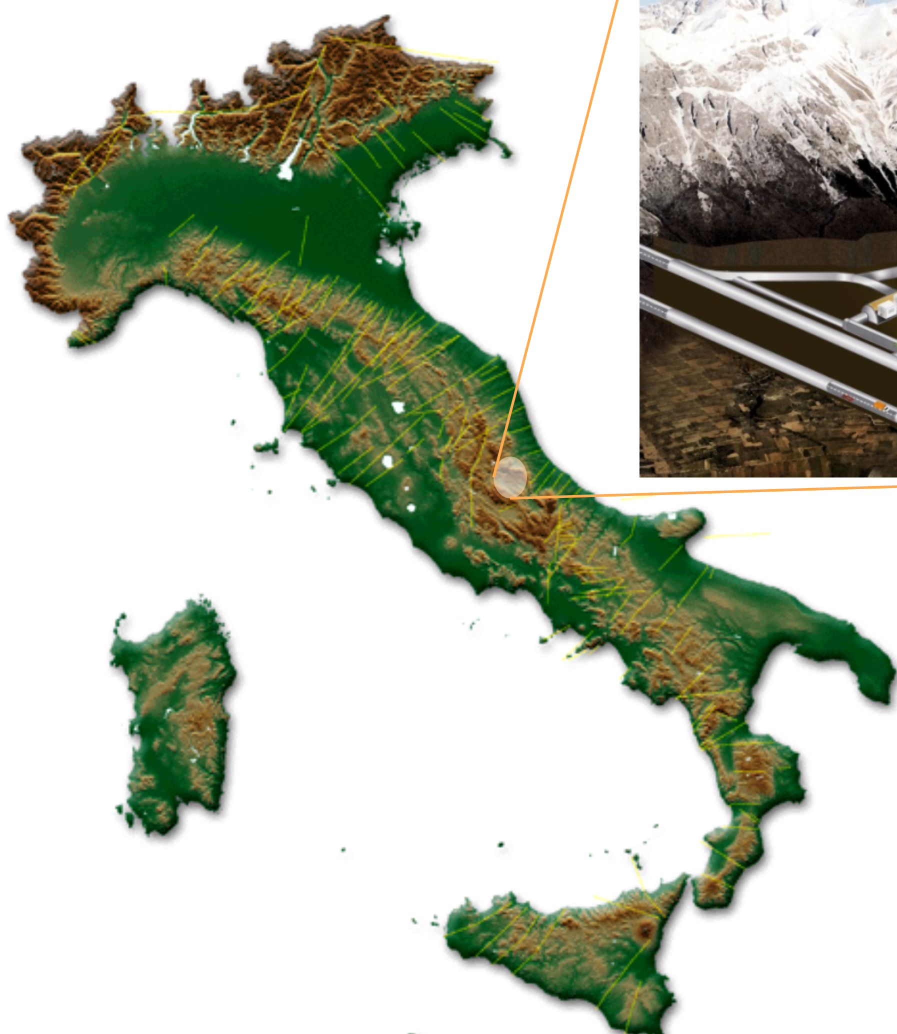

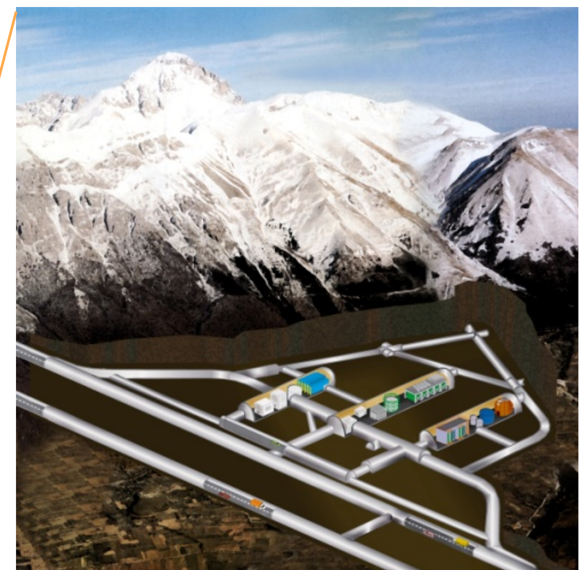

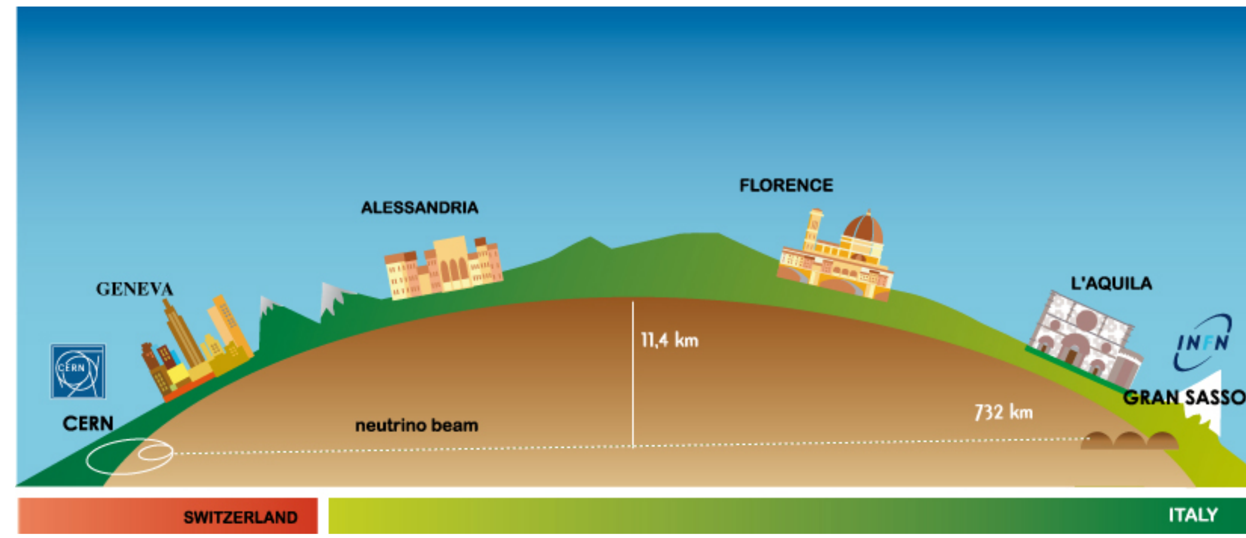

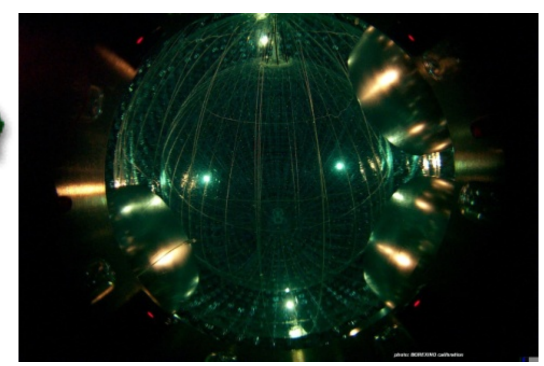

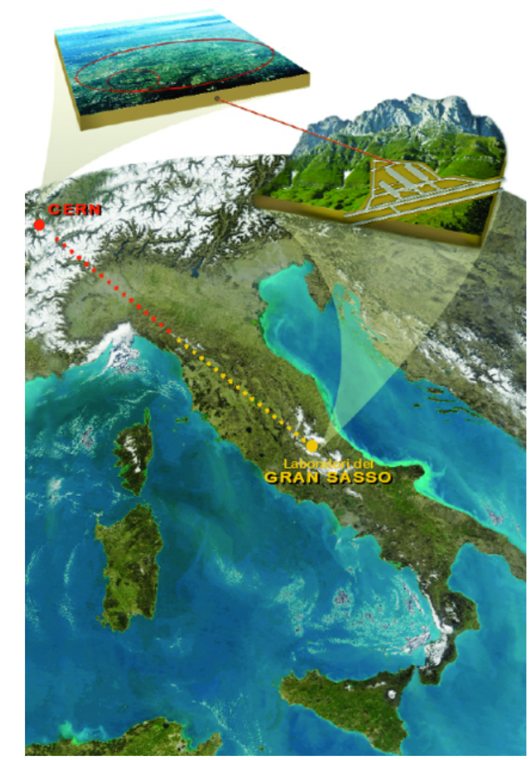

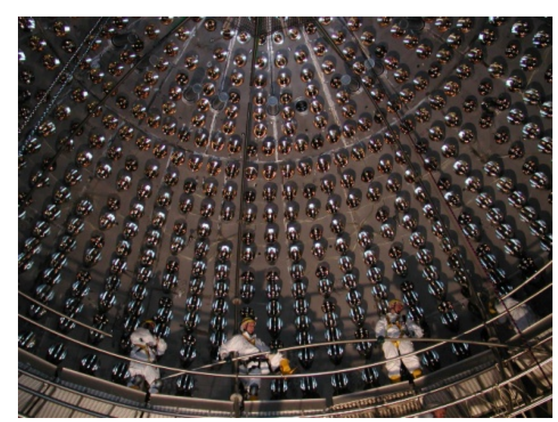

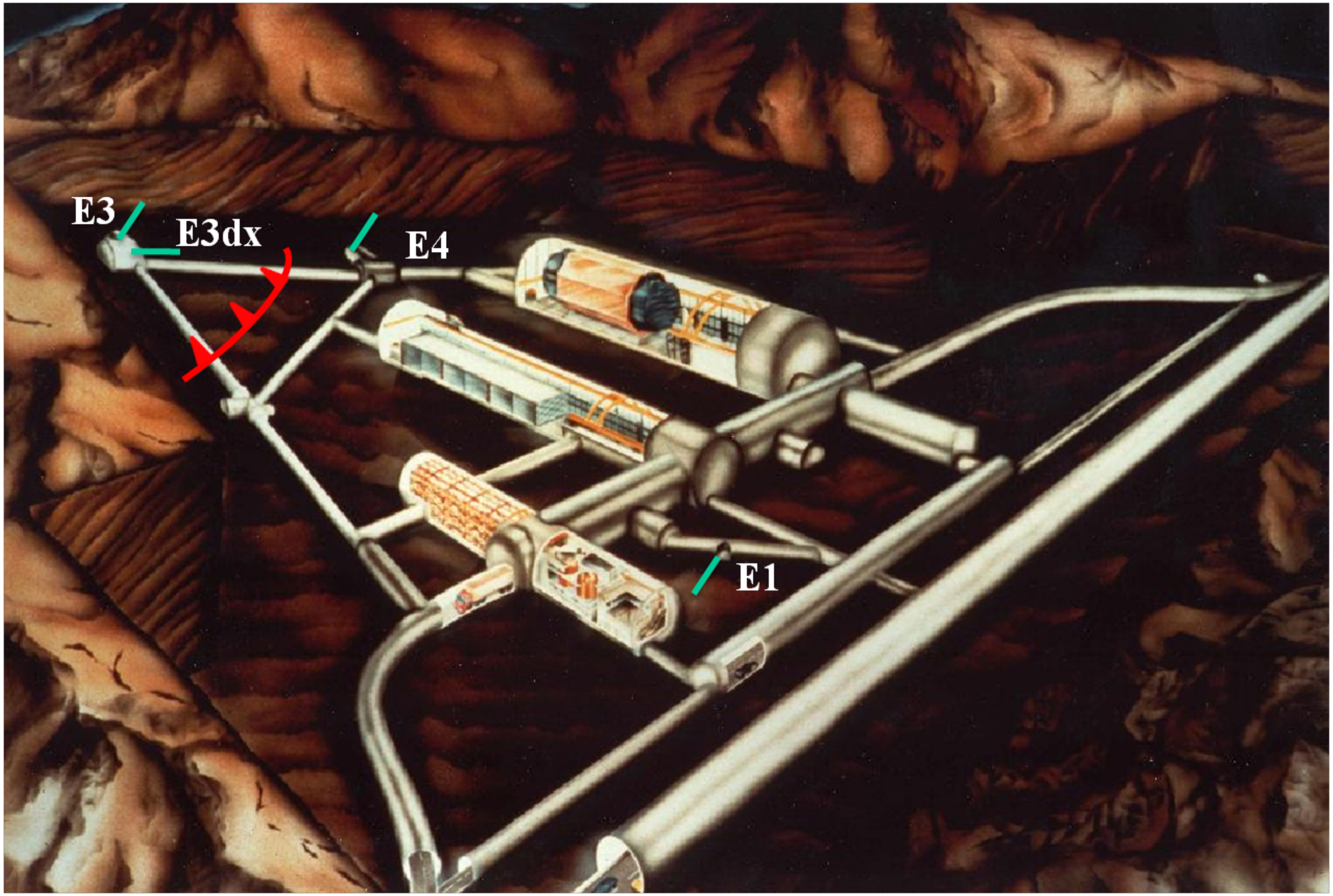

Plastino, W. et al., 2010. Uranium groundwater anomalies and L'Aquila earthquake, 6th April 2009 (Italy), Journal of Environmental Radioactivity, 101, 45-50.

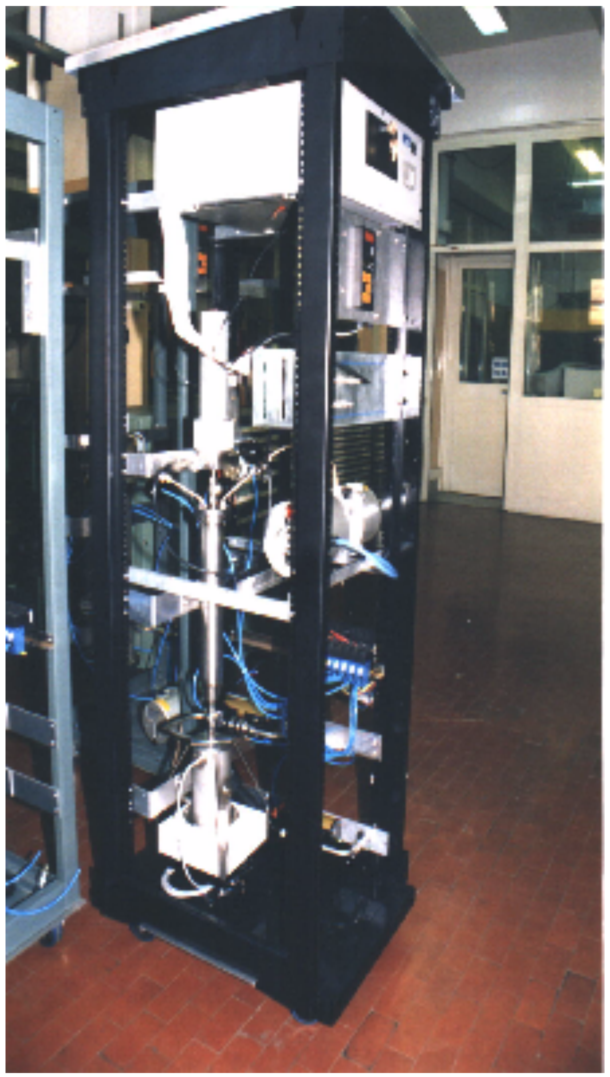

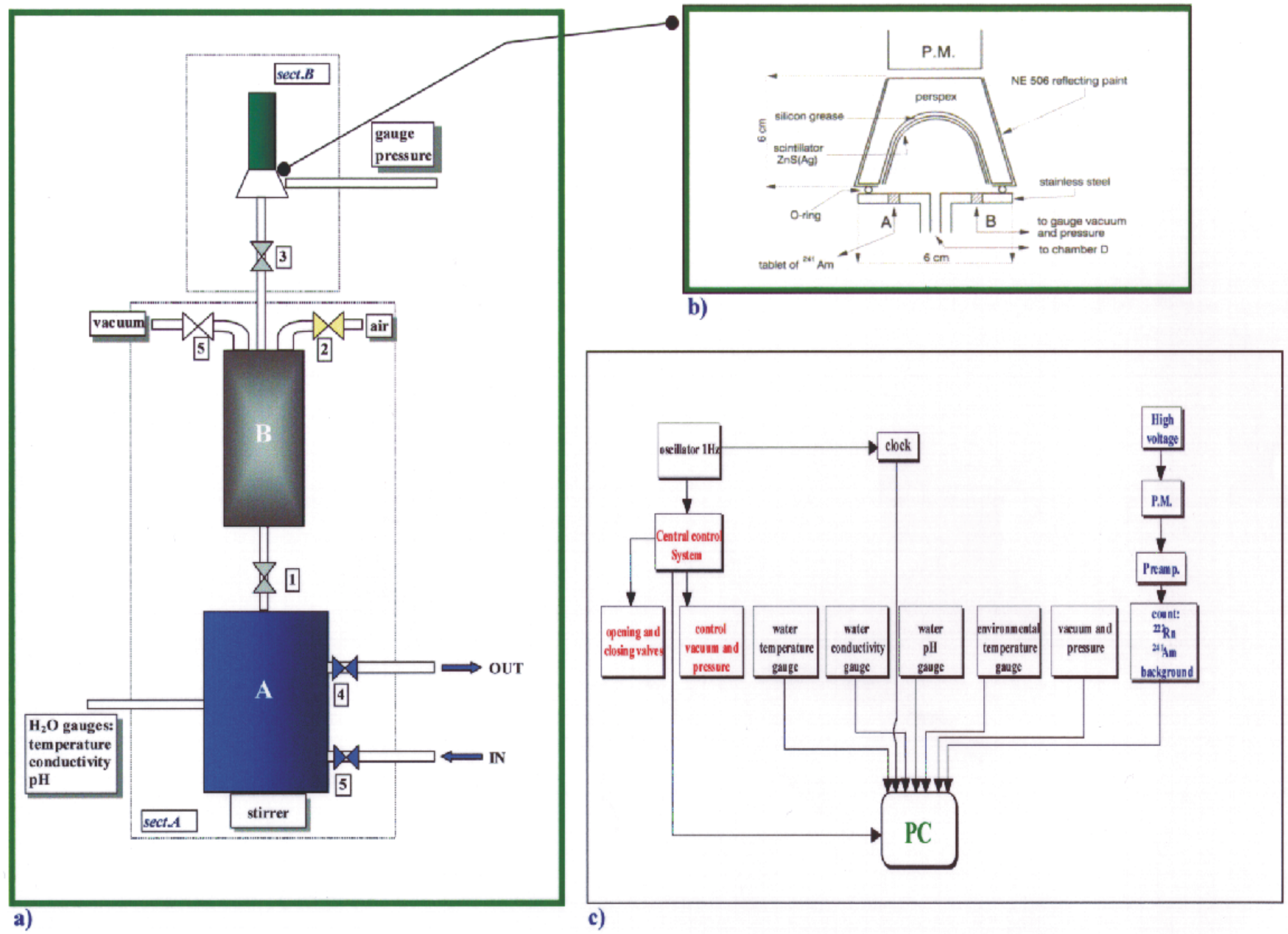

Plastino, W., Bella, F., 2001. Radon groundwater monitoring at underground laboratories of Gran Sasso(Italy). Geophysical Research Letters, 28, 2675-2677.

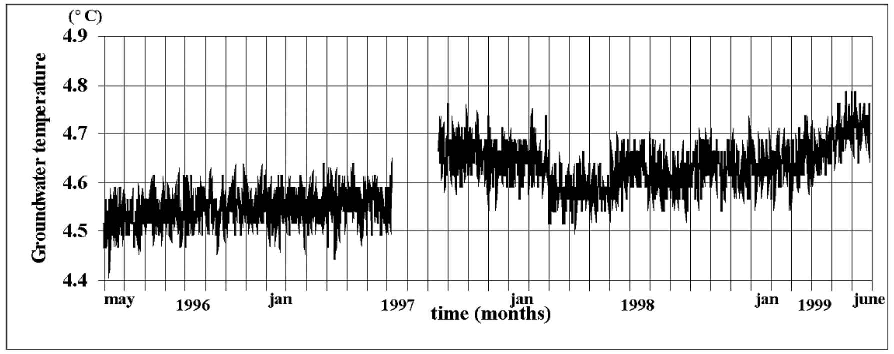

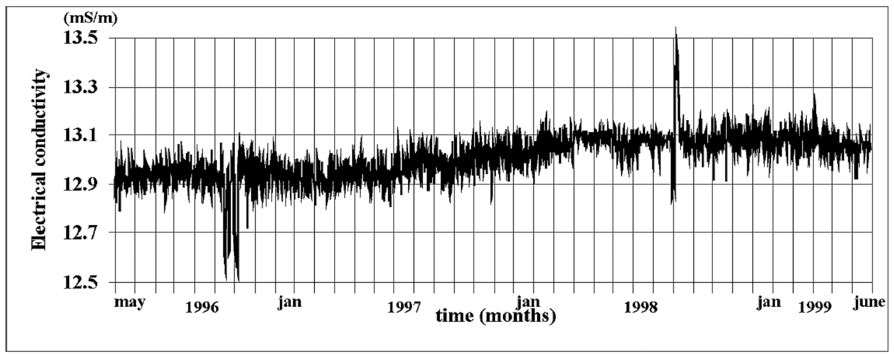

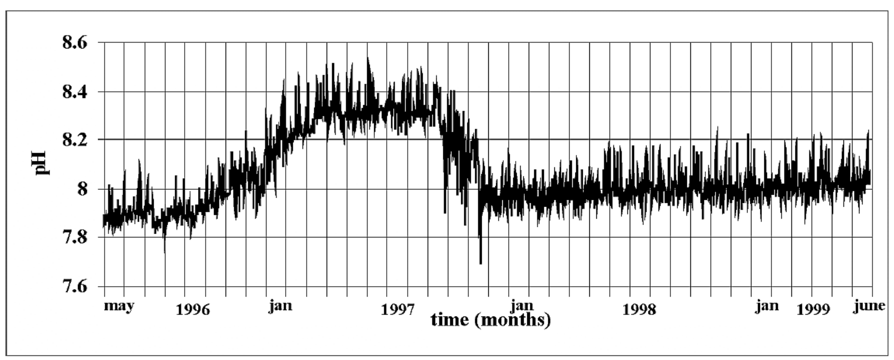

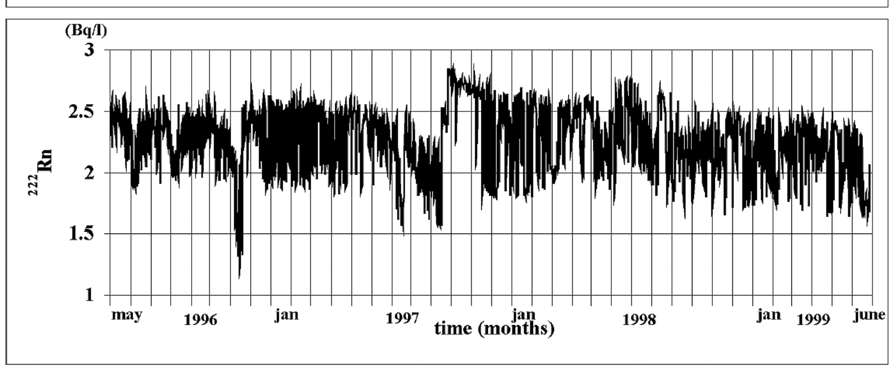

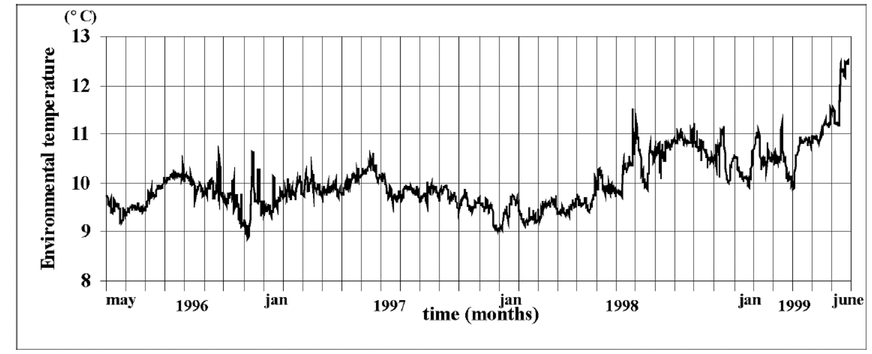

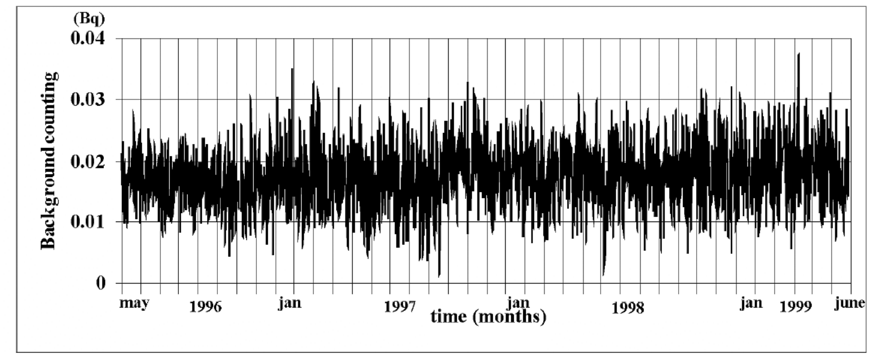

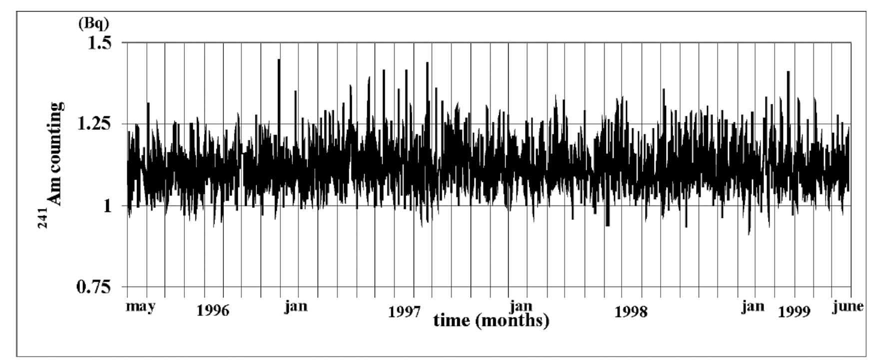

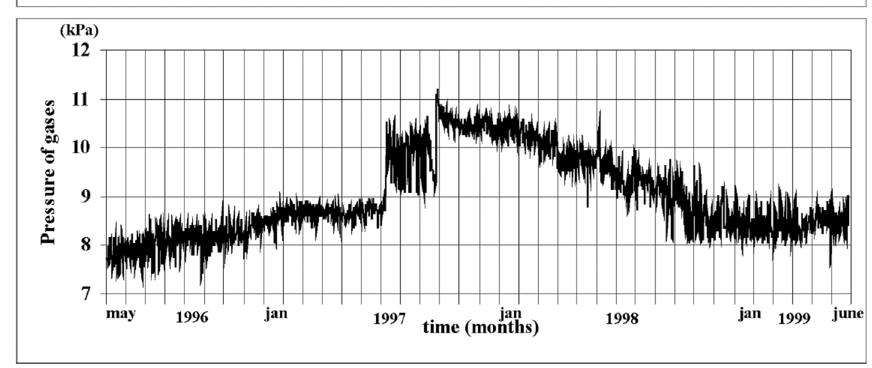

Plastino, W., 2006. Monitoring of geochemical and geophysical parameters in the Gran Sasso aquifer, Radionuclides in the Environment, Elsevier, 335-342,.

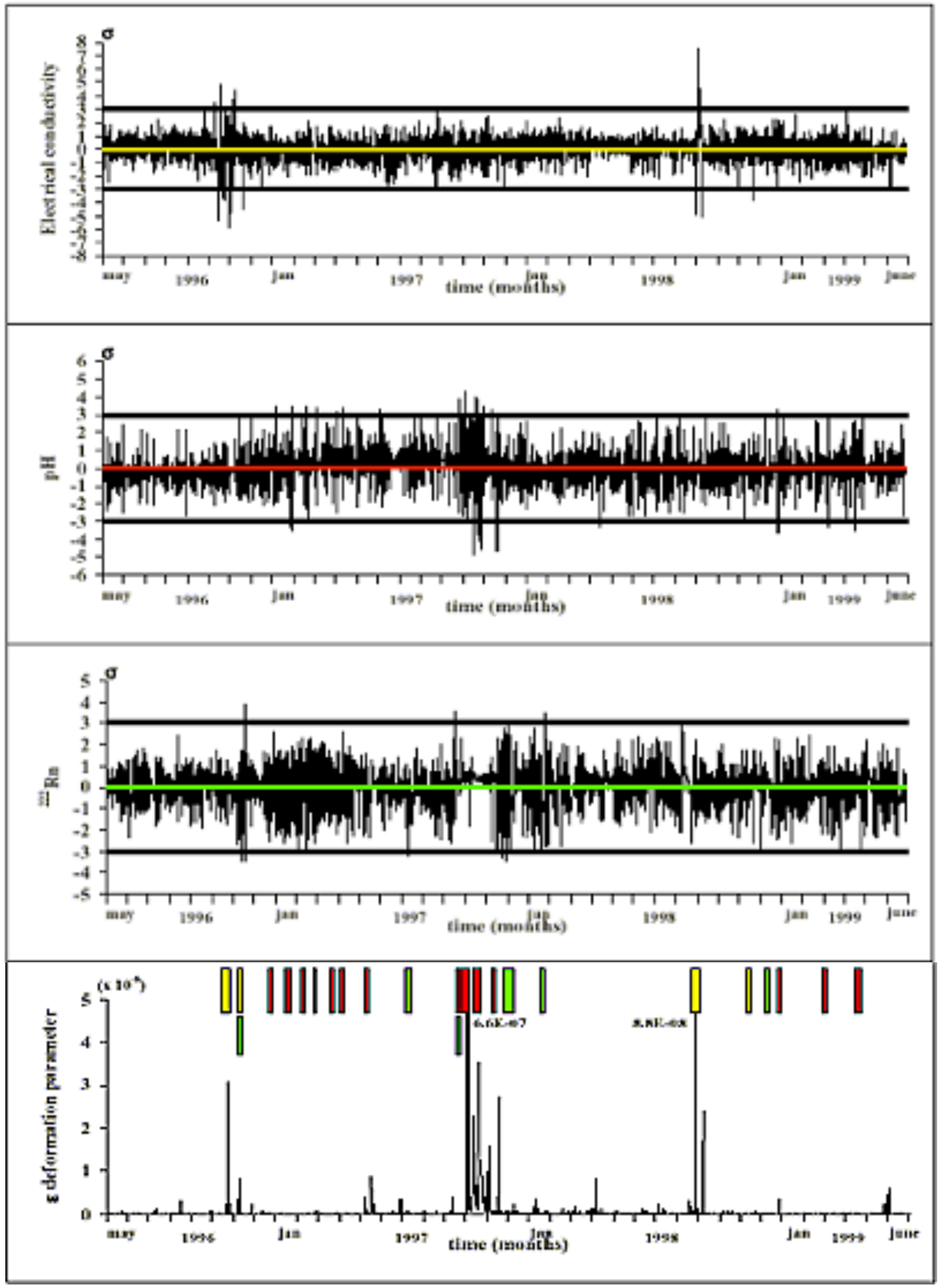

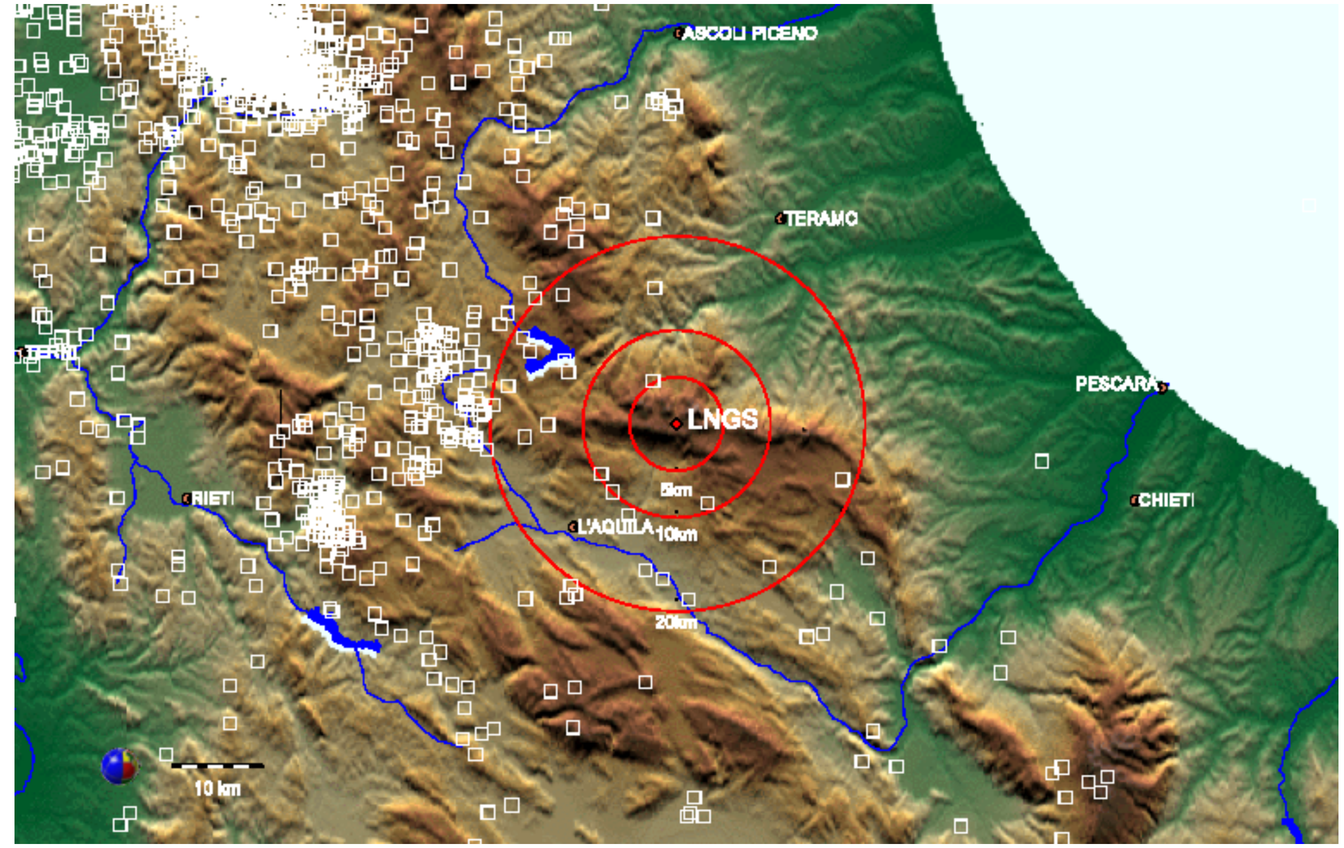

Plastino, W., 2006. Monitoring of geochemical and geophysical parameters in the Gran Sasso aquifer, Radionuclides in the Environment, Elsevier, 335-342,.

Geophys. J. Int. (2004) **158,** 385–396 doi: 10.1111/j.1365-246X.2004.02290.x

Diffusion in porous layers with memory

Michele Caputo[1] and Wolfango Plastino[2]

[1]*Department of Physics 'G. Marconi', University 'La Sapienza', Piazzale A. Moro,* 2, *Rome,* I-00185, *Italy*
[2]*Department of Physics 'E. Amaldi', University of Roma Tre, Via delle Vasca Navale,* 84, *Rome,* I-00146, *Italy. E-mail: plastino@fis.uniroma3.it*

Accepted 2004 March 13. Received 2004 February 10; in original form 2003 April 2

SUMMARY

The process of diffusion of fluid in porous media and biological membranes has usually been modelled with Darcy's constitutive equation, which states that the flux is proportional to the pressure gradient. However, when the permeability of the matrix changes during the process, solution of the equations governing the diffusion presents severe analytical difficulties because the variation of permeability is not known *a priori*.

A diverse formulation of the constitutive law of diffusion is therefore needed and many authors have studied this problem using various methods and solutions. In this paper Darcy's constitutive equation is modified with the introduction of a memory formalism. We have also modified the second constitutive equation of diffusion which relates the density variations in the fluid to the pressure, introducing rheology in the fluid represented by memory formalisms operating on pressure variations as well as on density variations. The memory formalisms are then specified as derivatives of fractional order, solving the problem in the case of a porous layer when constant pressures are applied to its sides.

For technical reasons many studies of diffusion are devoted to the flux rather than to the pressure; in this work we shall devote our attention to studying the pressure and compute the Green's function of the pressure in the layer when a constant pressure is applied to the boundary (Case A) for which we have found closed-form formulae. The described problem has already been considered for a half space (Caputo 2000); however, the results for a half space are mostly qualitative since in most practical problems the diffusion occurs in layers.

The solution is also readily extended to the case when a periodic pressure is applied to one of the boundary planes while on the other the pressure is constant (Case B) which mimics the effect of the tides on sea coasts. In this case we have found a skin effect for the flux which limits the flux to a surface layer whose thickness decreases with increasing frequency. Regarding the effect of pressure due to tidal waters on the coast, it has been observed that when the medium is sand and the fluid is water, for a sinusoidal pressure of 2×10^4 Pa and a period of 24 hr at one of the boundaries and zero pressure at the other boundary, the flux is sinusoidal with the same period and amplitude decaying exponentially with distance to become negligible at a distance of a few hundred metres.

A brief discussion is given concerning the mode of determination of the parameters of memory formalisms governing the diffusion using the observed pressure at several frequencies. We shall also see that, as in the classic case of pure Darcy's law behaviour, the equation governing the flux resulting in the diffusion through porous media with memory is the same as that governing the pressure.

Key words: Darcy, diffusion, filtering, flux, memory, porous media.

N·H ELSEVIER

Nuclear Instruments and Methods in Physics Research A 486 (2002) 146–149

NUCLEAR INSTRUMENTS & METHODS IN PHYSICS RESEARCH Section A

www.elsevier.com/locate/nima

Radon gamma-ray spectrometry with YAP:Ce scintillator

Wolfango Plastino[a,b,*], Pierino De Felice[c], Francesco de Notaristefani[a,b]

[a]*Department of Physics, University of Roma Tre, via della Vasca Navale 84, I-00146 Roma, Italy*
[b]*National Institute for Nuclear Physics, Section of Roma Tre, via della Vasca Navale, 84, I-00146 Roma, Italy*
[c]*ENEA, Department of Environment, National Institute for Metrology of Ionizing Radiations, C.R. Casaccia, P.O. Box 2400, I-00100 Roma, Italy*

Abstract

The detection properties of a YAP:Ce scintillator ($YAlO_3$:Ce crystal) optically coupled to a Hamamatsu H5784 photomultiplier with standard bialkali photocathode have been analyzed. In particular, the application to radon and radon-daughters gamma-ray spectrometry was investigated. The crystal response has been studied under severe extreme conditions to simulate environments of geophysical interest, particularly those found in geothermal and volcanic areas. Tests in water up to a temperature of 100°C and in acids solutions such as HCl (37%), H_2SO_4 (48%) and HNO_3 (65%) have been performed. The measurements with standard radon sources provided by the National Institute for Metrology of Ionizing Radiations (ENEA) have emphasized the non-hygroscopic properties of the scintillator and a small dependence of the light yield on temperature and HNO_3. The data collected in this first step of our research have pointed out that the YAP:Ce scintillator can allow high response stability for radon gamma-ray spectrometry in environments with large temperature gradients and high acid concentrations.

PACS: 07.85.−m; 07.89.+b; 23.60.+e; 29.30.Kv; 29.40.Mc; 93.85.+q

Keywords: Radon; Radon daughters; Gamma-ray spectrometry; Geophysics; YAP:Ce

1. Introduction

The YAP:Ce monocrystal has been emphasized as a good detector for gamma-ray spectrometry [1,2]. The properties of YAP:Ce can be summarized as follows [3–6]:

- high light output of 40–50% relative to NaI(Tl);
- density of 5.37 g/cm^3;
- short decay time constant of 27 ns;
- average Z of 39;
- broad spectrum emission peaking at 370 nm;
- very good mechanical and chemical properties; and
- light yield almost independent of the energy deposited by gamma rays in the crystal and negligible afterglow.

The properties of YAP:Ce monocrystal and particularly its emission peak are well coupled with the sensitivity curve of typical photomultipliers and make this detector a useful tool for potential applications in gamma-ray spectrometry in geophysical research.

*Corresponding author. Department of Physics, University of Roma Tre, via della Vasca Navale 84, I-00146 Roma, Italy. Tel.: +39-06-55177-277; fax: +39-06-5579-303.
E-mail address: plastino@fis.uniroma3.it (W. Plastino).

PII: S0168-9002(02)00692-7

Earth science

Radon and rock deformation

Evelyn Roeloffs

What happens when stress is applied to rocks in the Earth's crust so that the crust deforms? This is a question tackled by Trique *et al.* on page 137 of this issue[1]. They have used a natural laboratory in the French Alps — the Roselend reservoir — to monitor the geophysical signals that result from the greater or lesser pressure on the underlying crust exerted by the weight of water in the reservoir. This area is not itself prone to earthquakes. But the broader interest of this work is in what it may tell us about the events, induced by crustal deformation, that precede earthquakes.

The ability to predict earthquakes is of course highly desirable. But progress in this difficult and highly contentious science will depend on detecting and interpreting physical changes stemming from the processes of earthquake generation. Many possible precursors have been reported, but seismologists are sceptical of those that are not clearly linked to crustal deformation. This 'unproven' category includes the well-documented precursory decrease and increase of radon concentration before the 1978 Izu–Oshima earthquake in Japan[2] (Fig. 1), as well as the controversial assertion that

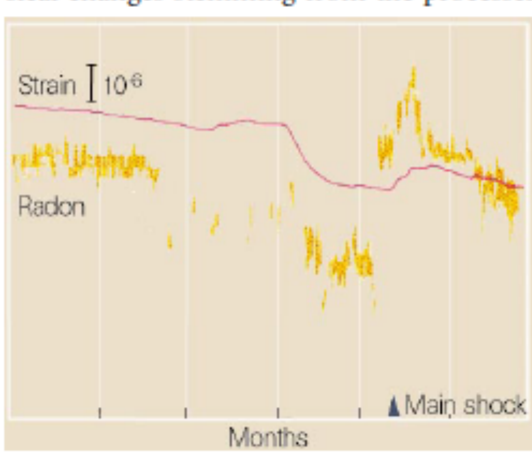

Figure 1 The radon and strain data for the magnitude-7 Izu–Oshima earthquake[2,9] of 14 January 1978 show changes preceding the earthquake. But they do not match the model shown in Fig. 2; in particular, neither change is monotonic, and in both cases the pre-earthquake change exceeds that produced by the earthquake itself.

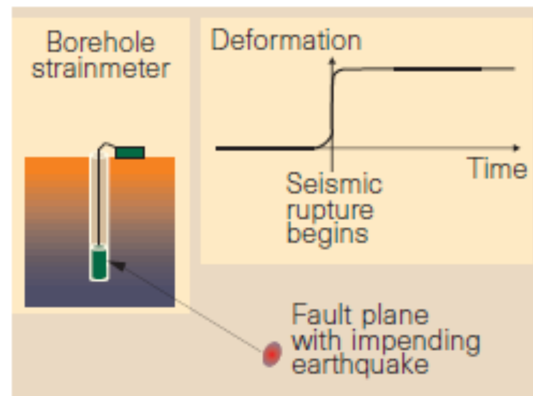

Figure 2 Rock friction, which depends on slip rate and sliding-induced changes on a fault surface, implies that seismic slip should be preceded by accelerating aseismic slip near the hypocentre of an impending earthquake. Sufficient aseismic slip would produce near-surface deformation detectable by a borehole strainmeter. Compared with the strain step recorded at the time of the earthquake, the precursory strain signal would be in the same direction but of much smaller amplitude. A magnitude-5 earthquake, 10 km deep, produces maximum near-surface strain of about 10^{-7} at a site 5 km from its fault plane; strain increases 30-fold for each unit increase of magnitude, but falls off as the third power of distance from the source. Estimates of pre-seismic slip duration and amplitude range widely because frictional parameters of natural faults are poorly known.

Seismologists expect earthquake precursors to take the form of transient crustal-strain signals from 'aseismic' fault slip near the earthquake's nucleation point (that is, fault slip that is too slow to radiate seismic waves) (Fig. 2). Numerical simulations show, however, that such signals would be exceedingly small[4]. Even the best existing instruments — borehole strainmeters with resolution exceeding a part per billion — would need to be within a few kilometres of the impending earthquake's epicentre to detect this aseismic strain. Although strain changes preceding two California earthquakes have been identified[5,6], they don't resemble the expected signals.

Proponents of earthquake prediction maintain that changes in radon emission, or in electrical or magnetic fields, represent a natural amplification of pre-earthquake deformation under special geological conditions. For example, the conductance by rock fractures of water or gas is proportional to the third power of the fracture's aperture[7]. Fluid flow past ions adsorbed on rock surfaces produces an electric field, termed a 'streaming potential', that varies with pressure gradient and permeability[8]. Fluid, gas or electromagnetic measurements might thus detect deformation indirectly, albeit at localized sites and with amplitudes related nonlinearly to strain.

Silver and Wakita[9] list many potential examples of such pre-earthquake 'strain indicators'. Unfortunately, these indicators are irreproducible: they can be detected only in certain locations, but in any one location earthquakes recur infrequently. What is needed is evidence that transient strain leads consistently, if not linearly or uniformly, to observable phenomena. The radon, electrical and ground-tilt measurements from Roselend lake constitute this kind of reproducible evidence.

The shallow crust's reaction to large changes in lake level may also illuminate the

^{226}Ra

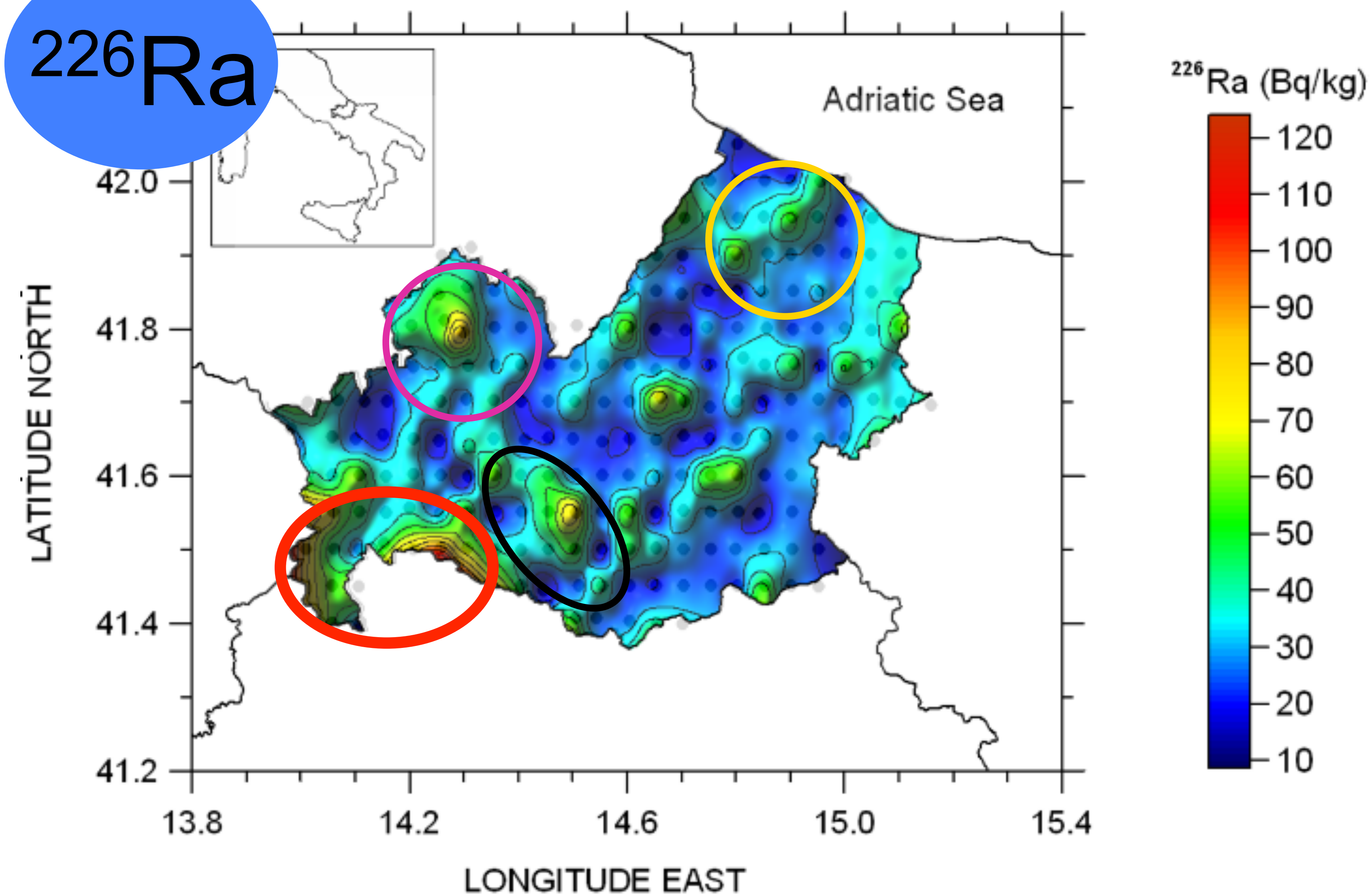
Adriatic Sea
LATITUDE NORTH
42.0
41.8
41.6
41.4
41.2
13.8
14.2
14.6
15.0
15.4
LONGITUDE EAST
226Ra (Bq/kg)
120
110
100
90
80
70
60
50
40
30
20
10

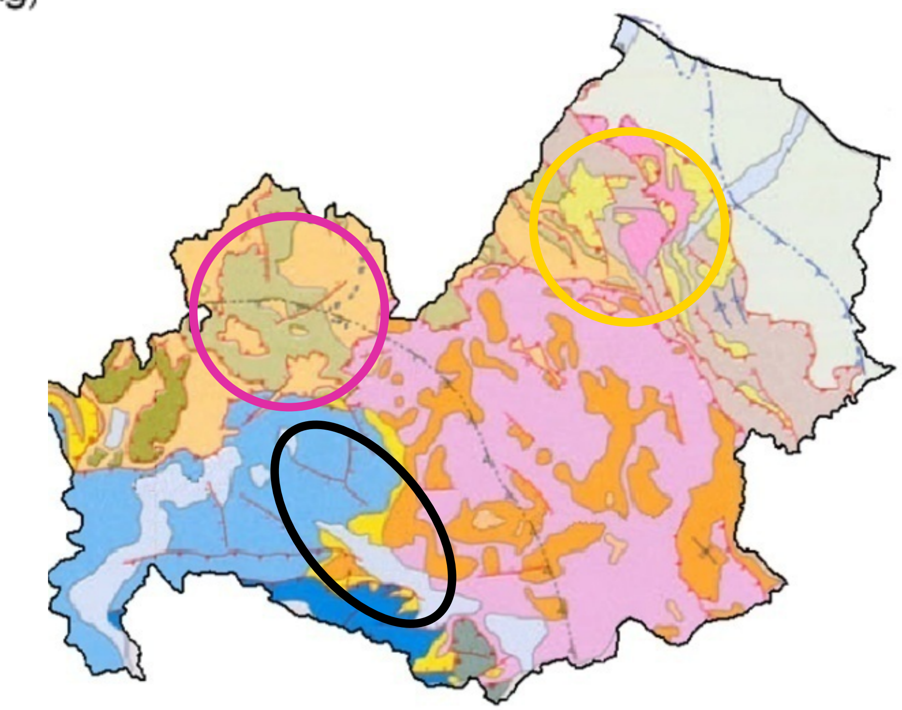

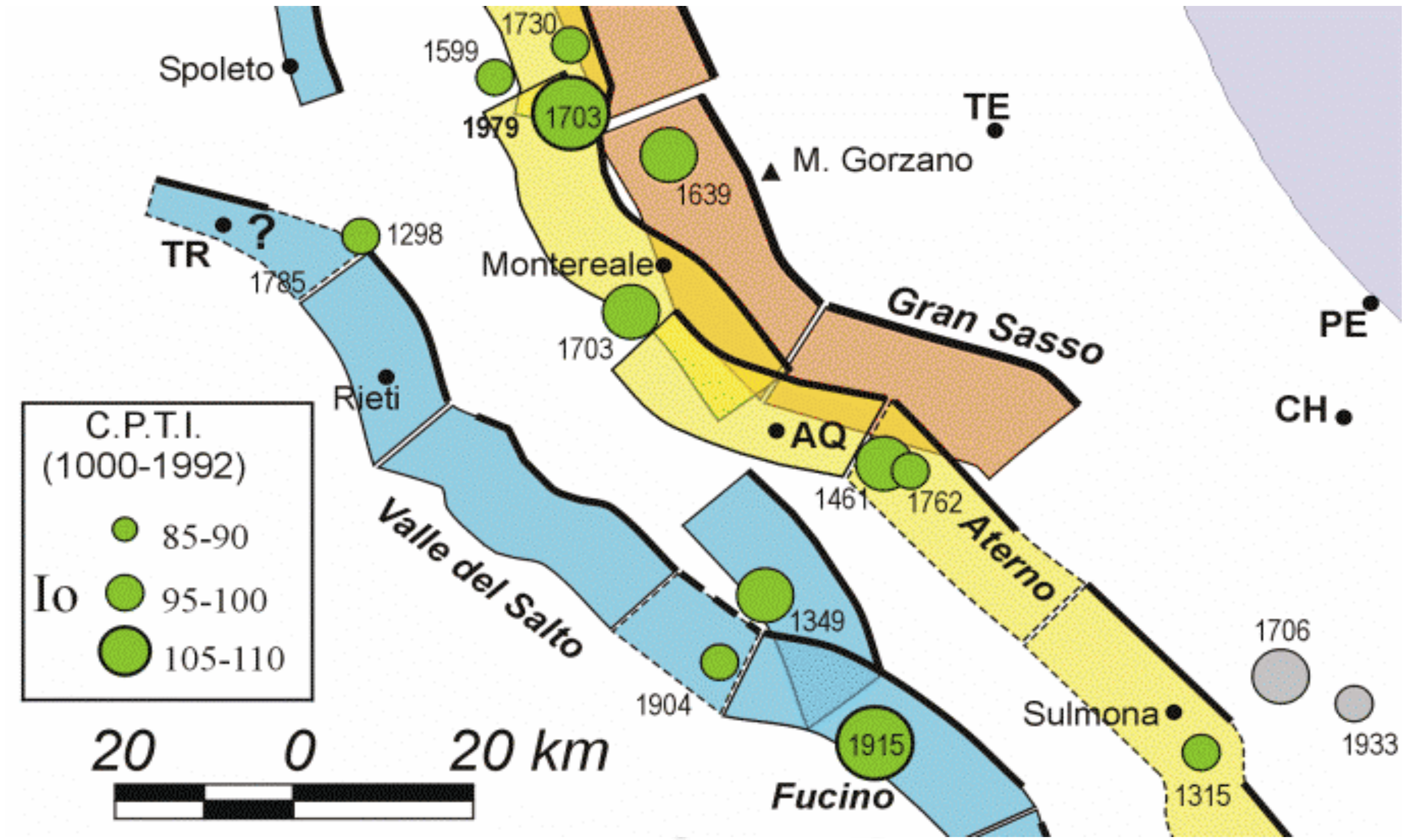

Lavecchia, G. et al. 1999. Analisi delle relazioni tra sismicita` e strutture tettoniche in Umbria–Marche–Abruzzo finalizzata alla realizzazione della mappa delle zone sismogenetiche. Progetto 5.1.1 — PE 98 (CNR-GNDT): Mappa delle zone sismogenetiche e probabilita` degli eventi associati, http://emidius.itim.mi.cnr.it/GNDT/P511/UNI_CHI/rel990703.html

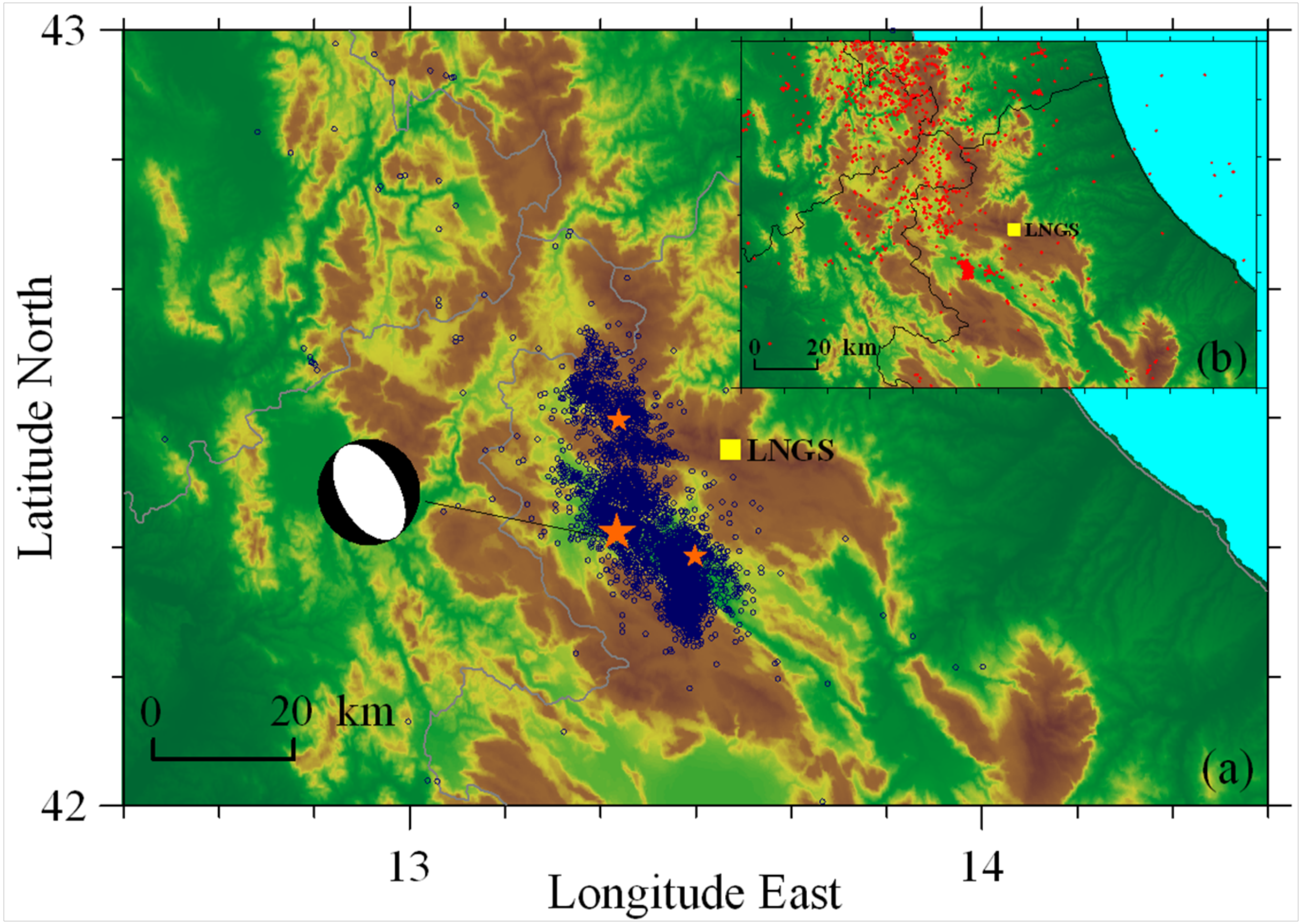

Plastino, W. et al., 2010. Uranium groundwater anomalies and L'Aquila earthquake, 6th April 2009 (Italy), Journal of Environmental Radioactivity, 101, 45-50.

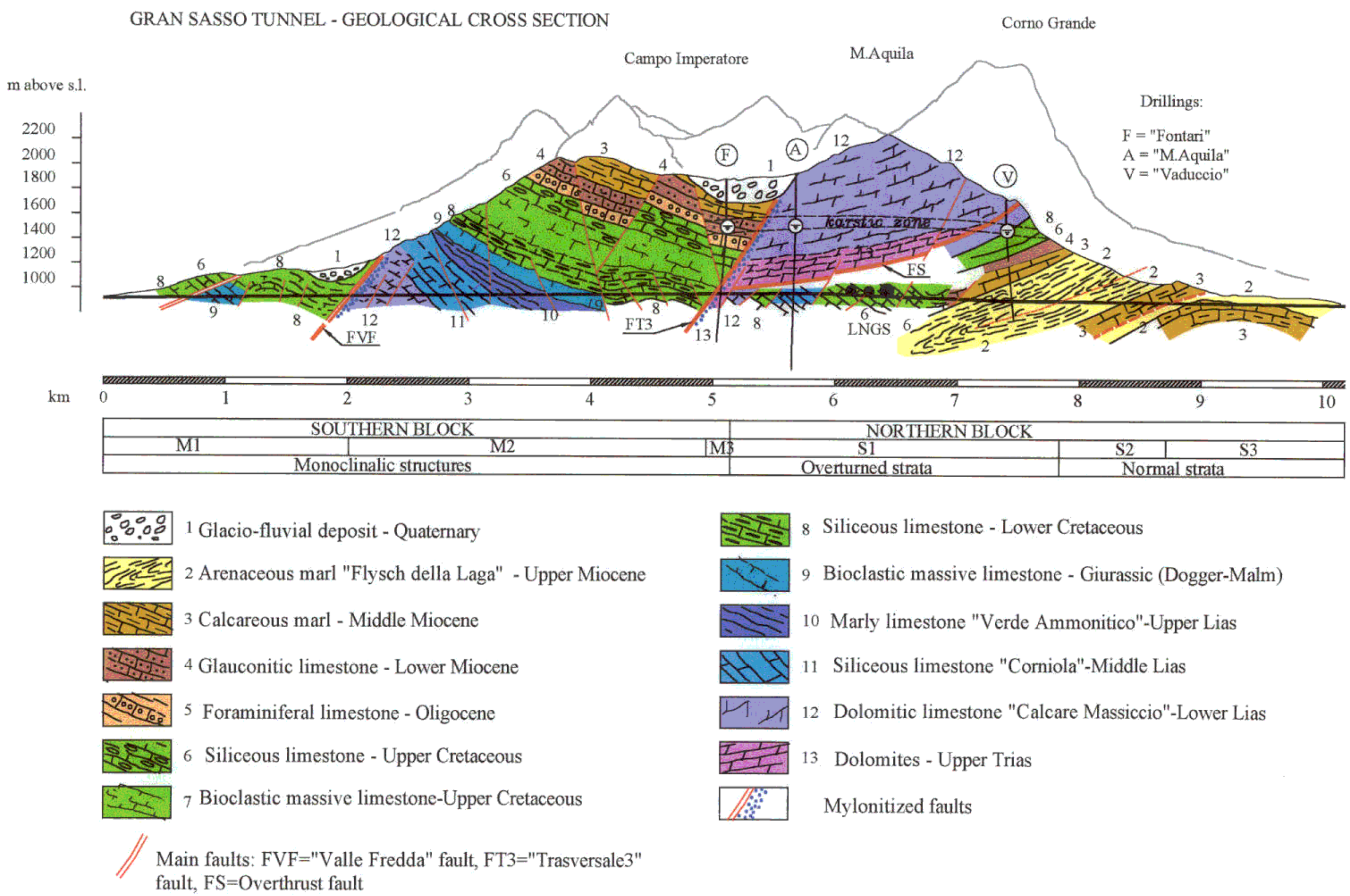

Plastino, W. et al., 2010. Uranium groundwater anomalies and L'Aquila earthquake, 6th April 2009 (Italy), Journal of Environmental Radioactivity, 101, 45-50.

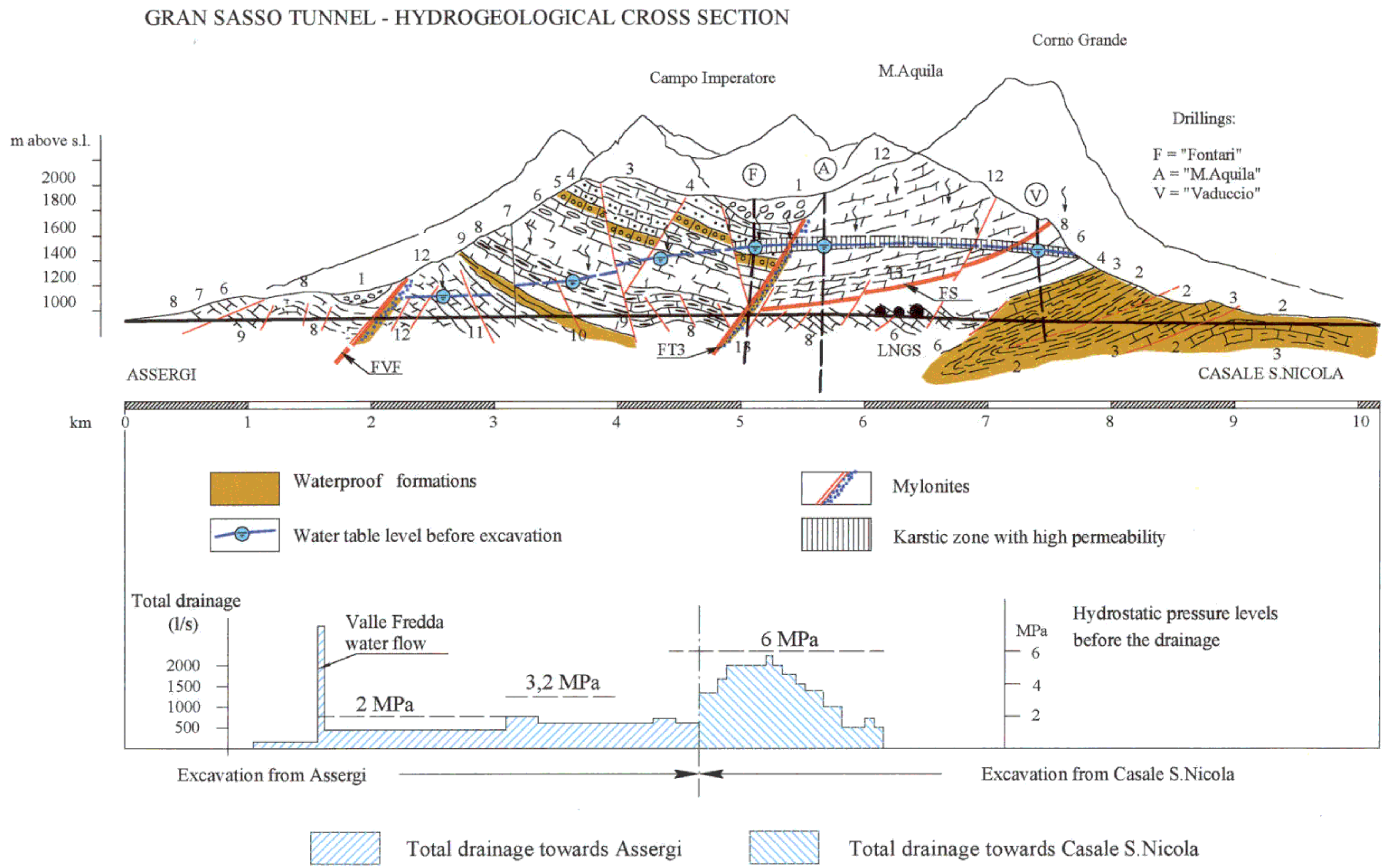

Plastino, W. et al., 2010. Uranium groundwater anomalies and L'Aquila earthquake, 6th April 2009 (Italy), Journal of Environmental Radioactivity, 101, 45-50.

^{238}U and ^{232}Th activities in LNGS rock

Hall	Activities (ppm)	
	^{238}U	^{232}Th
A	6.80 ± 0.67	2.167 ± 0.074
B	0.42 ± 0.10	0.062 ± 0.020
C	0.66 ± 0.14	0.066 ± 0.025

Wulandari, H. et al., 2004. Neutron flux at the Gran Sasso underground laboratory revisited. Astroparticle Physics, doi: 10.1016/j.astropartphys.2004.07.005

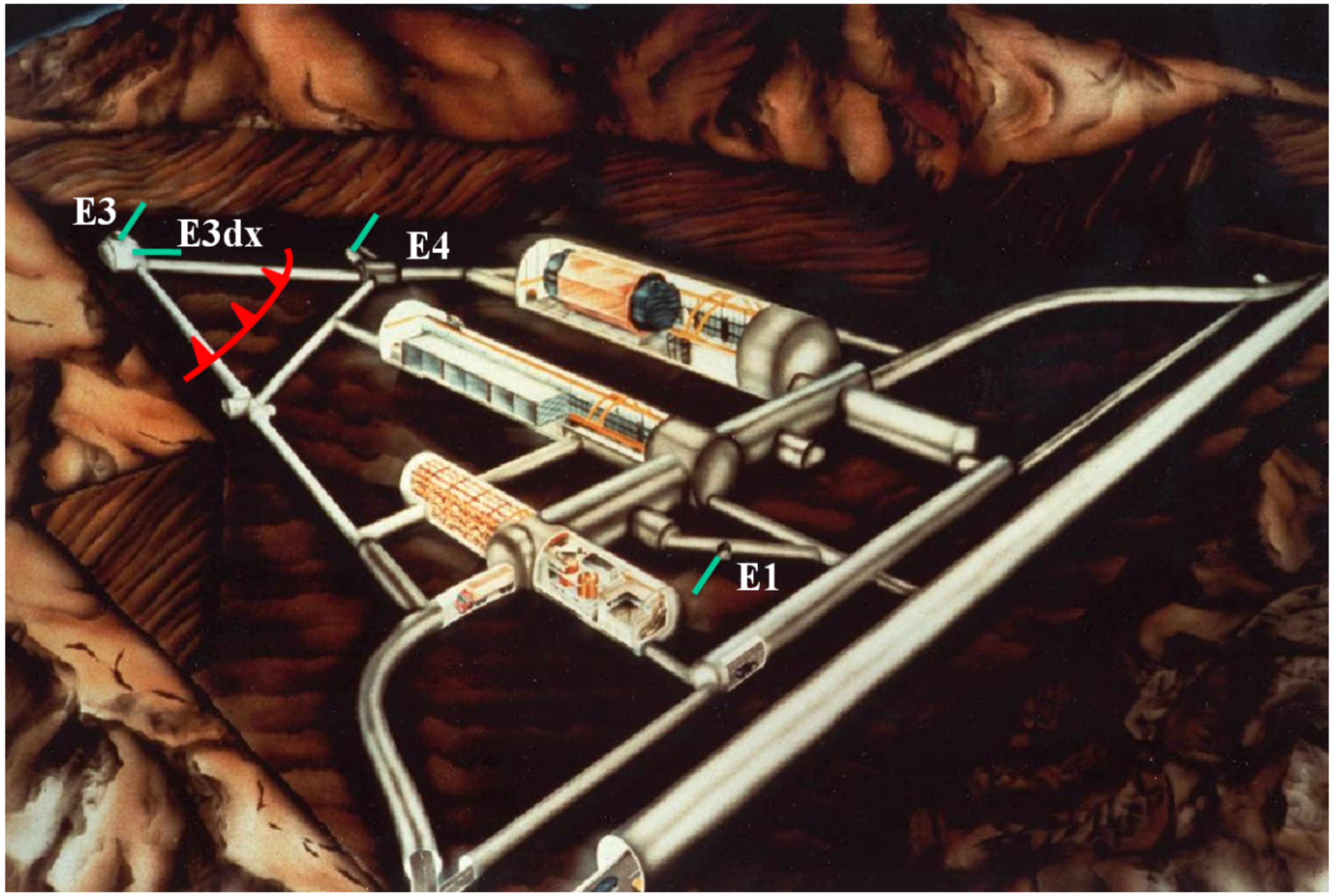

	U 10^{-9} g/g	^{3}H TU	^{14}C pMC	δ^{13}C ‰	δ^2H ‰	δ^{18}O ‰	pH	ORP/mV	EC µS/cm
E1	0.29 ± 0.01	6.6 ± 0.4	59.5 ± 1.0	−9.64	−72.2	−10.93	8.2 ± 0.1	231 ± 22	255.4 ± 3.0
E3	1.79 ± 0.02	8.8 ± 0.5	57.1 ± 1.0	−6.68	−74.6	−11.28	8.2 ± 0.1	232 ± 22	169.3 ± 2.0
E3dx	1.47 ± 0.02	11.2 ± 0.6			−74.4	−11.22	8.3 ± 0.1	228 ± 22	169.1 ± 2.0
E4	0.54 ± 0.01	10.1 ± 0.6	71.7 ± 1.0	−5.74	−72.6	−11.07	8.2 ± 0.1	240 ± 22	159.1 ± 2.0

Plastino, W., et al. 2009. Environmental radioactivity in the ground water at the Gran Sasso National Laboratory (Italy): a possible contribution to the variation of the neutron flux background, Journal of Radioanalytical and Nuclear Chemistry, 282, 809-813.

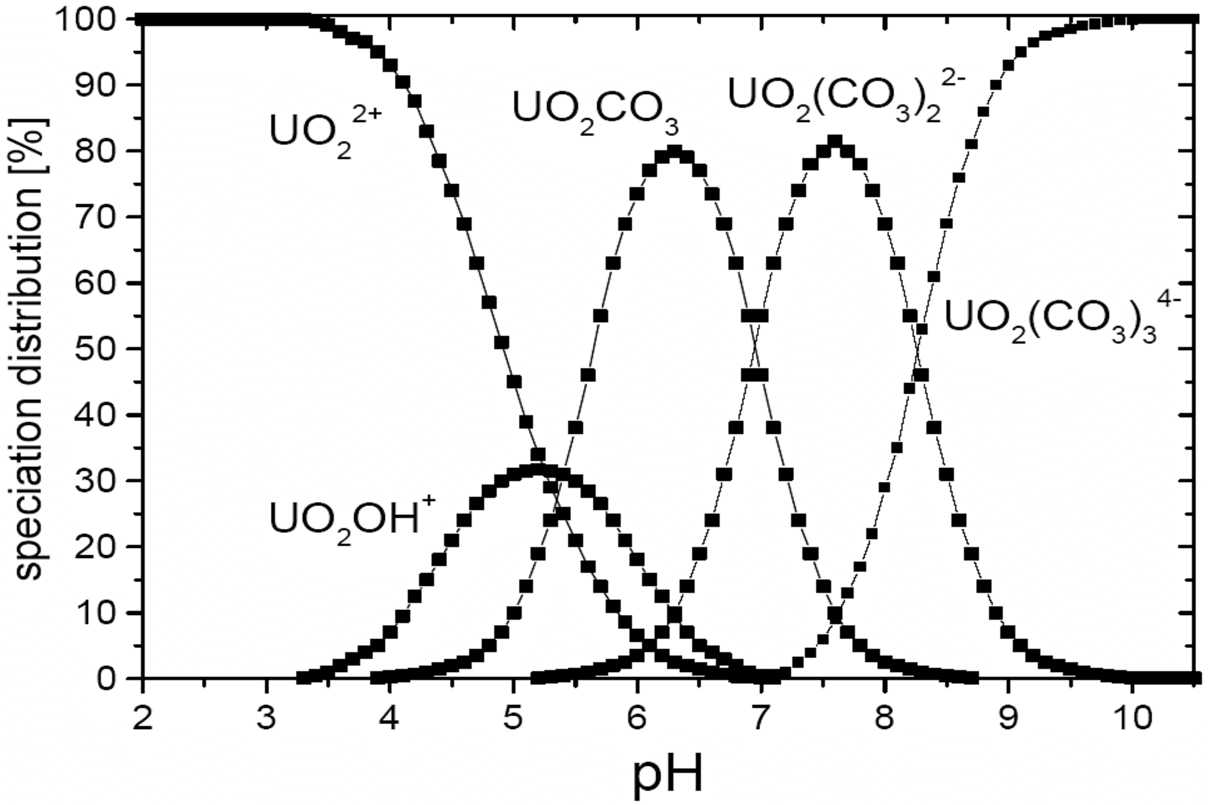

Langmuir, Geoch. Cosmoch. Acta, 1978

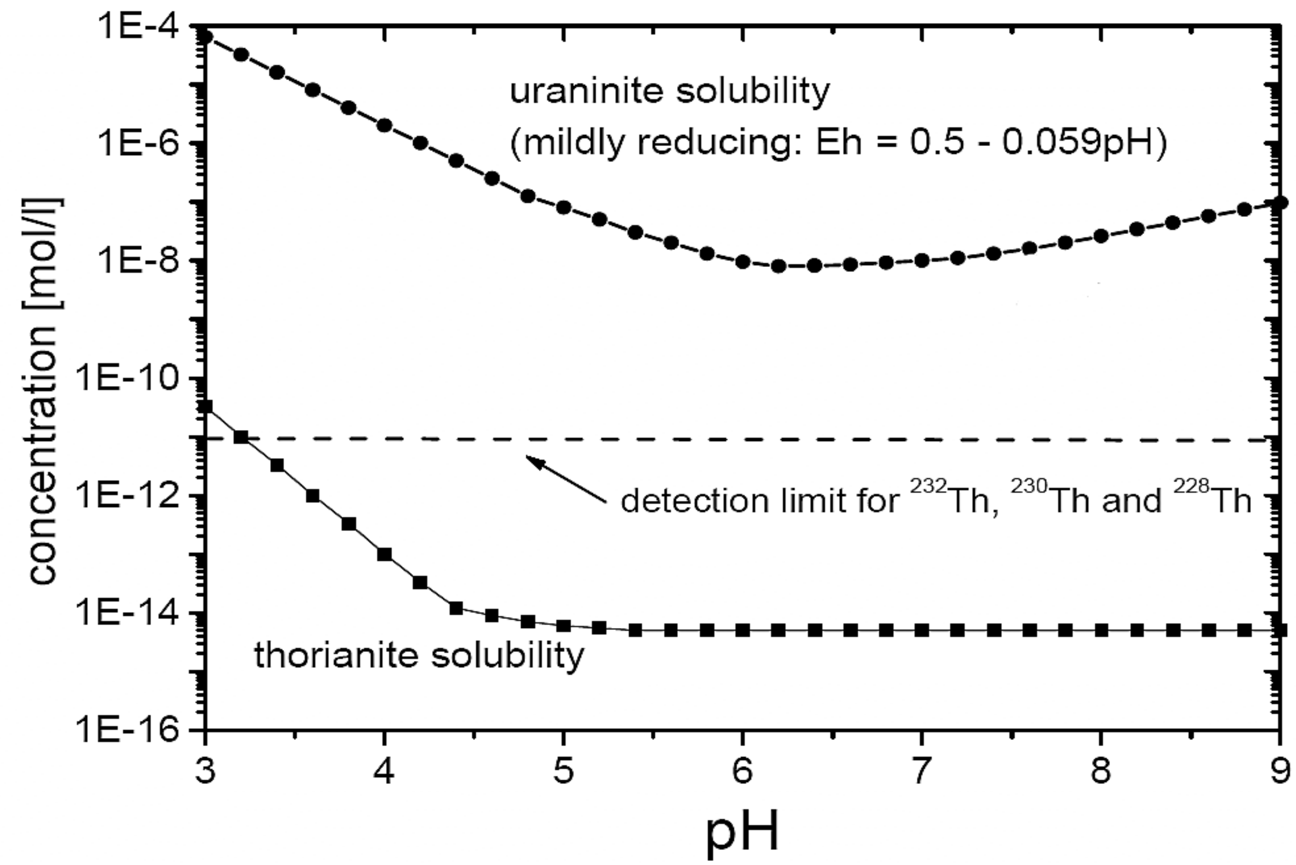

© J. Eikenberg, Paul Scherrer Institute

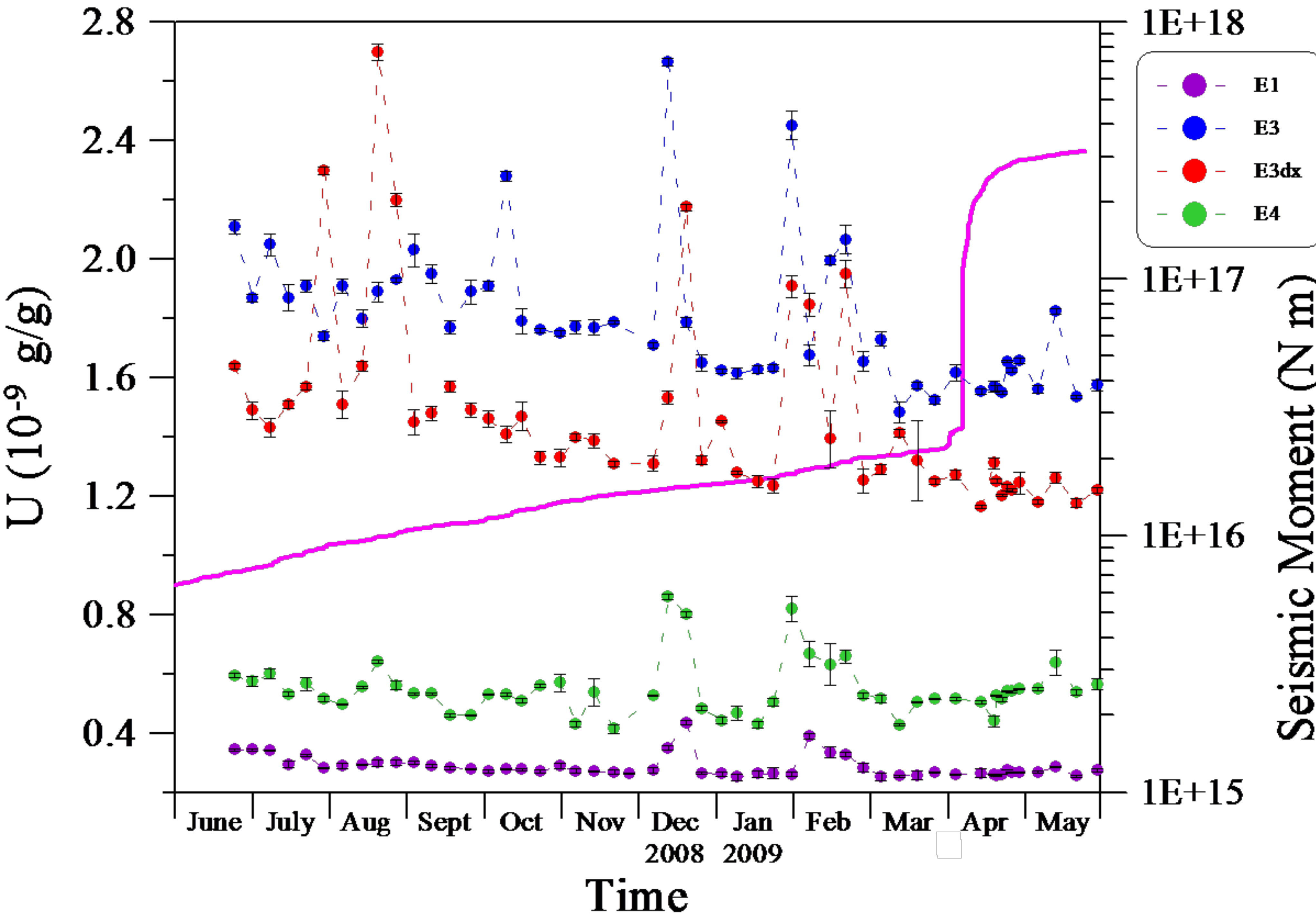

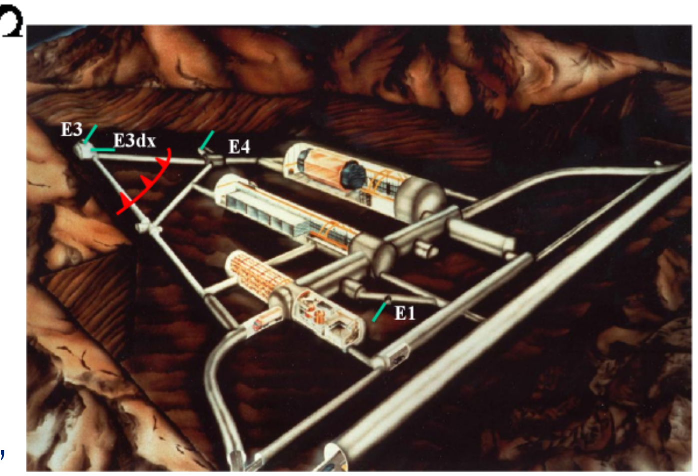

Plastino, W. et al., 2010. Uranium groundwater anomalies and L'Aquila earthquake, 6th April 2009 (Italy), Journal of Environmental Radioactivity, 101, 45-50.

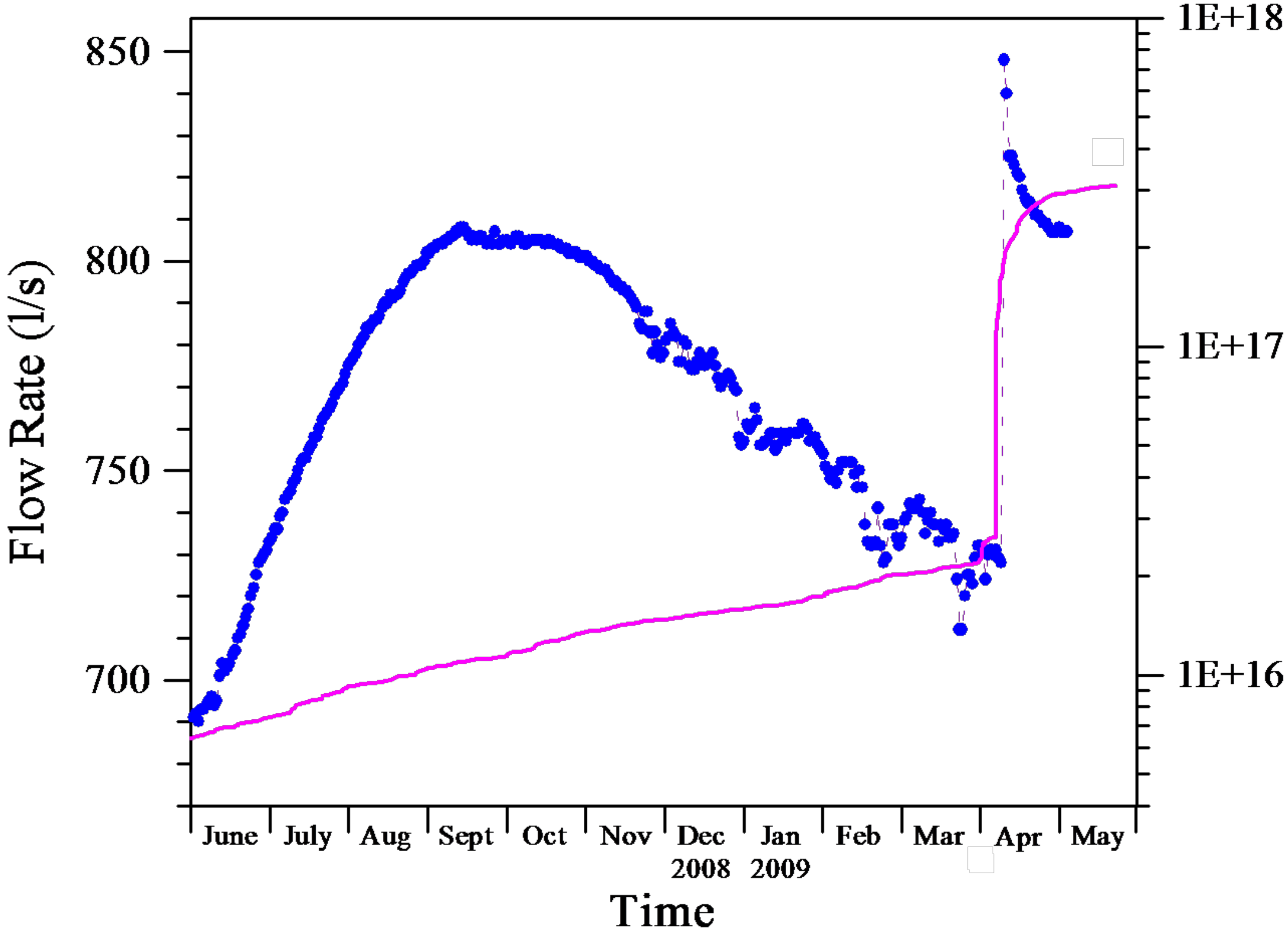

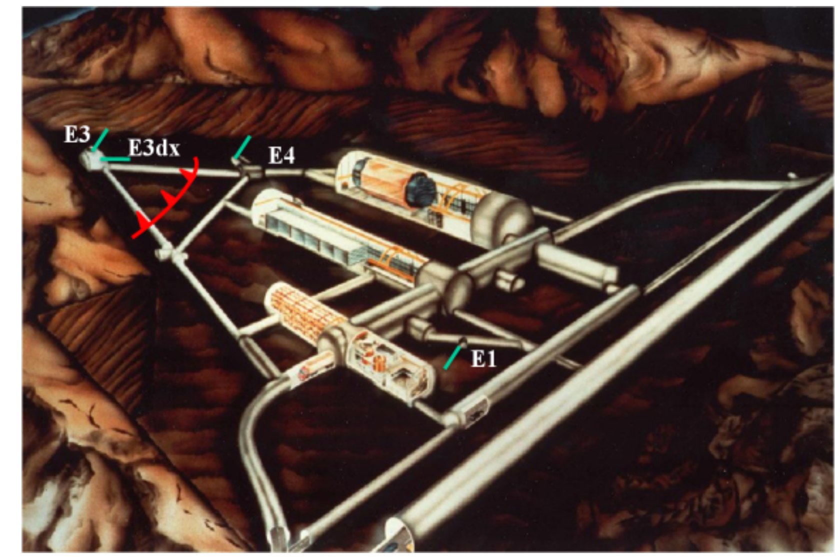

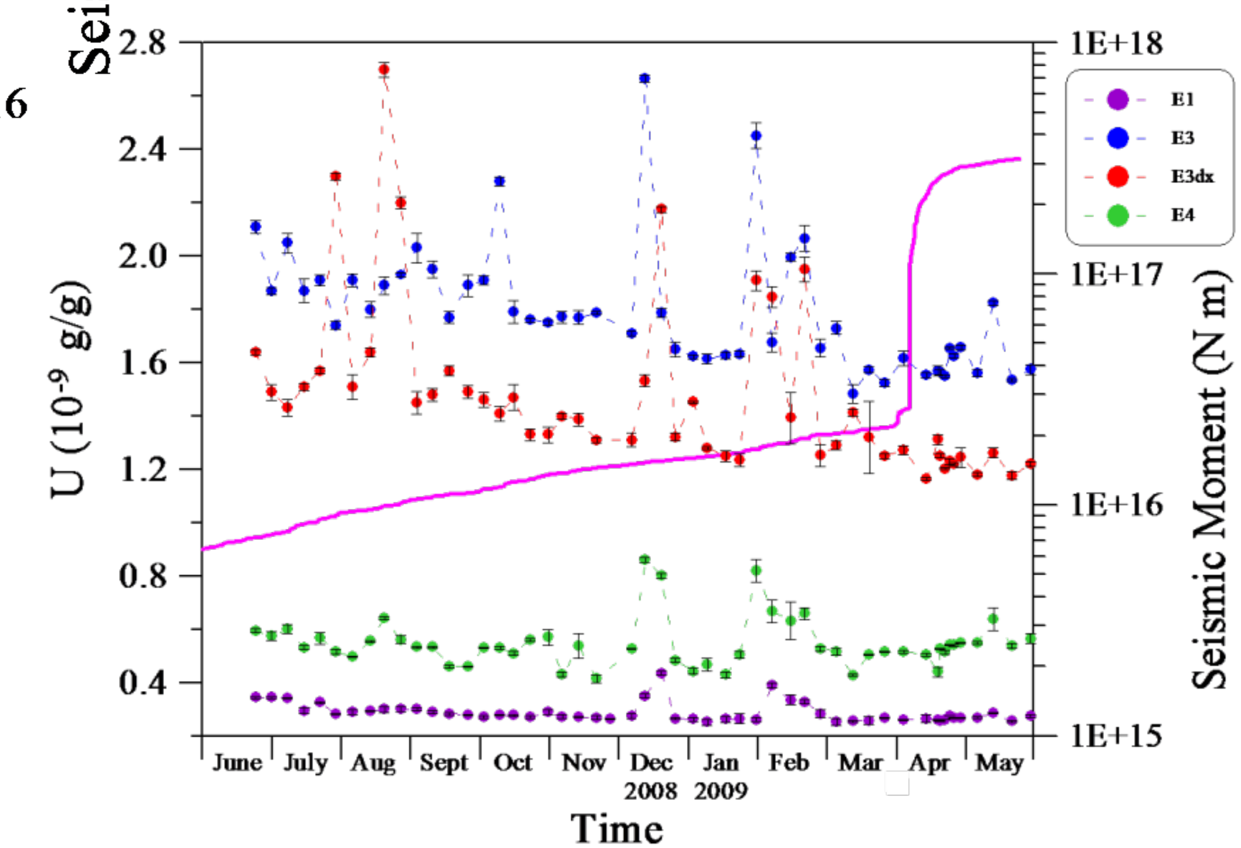

Plastino, W. et al., 2010. Uranium groundwater anomalies and L'Aquila earthquake, 6th April 2009 (Italy), Journal of Environmental Radioactivity, 101, 45-50.

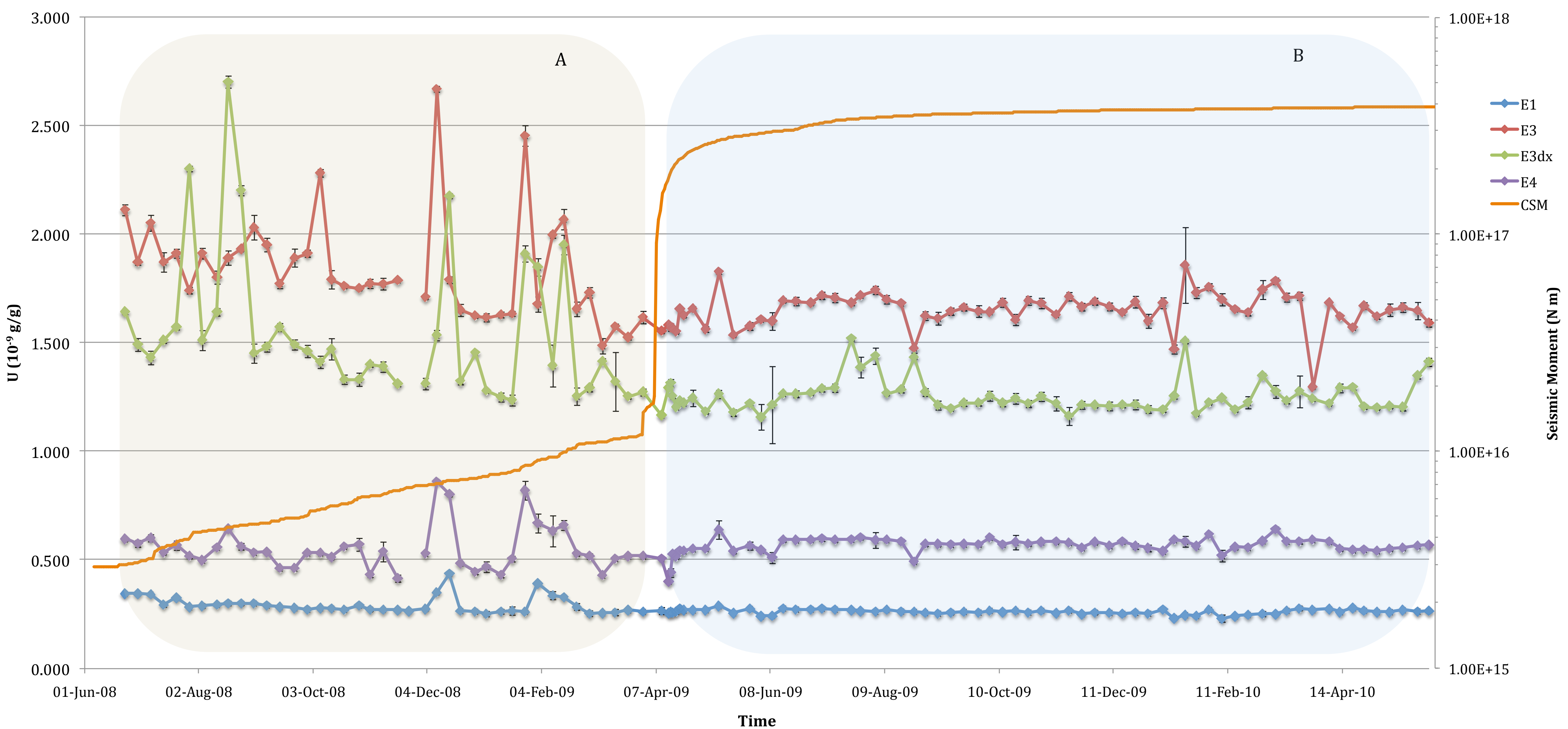

Plastino, W. et al., 2011. Uranium groundwater anomalies and active normal faulting, Journal of Radioanalytical and Nuclear Chemistry, 288, 101-107.

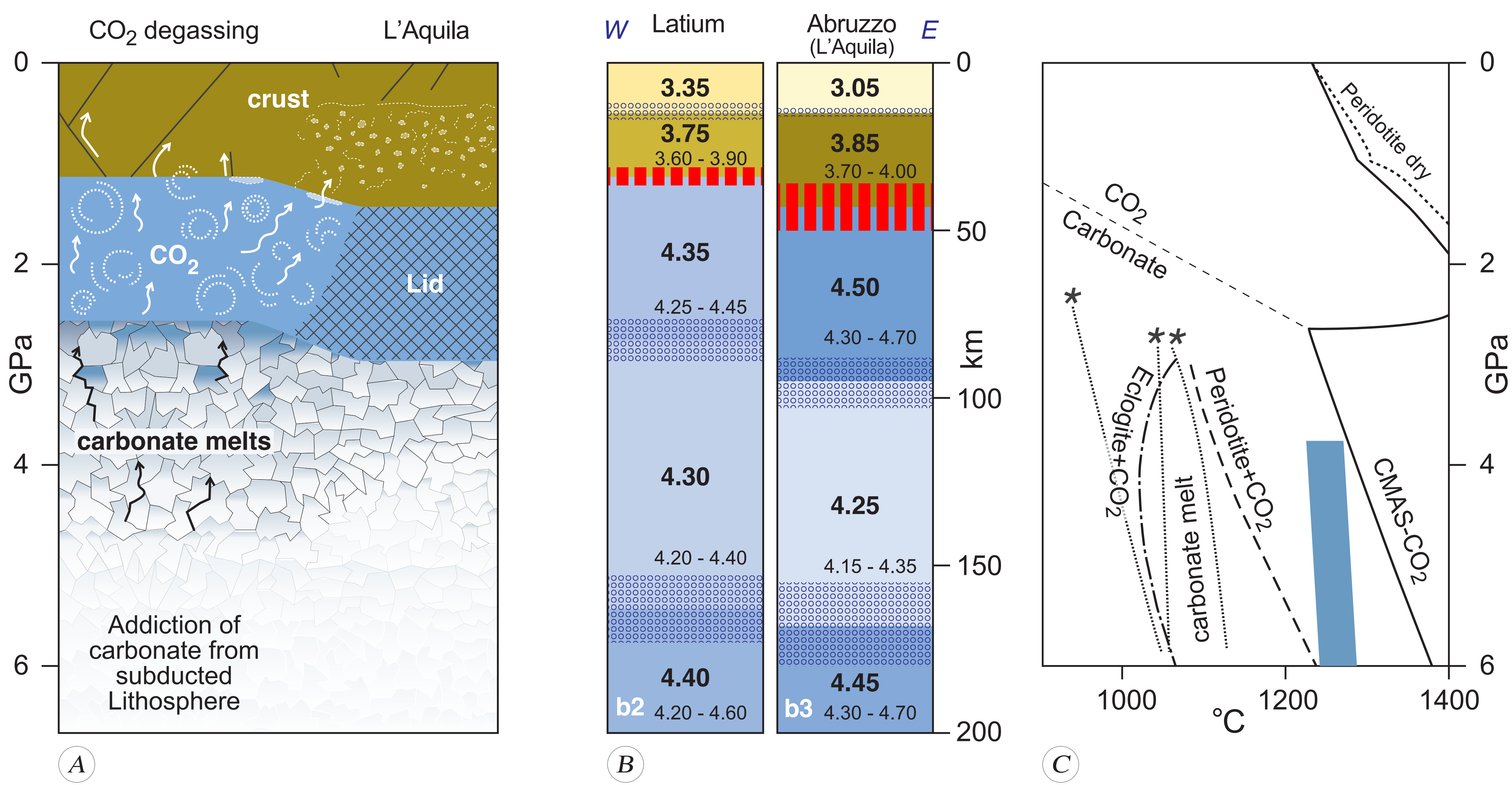

Plastino, W. et al., 2011. Uranium groundwater anomalies and active normal faulting, Journal of Radioanalytical and Nuclear Chemistry, 288, 101-107.

Hydrological Cycle and Water Resources

Development of an integrated view of the water resource management, bridging the evaluation of the water resources area with the study of the large and basin-scale hydrological cycle

Development of effective, internationally shared tools for public and private institutions for the correct management of the water resources as well as for planning future development

Development of set of standards for the collection, evaluation, storage and interpretation of the hydro-meteorological data, with particular regard to extreme events of great potential impact on the welfare of the population and on the state of the environment

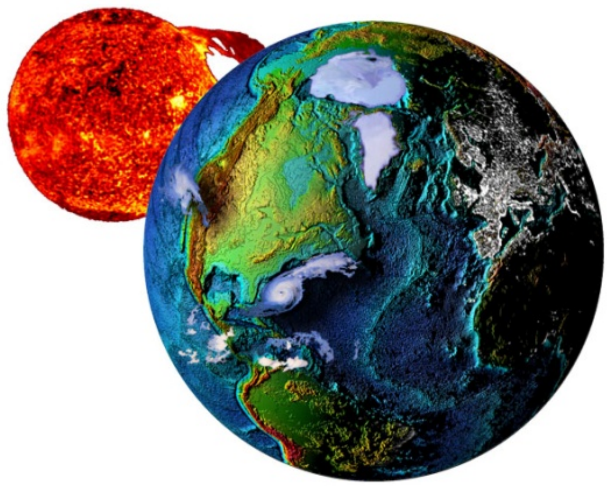

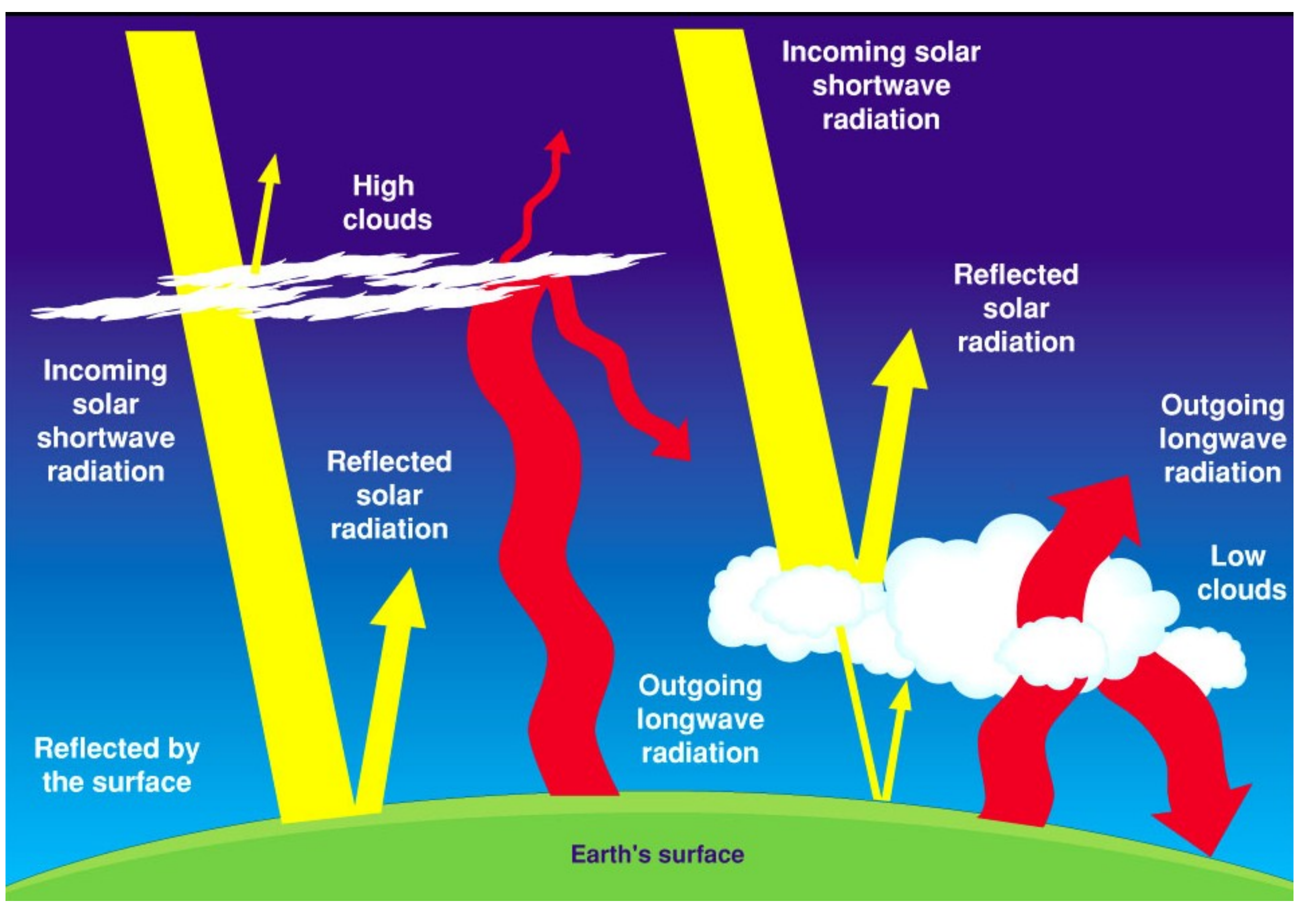
Incoming solar shortwave radiation
High clouds
Reflected solar radiation
Incoming solar shortwave radiation
Reflected solar radiation
Outgoing longwave radiation
Low clouds
Outgoing longwave radiation
Reflected by the surface
Earth's surface

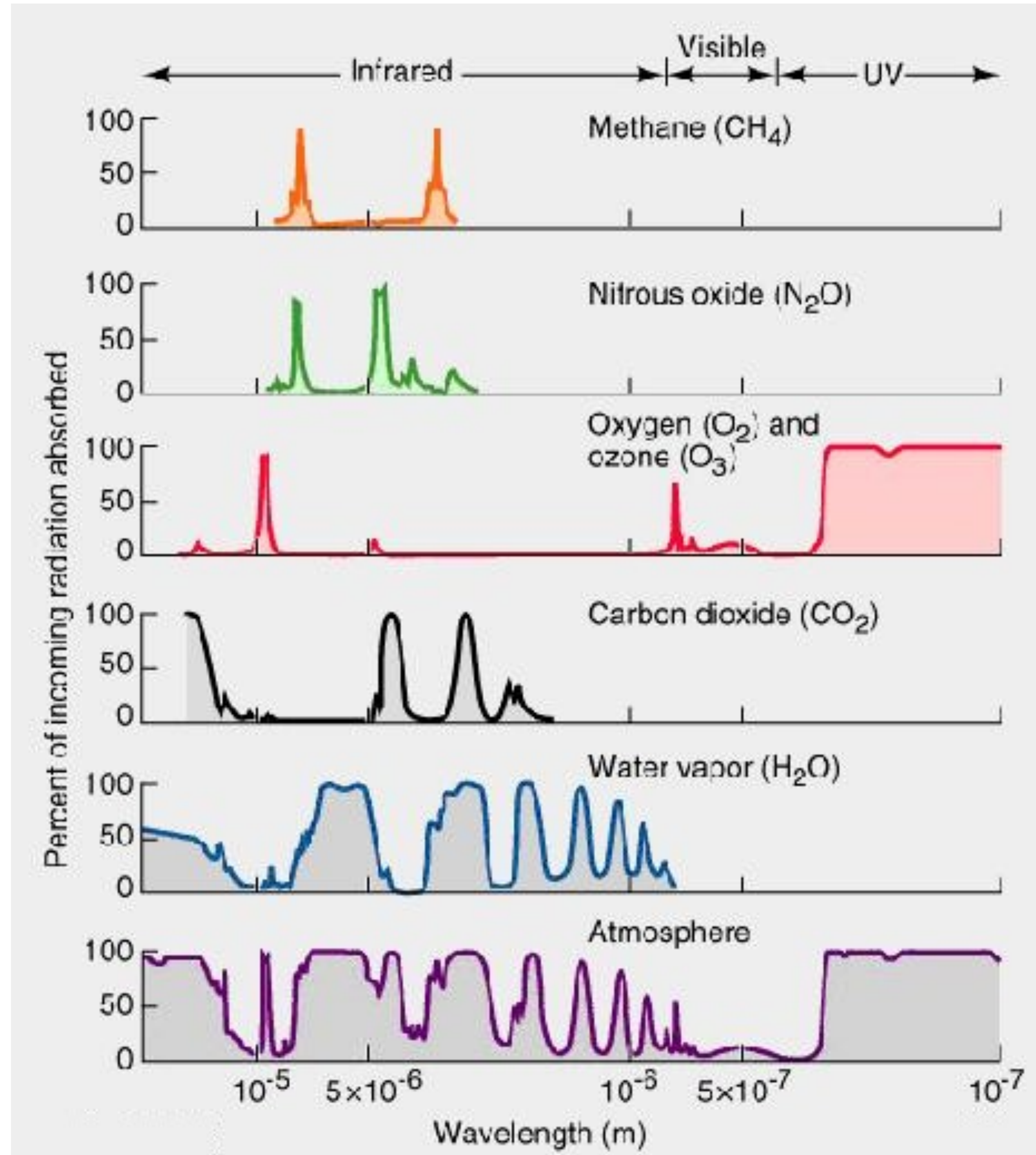
Infrared
Visible
UV
Methane (CH4)
Nitrous oxide (N2O)
Oxygen (O2) and ozone (O3)
Carbon dioxide (CO2)
Water vapor (H2O)
Atmosphere
Percent of incoming radiation absorbed
100
50
0
10-5
5×10-6
10-6
5×10-7
10-7
Wavelength (m)

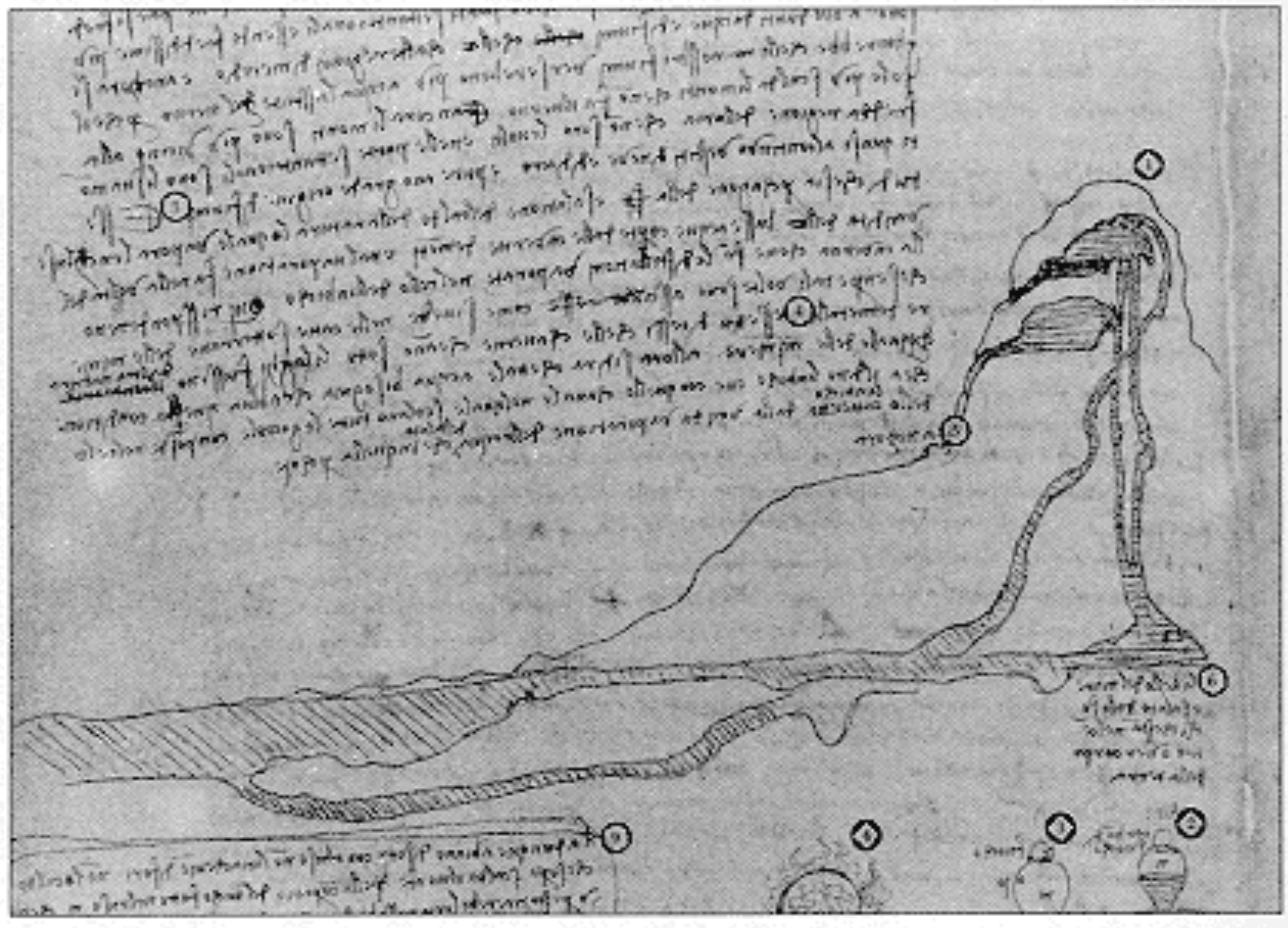

[..] Il corpo della Terra, a similitudine de' corpi de li animali, è tessuto di ramificazione di vene, le quali son tutte insieme congiunte, e son costituite a nutrimento e vivificazione d'essa Terra e de' suoi creati, e si partano dalle profondità del mare, e a quelle dopo molta revoluzione, ànno a tornare per li fiumi creati dalle altre rotture d'esse vene. [..] (Leonardo Da Vinci, 1508 -1510)

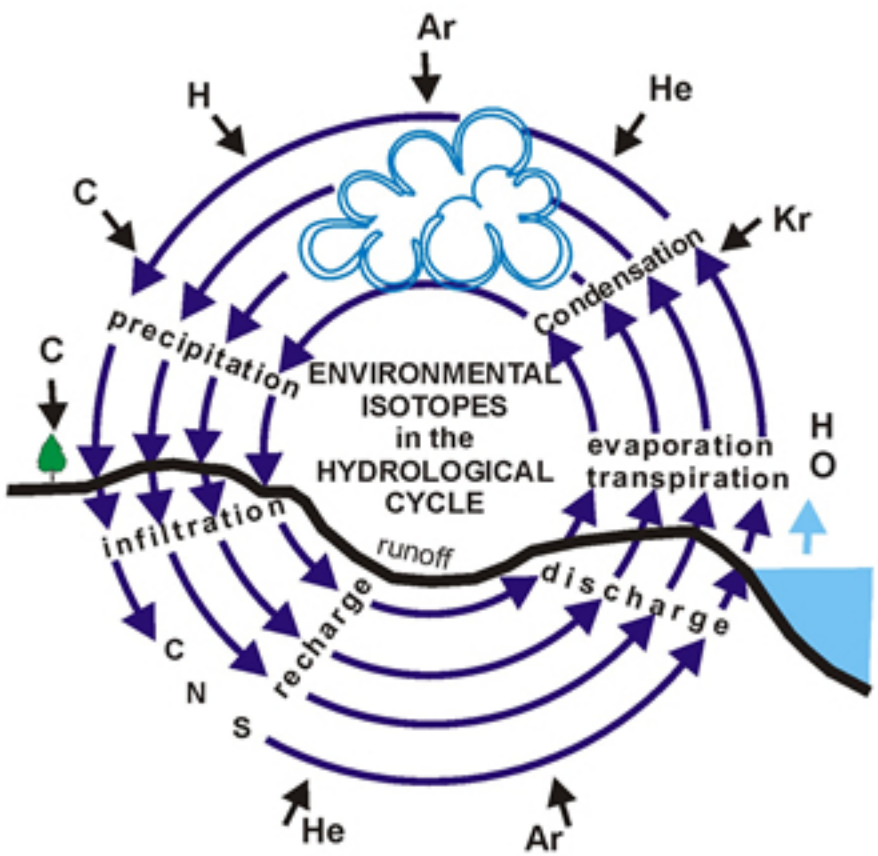
Ar
He
H
C
Kr
C
precipitation
condensation
ENVIRONMENTAL ISOTOPES in the HYDROLOGICAL CYCLE
evaporation transpiration
H
O
infiltration
runoff
discharge
recharge
C
N
S
He
Ar

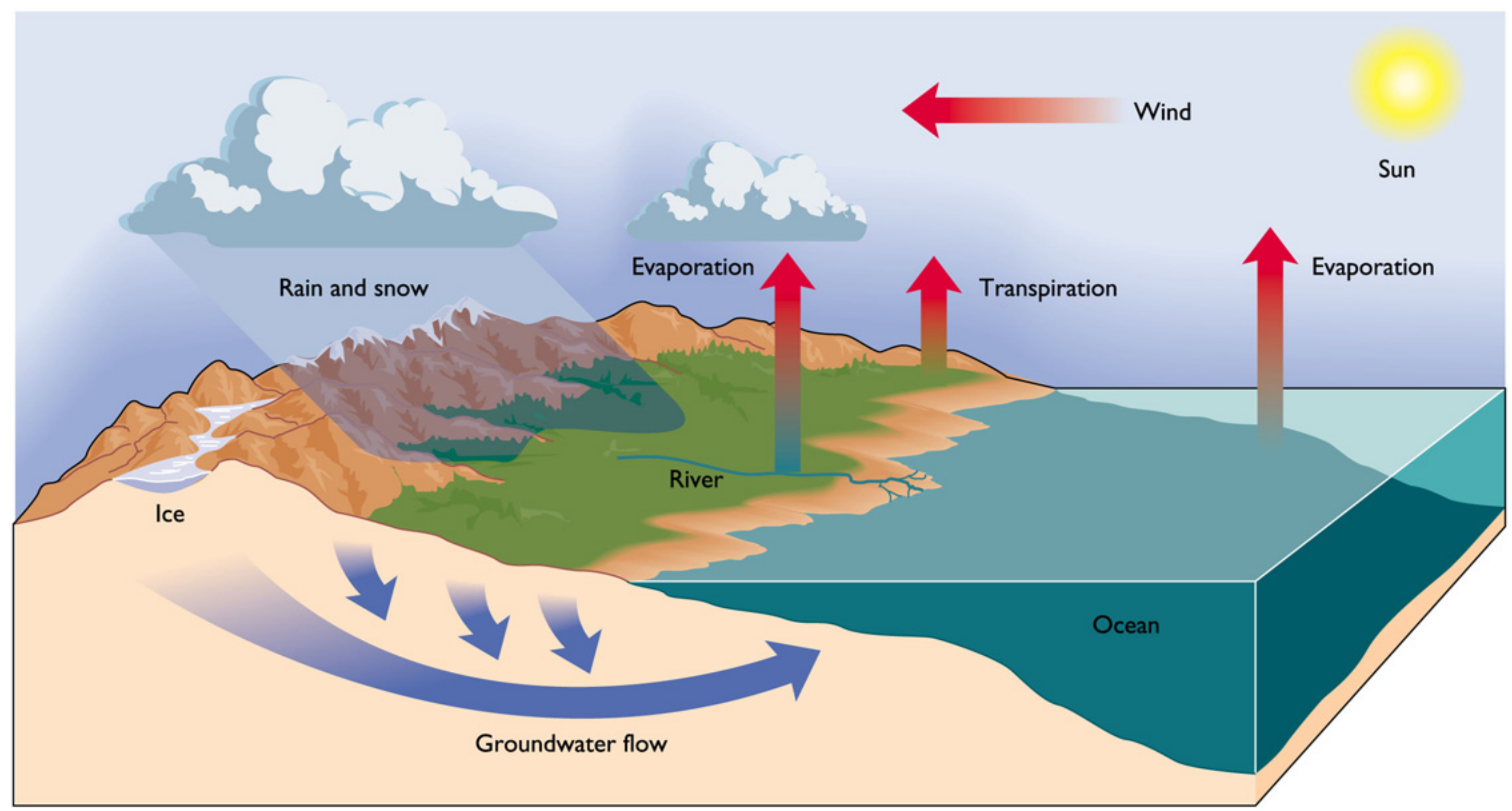
Wind
Sun
Evaporation
Transpiration
Evaporation
Rain and snow
River
Ice
Ocean
Groundwater flow

Radiocarbon

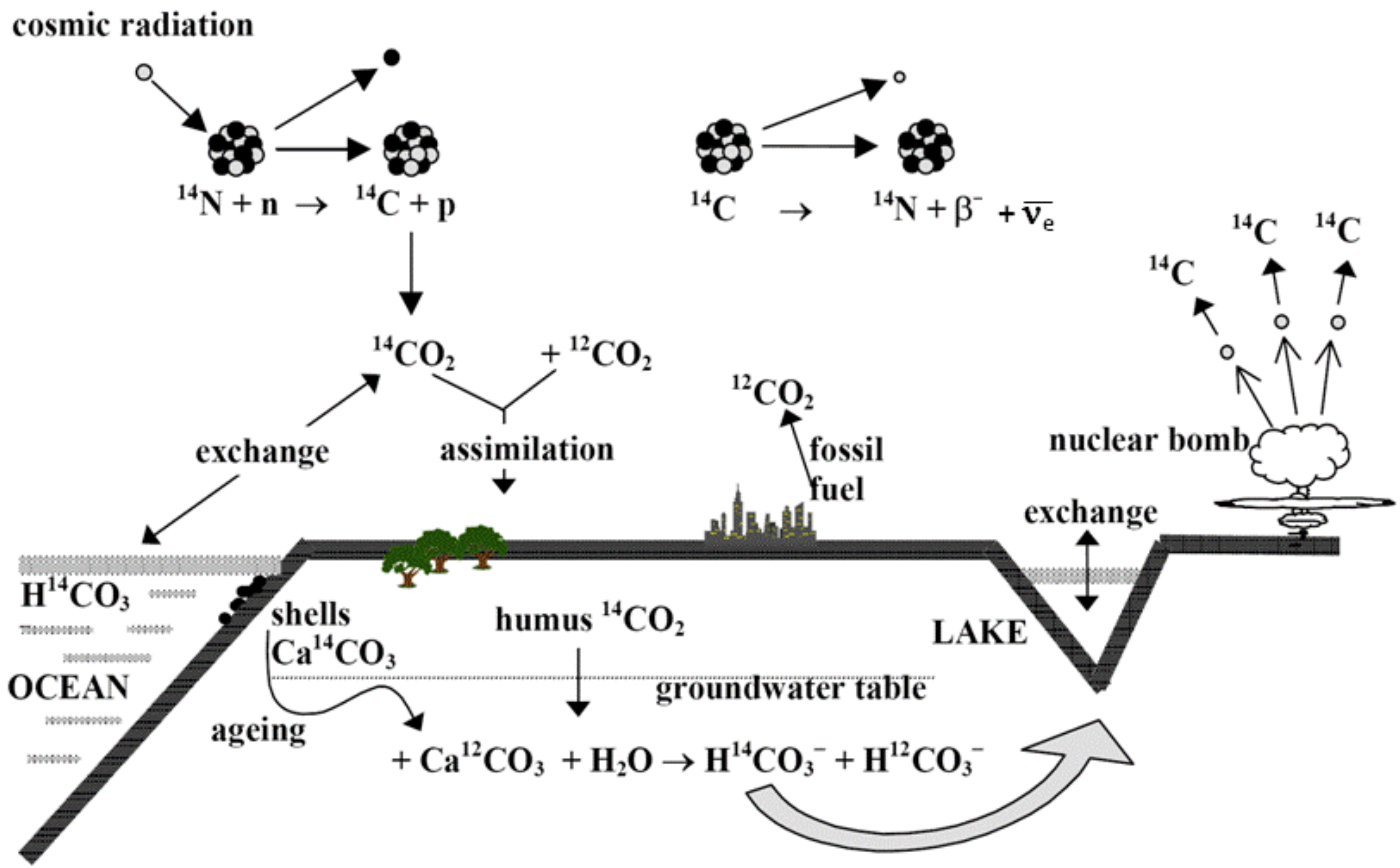

Tritium

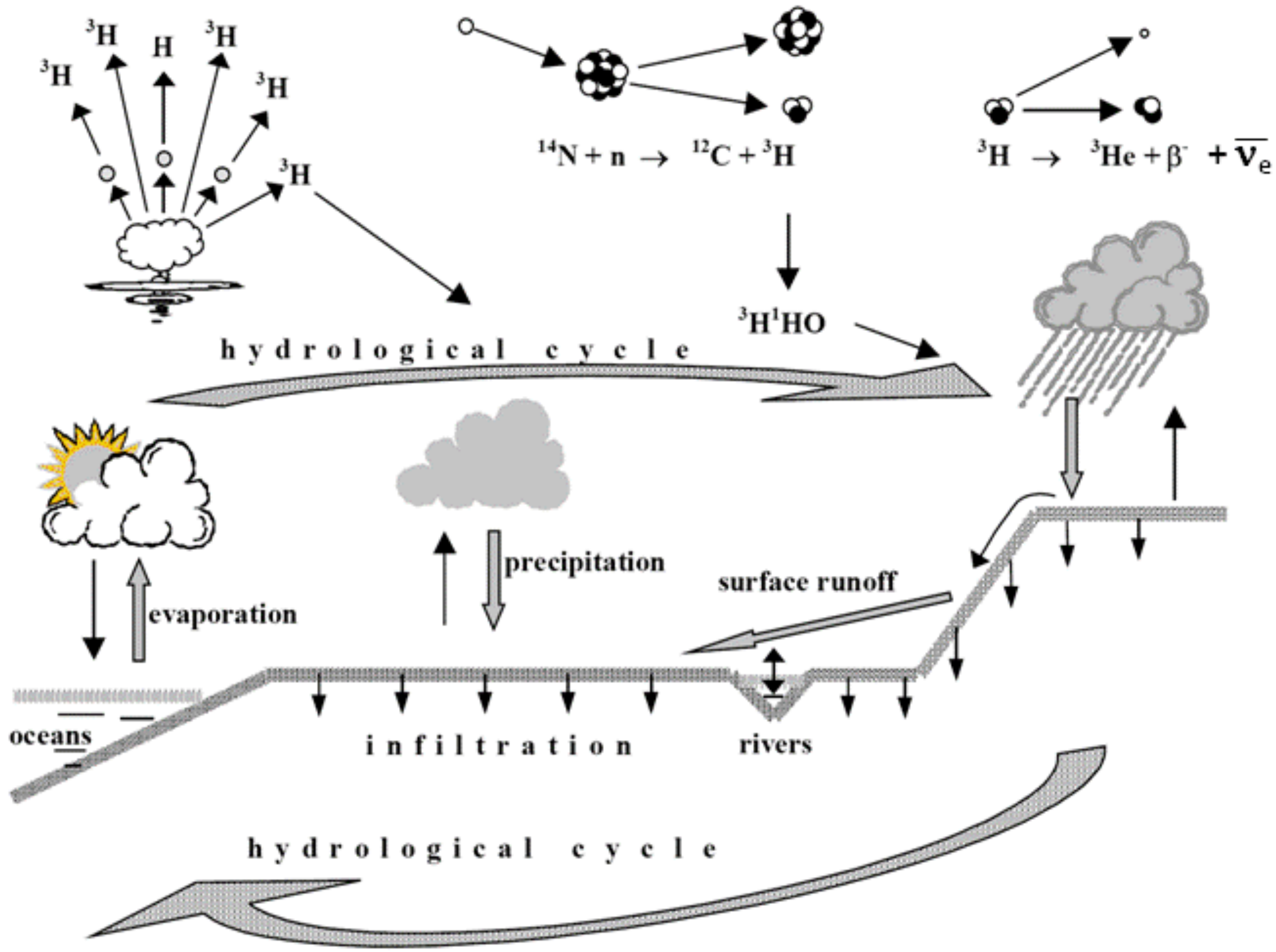
3H
H
3H
3H
3H
3H
14N + n → 12C + 3H
3H → 3He + β- + ν̄e
3H1HO
hydrological cycle
precipitation
evaporation
surface runoff
oceans
infiltration
rivers
hydrological cycle

RADIOCARBON, Vol 43, Nr 2A, 2001, p 157–161

COSMIC BACKGROUND REDUCTION IN THE RADIOCARBON MEASUREMENTS BY LIQUID SCINTILLATION SPECTROMETRY AT THE UNDERGROUND LABORATORY OF GRAN SASSO

Wolfango Plastino[1] • Lauri Kaihola[2] • Paolo Bartolomei[3] • Francesco Bella[4]

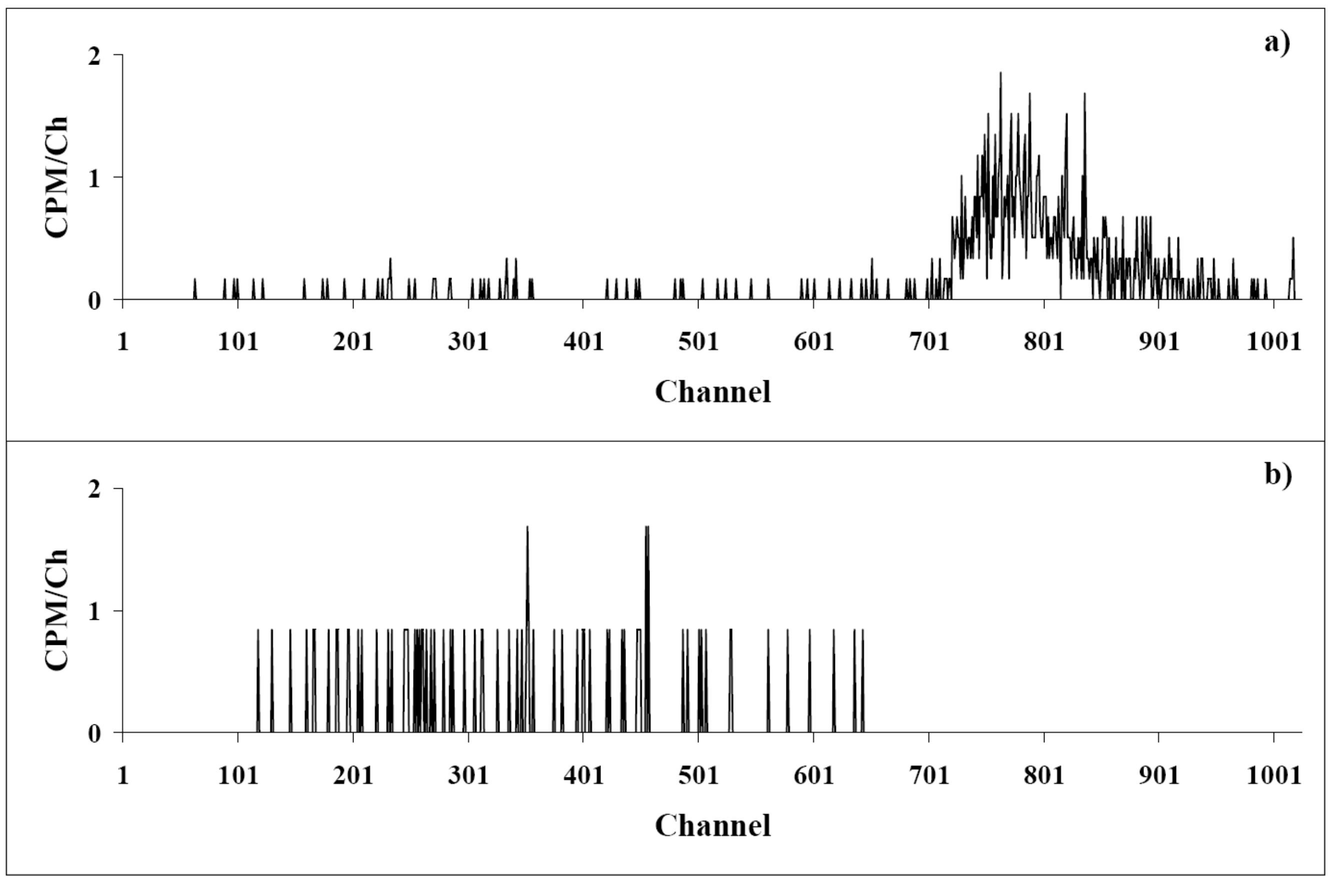

Figure 2 The coincidence count rate of guard with sample events recorded at the surface (a) and the underground (b) laboratories. To a better graphical representation the CPM/Ch of surface (a) and underground (b) laboratories are multiplied by factors 10E+01 and 10E+03, respectively.

Table 1 The count rate of the set A of teflon vials with benzene volumes of 1, 3, and 5 mL related to surface and underground (italic) laboratories. The labels L and H indicate background and modern standards, respectively.

Sample	Count rate (cpm)	Count error (cpm)	Modern activity (dpm)	Modern activity error (dpm)	Eff (%)	FM	fM	T_{max} (BP)
L1A	0.278	0.022						
H1A	12.949	0.148	8.853	0.088	80.93	25,531.503	17	48,200
L1A	*0.059*	*0.010*						
H1A	*12.282*	*0.144*	*8.540*	*0.094*	*76.76*	*99,734.000*	*35*	*54,000*
L3A	0.398	0.026						
H3A	39.140	0.257	27.068	0.161	83.28	17,419.104	43	55,900
L3A	*0.150*	*0.016*						
H3A	*38.235*	*0.254*	*26.609*	*0.166*	*81.35*	*44,052.587*	*69*	*59,600*
L5A	0.655	0.033						
H5A	65.206	0.332	45.101	0.209	83.60	10,676.865	57	58,000
L5A	*0.235*	*0.020*						
H5A	*63.874*	*0.328*	*44.464*	*0.215*	*81.89*	*28,580.867*	*92*	*61,900*

...the best result around the World!

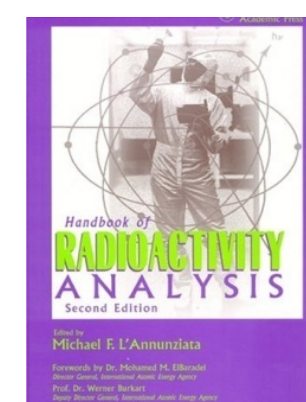

ELSEVIER

Tritium in water el

Wolfango Plastino[a]
Nicolae Lupsa[b],

[a]Department
[b]National Institute
d
[e]Facu

Received

Table 3
Results of the measurements in wide tritium window (Channels 5–200)

Sample in PE vials	Count rate (min^{-1})	Reference to mean BKG (Bq)	Error reference to mean BKG (Bq)	Measured EFT	Calculated EFT
STD	3006	210.500			
1A0	1.418	−0.004	0.001		
1B0	1.511	0.003	0.001		
1A1	1.573	0.007	0.001	−1.8	11.2
1B1	1.404	−0.005	0.001	−1.8	12.0
1A2	1.418	−0.004	0.001	1.0	21.4
1B2	1.517	0.003	0.001	1.2	22.2
2A0	4.651	0.223	0.015		
2B0	5.731	0.298	0.017		
2A1	37.79	2.545	0.041	11.4	11.4
2B1	32.74	2.190	0.038	7.3	11.0
2A2	55.48	3.783	0.051	17.0	22.9
2B2	78.58	5.402	0.064	18.1	22.4
3A0	42.57	2.880	0.044		
3B0	42.66	2.885	0.044		
3A1	458.1	31.98	0.24	11.1	11.2
3B1	453.9	31.70	0.24	11.0	11.0
3A2	896.8	62.73	0.43	21.8	22.0
3B2	878.5	61.45	0.42	21.3	21.8

STD ^3H activity = 12.630 decays min^{-1} = 210.500 ± 1.100 Bq
Mean BKG (mean count rate of 1A1–1B2) = 1.473 ± 0.026 min^{-1}
Eff = 23.8%

Sample notations: 1A0, 1B0 = tap water before e.; 2A0, 2B0 = rain water before e.; 3A0, 3B0 = moisture before e.; 1A1, 1B1 = tap water after l.e.; 2A1, 2B1 = rain water after l.e.; 3A1, 3B1 = moisture after l.e.; 1A2, 1B2 = tap water after h.e.; 2A2, 2B2 = rain water after h.e.; 3A2, 3B2 = moisture after h.e.;

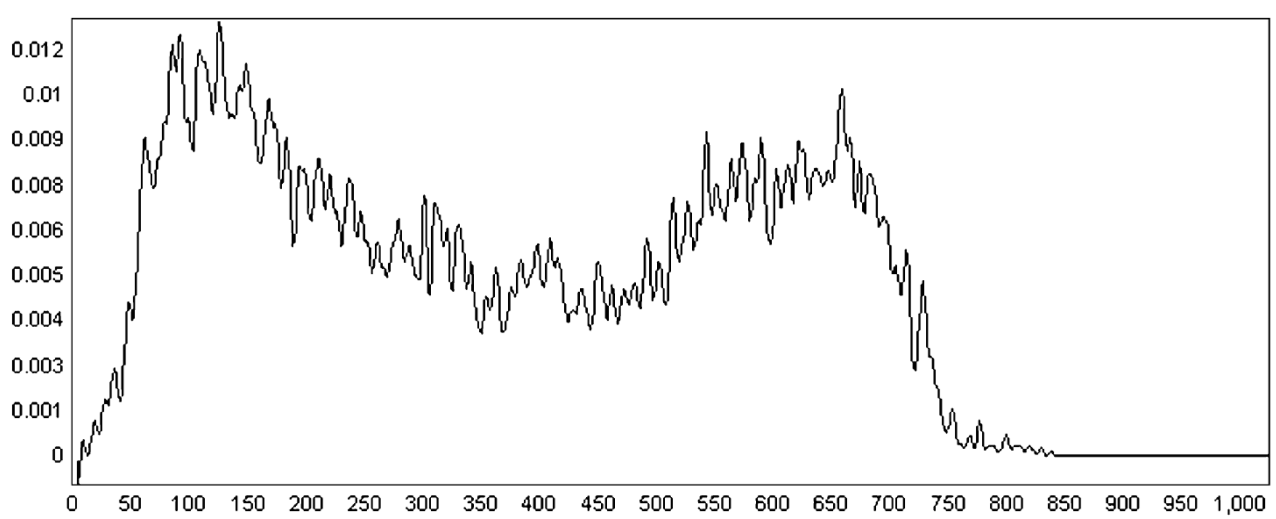

Fig. 3. Composite background spectrum of the samples 1A0, 1B0, 1A1, 1B1, 1A2 and 1B2.

$$\begin{aligned} \text{MDA or MDC/EFT} &= 0.95/11 \cong 0.08\ \text{Bq kg}^{-1} \text{ or} \\ &\cong 0.7\ \text{TU for l.e. and} \\ &= 0.95/22 = 0.04\ \text{Bq kg}^{-1} \text{ or} \\ &\leqslant 0.4\ \text{TU for h.e.,} \end{aligned}$$

Most of the major floodings occurred in central-eastern Europe are due to a typical Mediterranean meteorological pattern, the Genoa cyclone

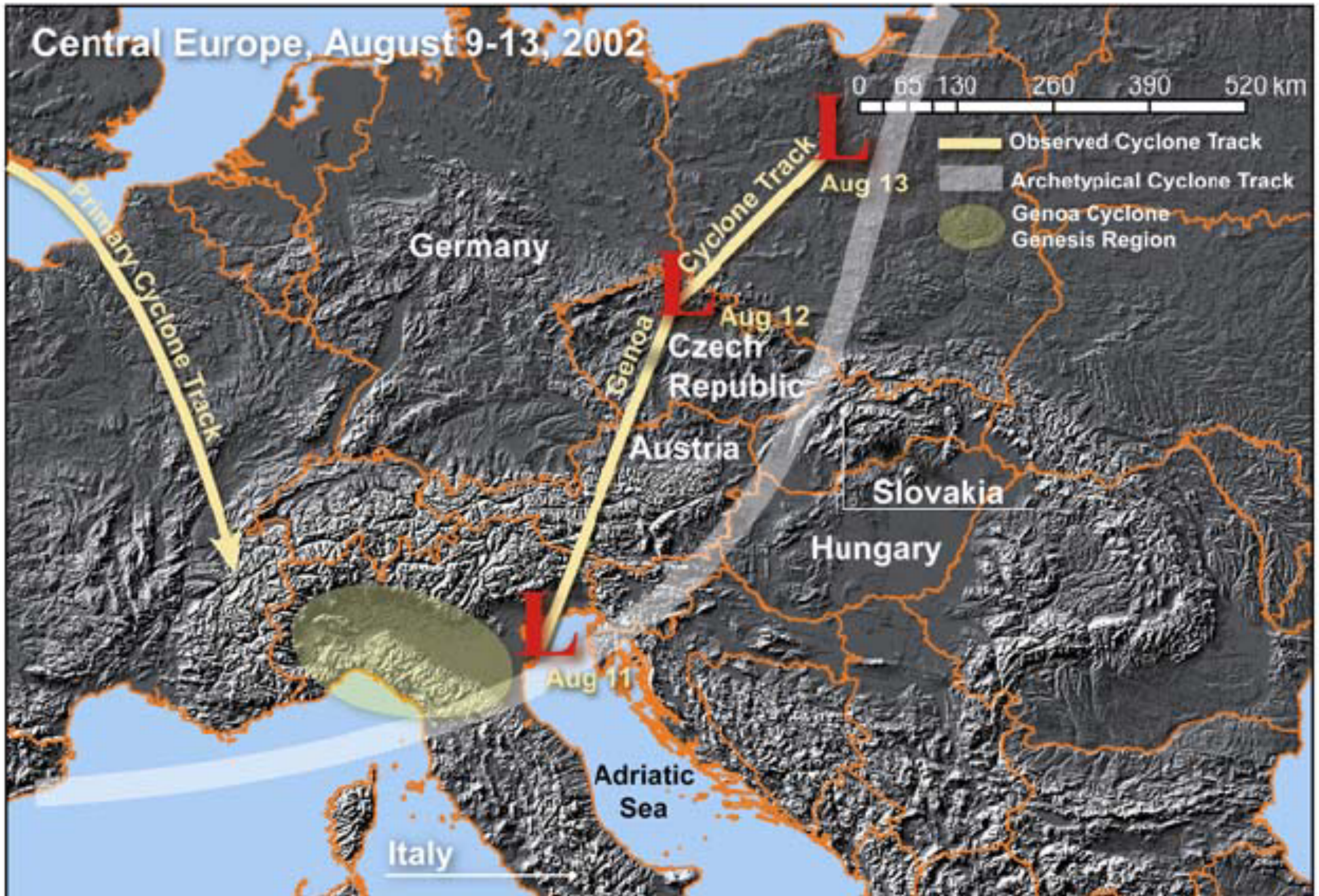

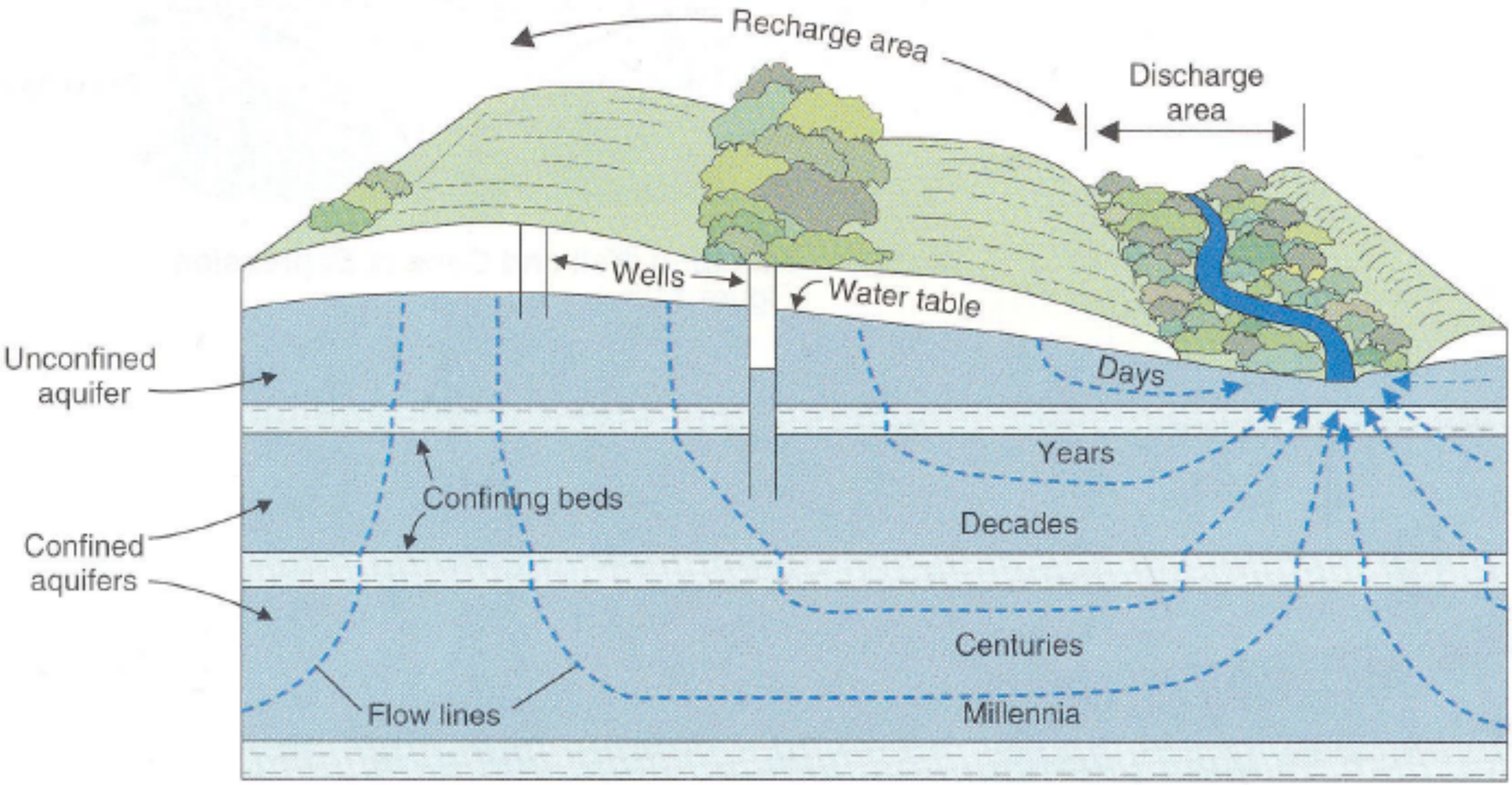
Recharge area
Discharge area
Wells
Water table
Unconfined aquifer
Confining beds
Confined aquifers
Flow lines
Days
Years
Decades
Centuries
Millennia

Oceanographic Processes in the Benthic Boundary Layer

The Benthic Boundary Layer is the dynamic interface between litosphere (seafloor) and ocean (seawater) where many physical, geochemical and biological processes occur playing an important role in environmental global change

Geohazards, carbon cycle, heat flow, life generation, climatic oceanography, are only some examples of local or global processes whose comprehension is today limited

Earthquakes produce short-term effects (landslides and tsunamis) that threaten the lives and economy of coastal communities, while outgassing of greenhouse gases impact long-term global climates

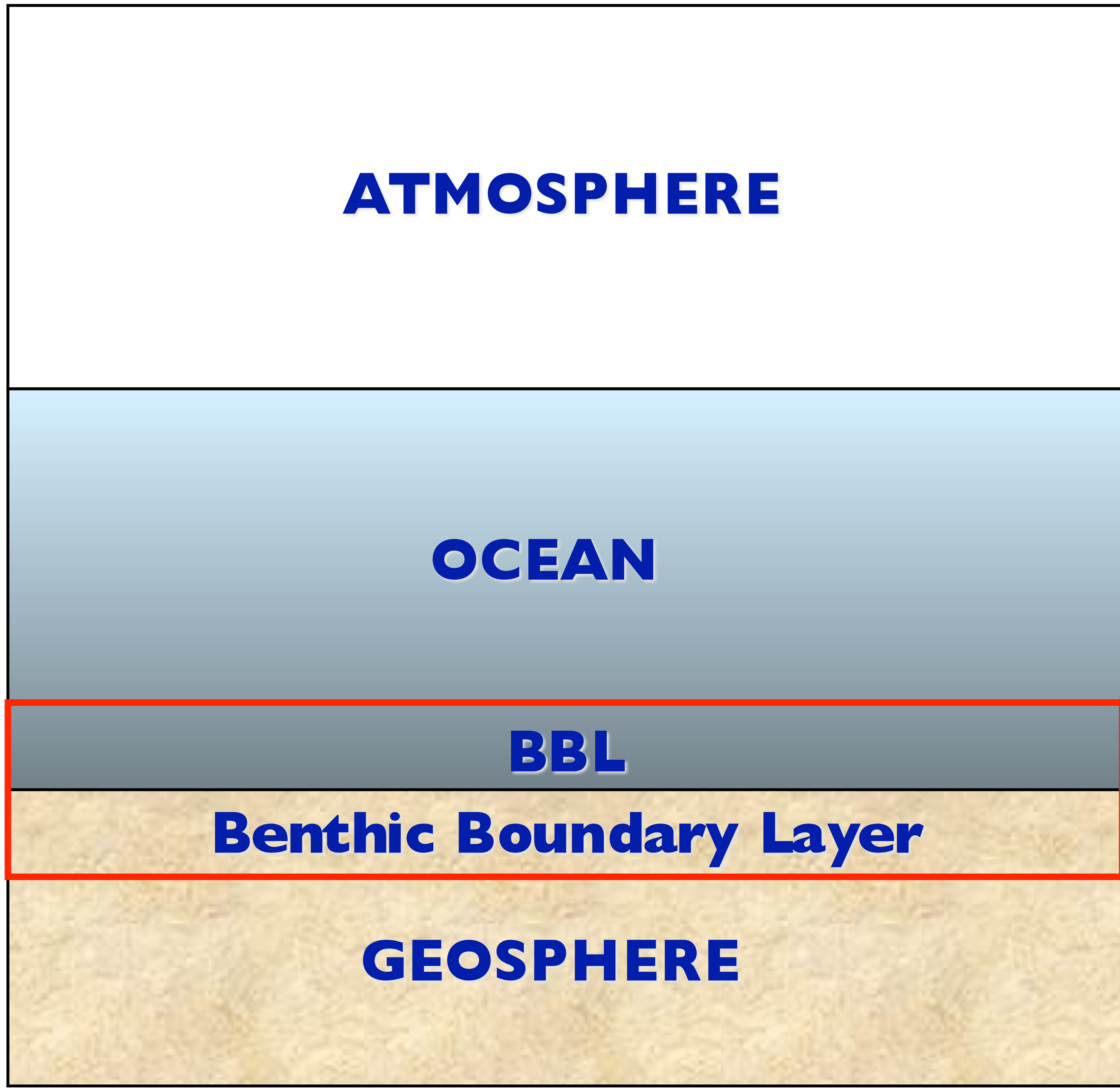

Key point:

AS OBSERVING SITE OF SOLID EARTH PROCESSES

-GEOPHYSICAL MONITORING-

(seismicity, geomagnetic field)

AS SITE OF PHYSICAL, GEOCHEMICAL AND BIOLOGICAL PROCESSES playing important roles in environmental global changes

(e.g., geohazards, carbon cycle, heat flow, life generation, climatic oceanography).

Plastino, W. et al., 2004, The Benthic Boundary Layer, IAEA

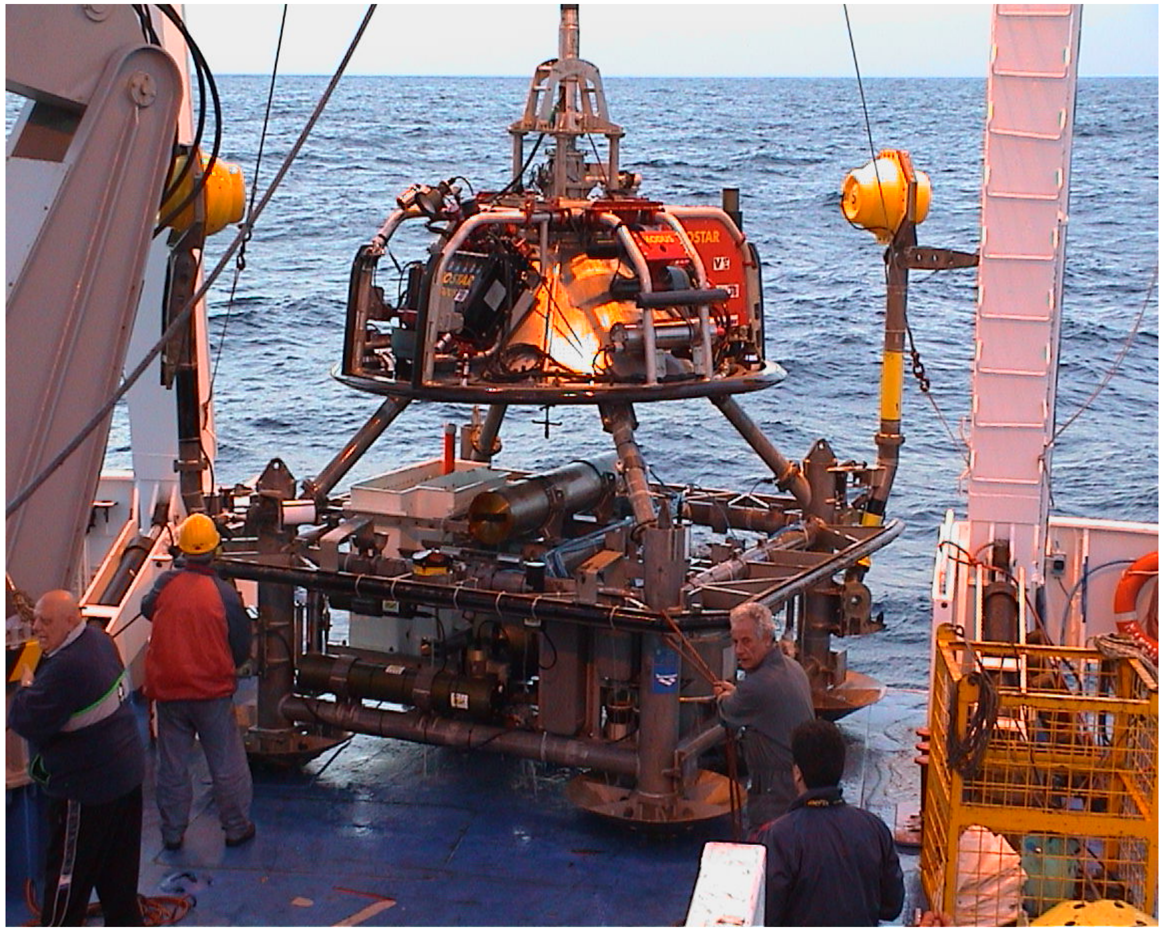

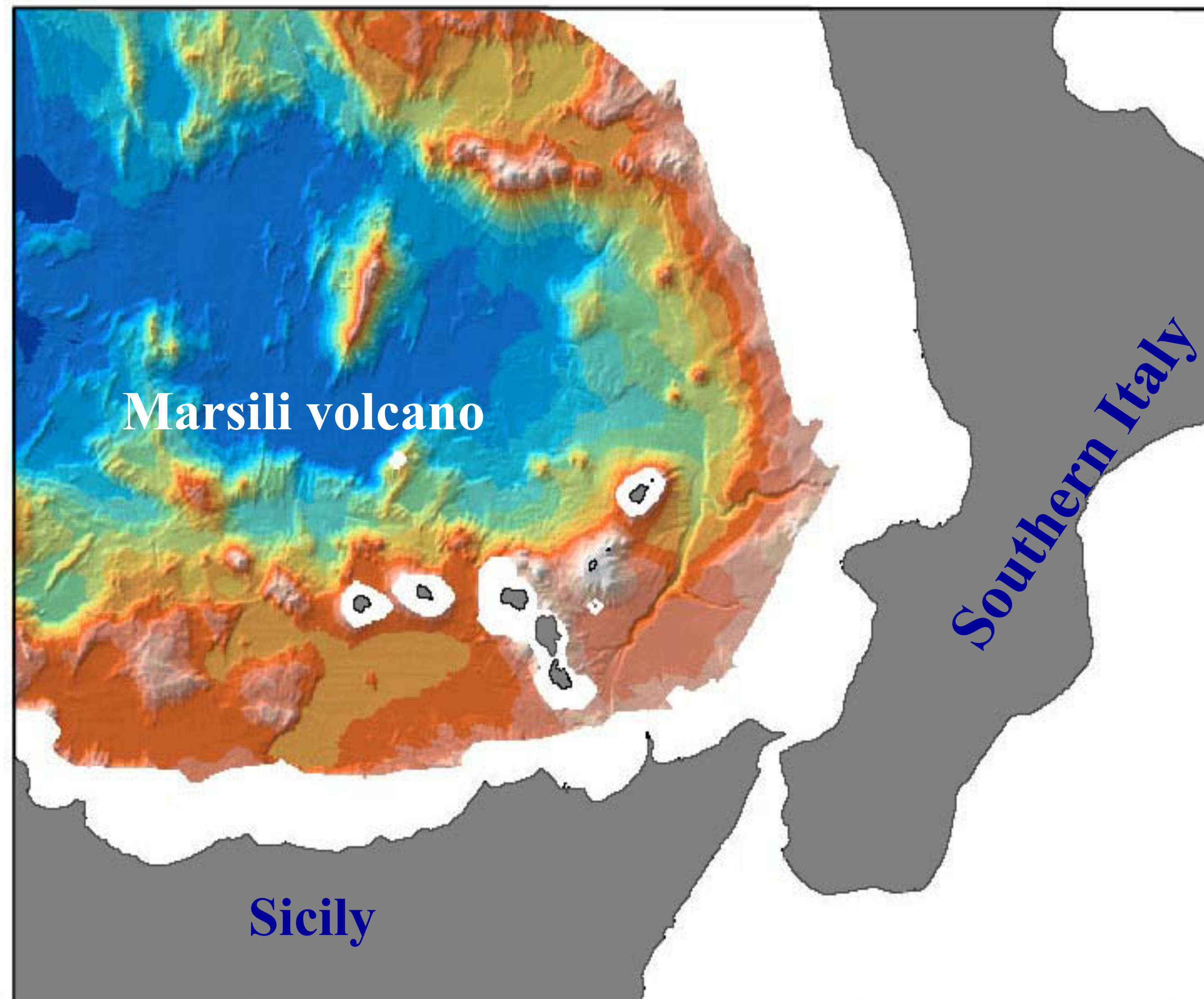
Marsili volcano
Southern Italy
Sicily

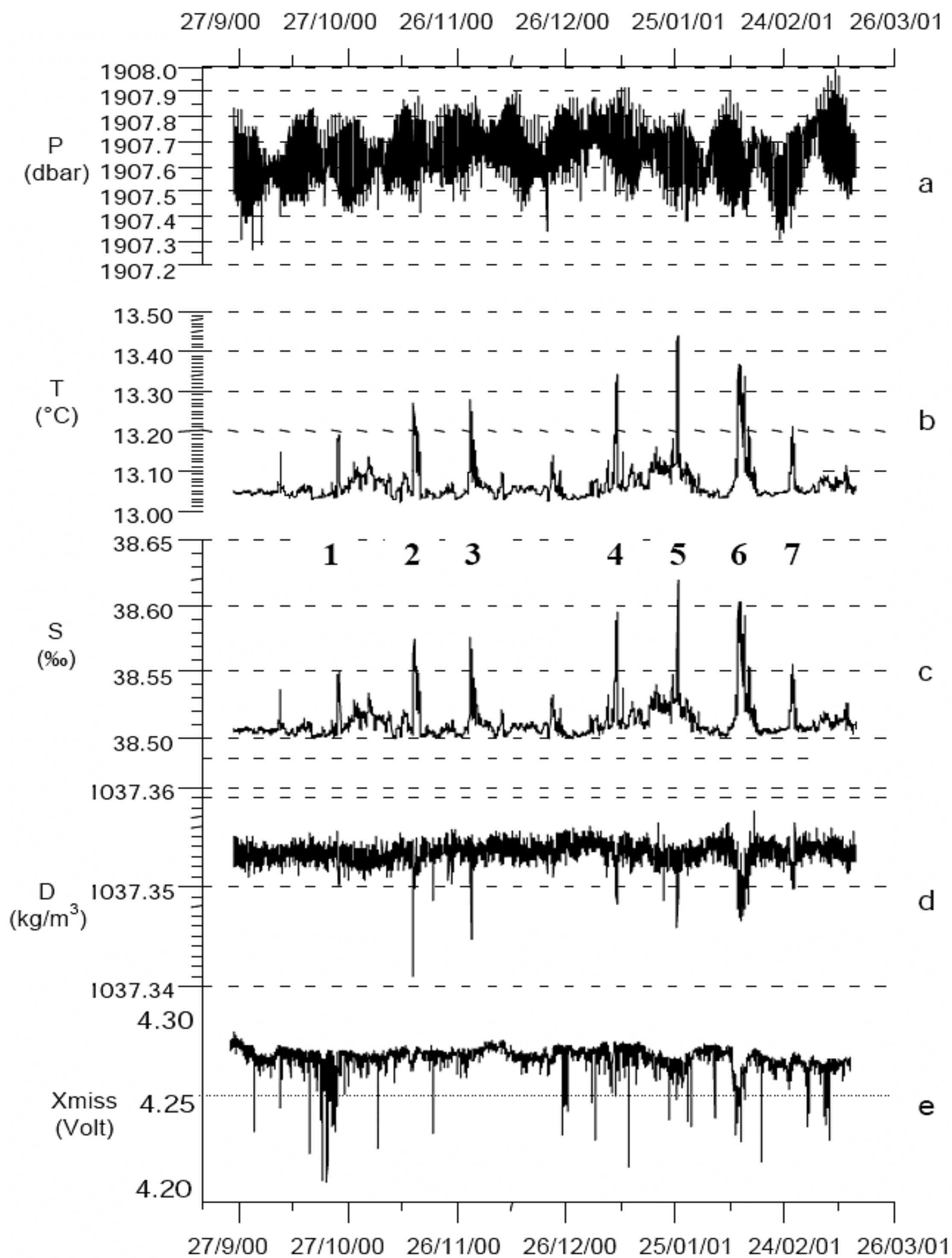

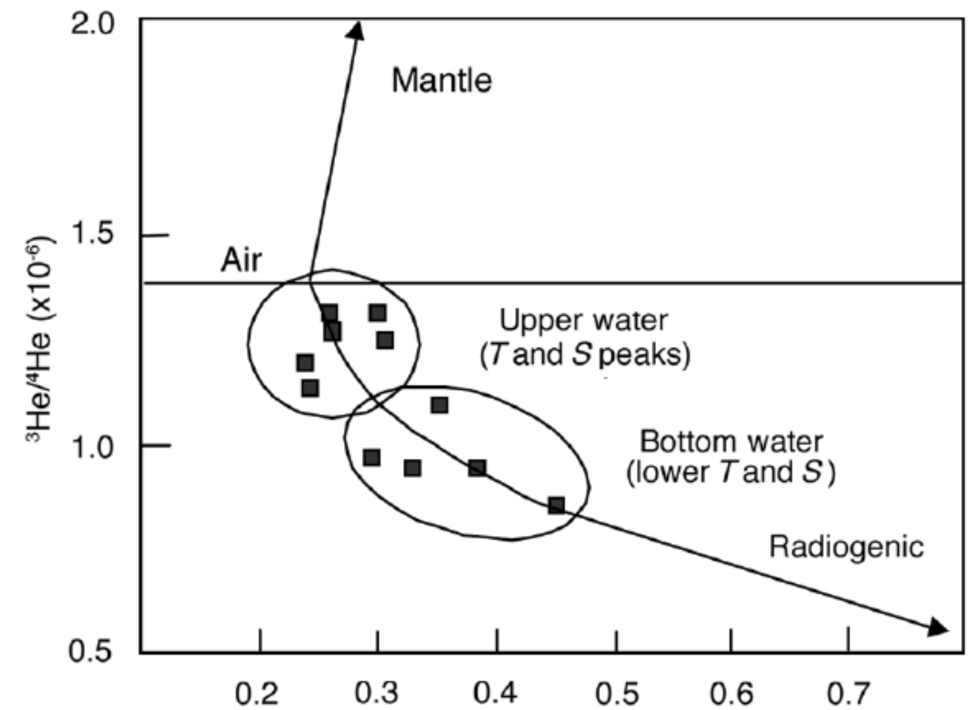

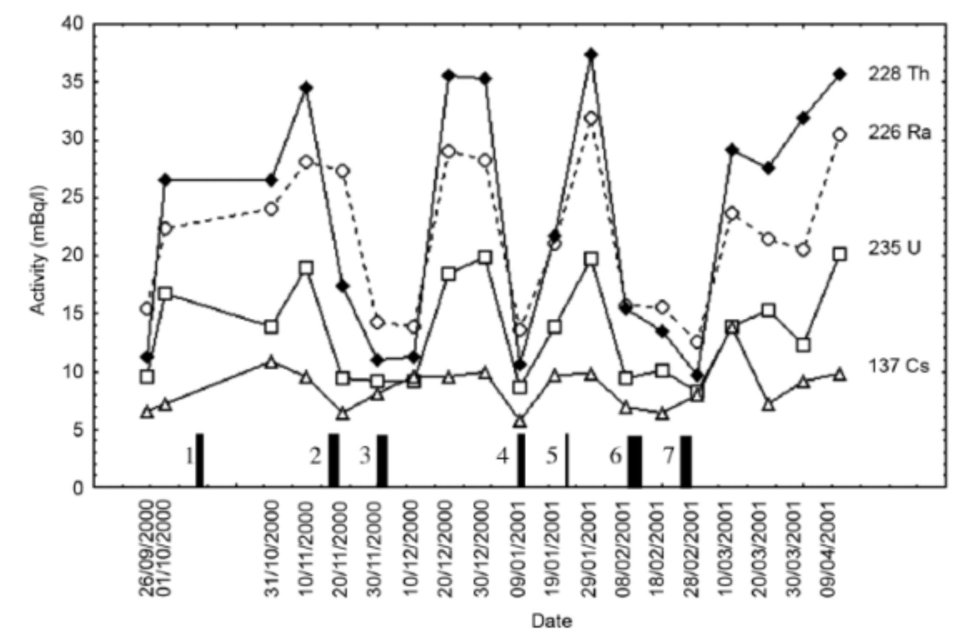

Plastino, W. et al., 2004, The Benthic Boundary Layer, IAEA

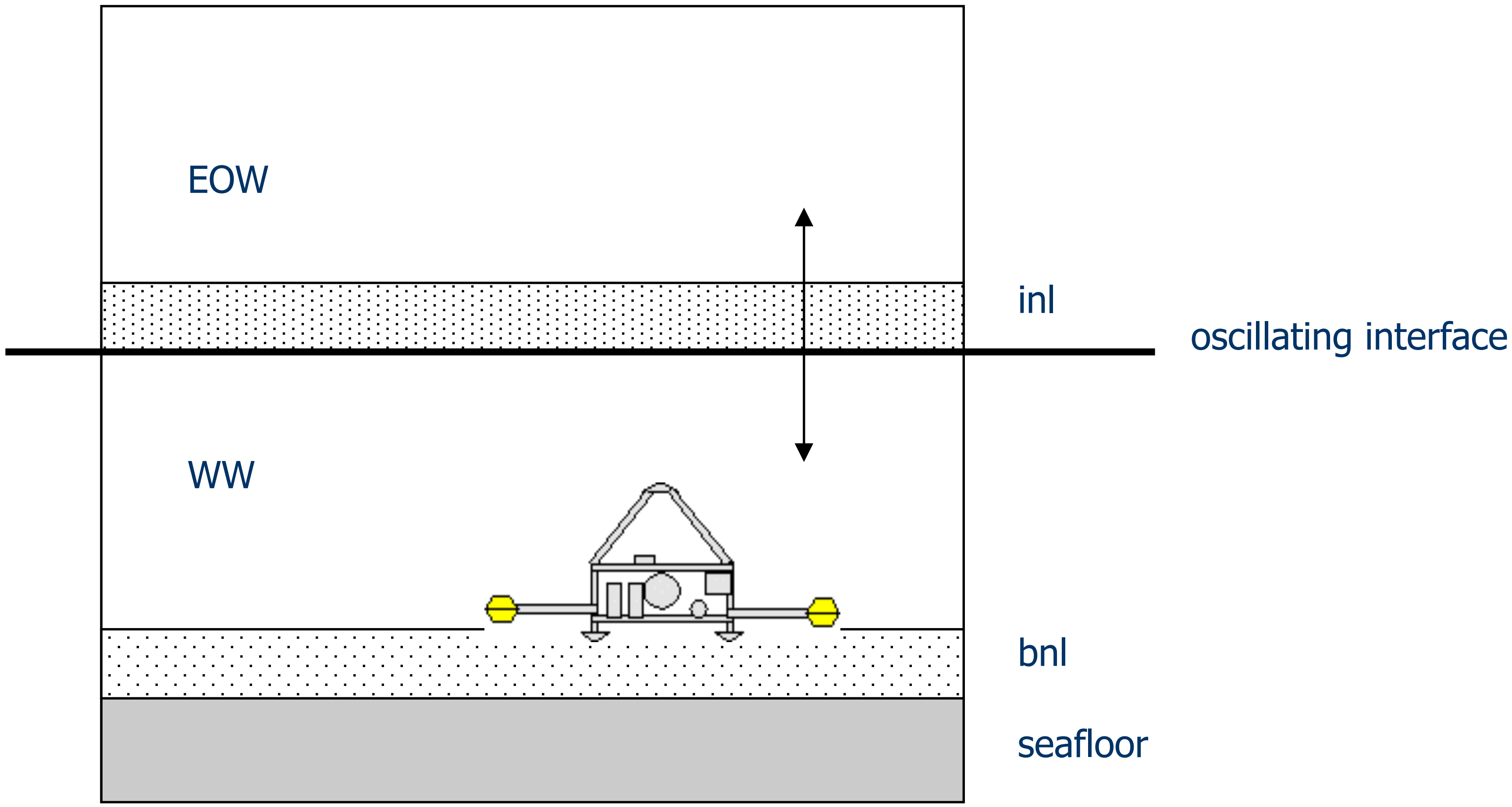

Sketch of the oscillating water mass interface in the BBL. EOW: Eastern Overflow Water; **WW**: Western Water; bnl: benthic nepheloyd layer; **inl**: intermediate nepheloyd layer. GEOSTAR detected WW for most of the time and events of EOW cascading, as suggested by T/S peaks, lower gas and radiogenic helium contents and lower radionuclide activities

Plastino, W. et al., 2004, The Benthic Boundary Layer, IAEA

Atmospheric Transport Modeling

Lagrangian particle models compute trajectories of a large number of so-called particles to describe the transport and diffusion of tracers in the atmosphere

The models simulate the long-range and mesoscale transport diffusion, dry and wet deposition, and radioactive decay of tracers released from point, line, area and volume sources

The models can be used backward in time to determine the potential source contributions for given receptors, or forward in time to simulate the dispersion of tracers from their sources

The most suitable resolution of the input data is equivalent to the characteristic scales in space and time (scale: typical orders of magnitude) considered to be relevant for the ATM output

– Spatial and temporal scales of physical processes taking place in the atmosphere are closely linked together

– A spatial grid resolution of 1° (≈100 km) fits well to a temporal resolution of 6 hours

– ($2\Delta x$ = 200 km corresponds with $\Delta t = 2\times10^4$ s, i.e. 5.6 hours)

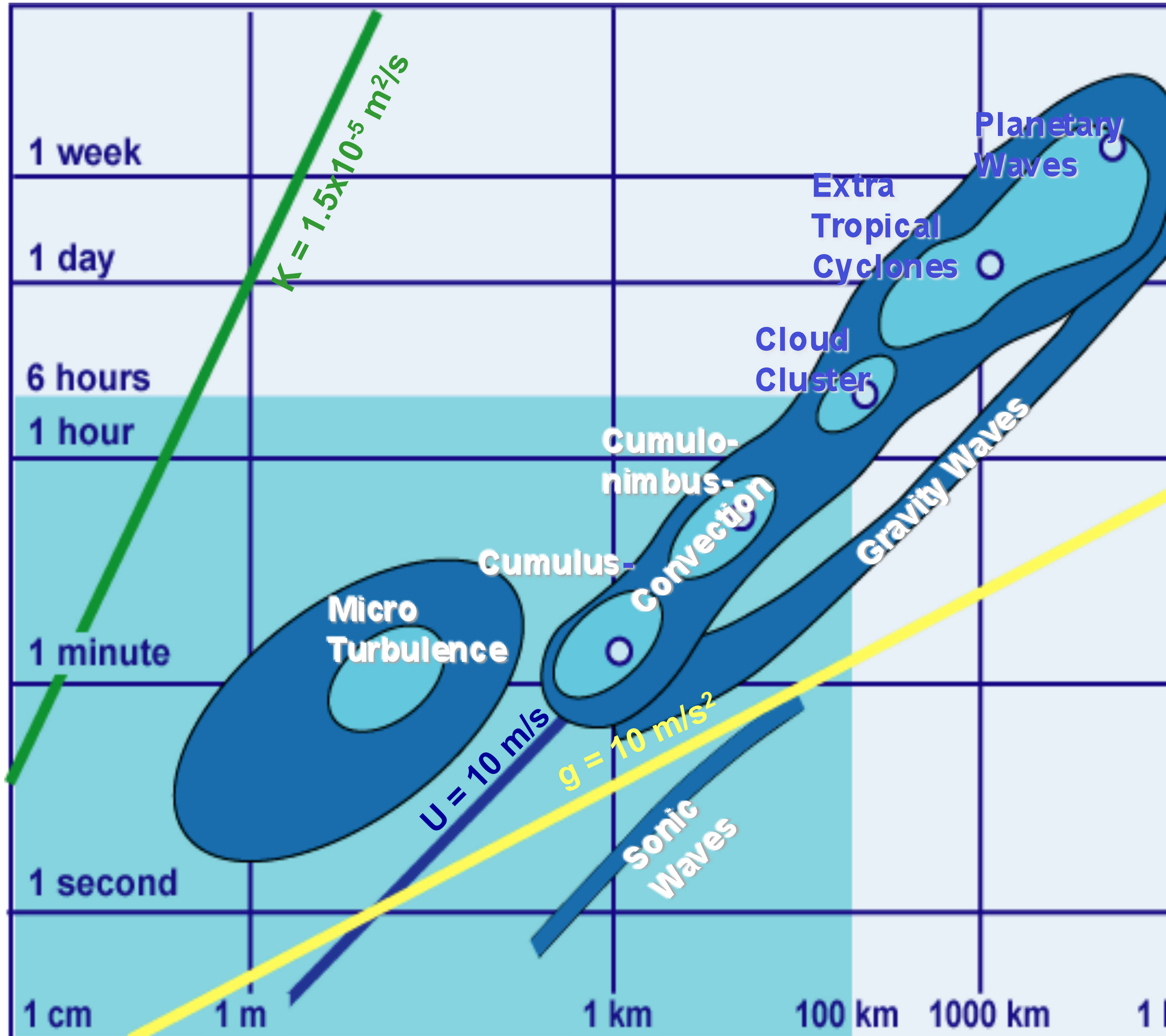

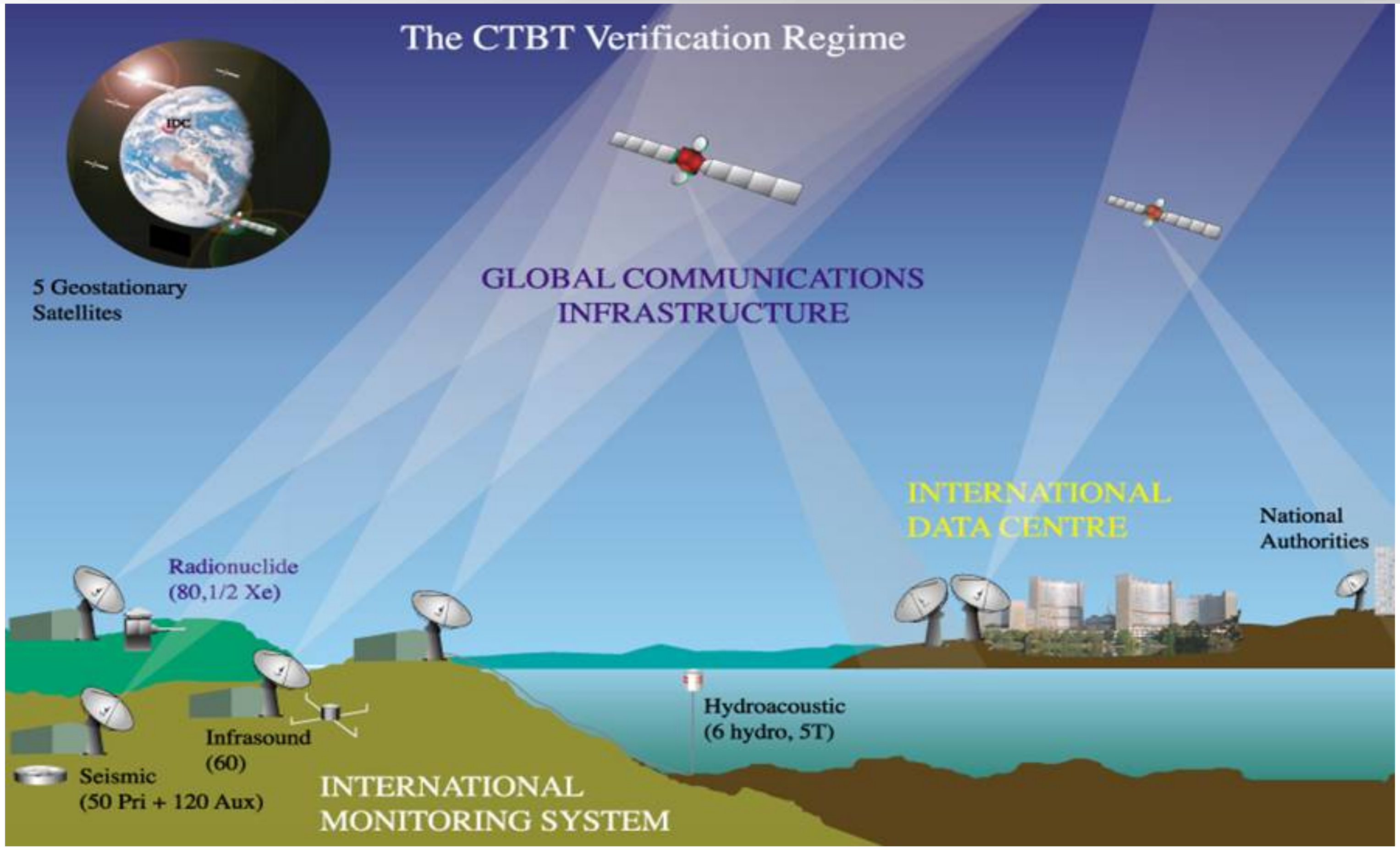
The CTBT Verification Regime
5 Geostationary Satellites
GLOBAL COMMUNICATIONS INFRASTRUCTURE
INTERNATIONAL DATA CENTRE
National Authorities
Radionuclide (80,1/2 Xe)
Hydroacoustic (6 hydro, 5T)
Infrasound (60)
Seismic (50 Pri + 120 Aux)
INTERNATIONAL MONITORING SYSTEM

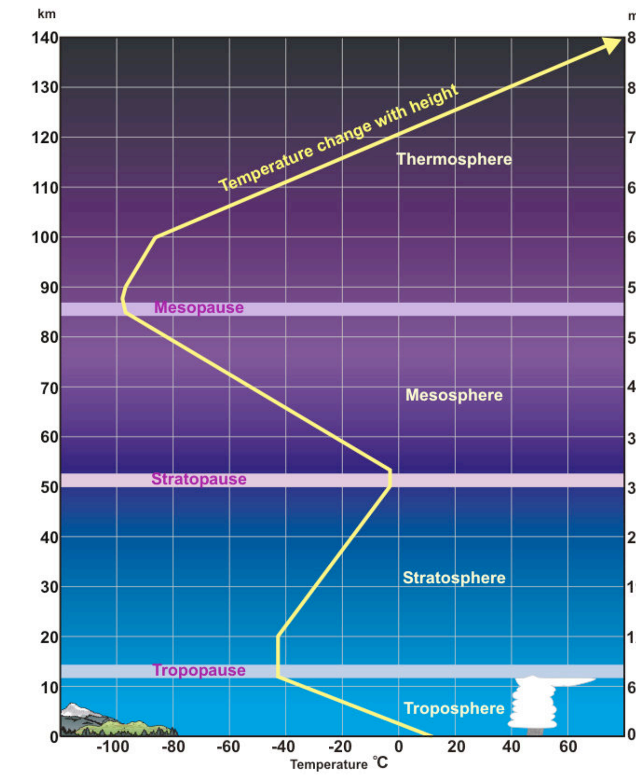
km
140
130
120
110
100
90
80
70
60
50
40
30
20
10
0
Temperature change with height
Thermosphere
Mesopause
Mesosphere
Stratopause
Stratosphere
Tropopause
Troposphere
-100
-80
-60
-40
-20
0
20
40
60
Temperature °C

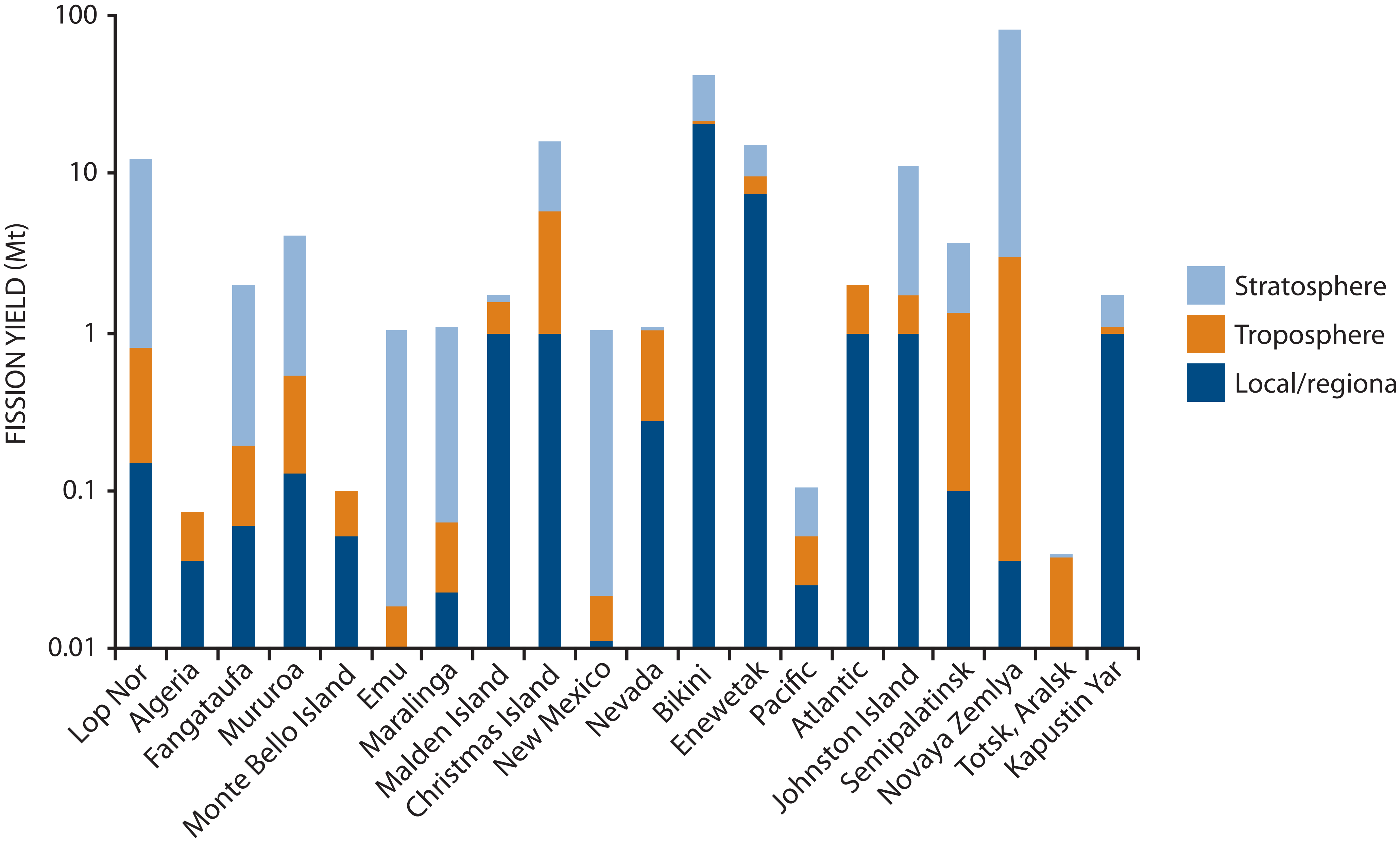
FISSION YIELD (Mt)
100
10
1
0.1
0.01
Lop Nor
Algeria
Fangataufa
Mururoa
Monte Bello Island
Emu
Maralinga
Malden Island
Christmas Island
New Mexico
Nevada
Bikini
Enewetak
Pacific
Atlantic
Johnston Island
Semipalatinsk
Novaya Zemlya
Totsk, Aralsk
Kapustin Yar
Stratosphere
Troposphere
Local/regional

Type	*United States*	*Former Soviet Union*	*United Kingdom*	*France*	*China*	*India*	*Pakistan*	*Democratic People's Republic of Korea*	*Total*
Atmospheric nuclear tests									
Airburst	13	8	9	0	0	0	0	0	30
Air drop	52	174	1	3	16	0	0	0	246
Balloon	24	0	1	34	0	0	0	0	59
Tower/surface	66	34	10	4	6	0	0	0	120
Barge	35	0	0	4	0	0	0	0	39
Underwater	5	3	0	0	0	0	0	0	8
Total	195	219	21	45	22	0	0	0	502
Fission (Mt)	82	85	4	6	12	0	0	0	189
Fusion (Mt)	72	162	4	4	9	0	0	0	251
Underground nuclear tests									
Number of tests	908	750	24	160	22	6	6	1	1 877
Yield (Mt)	46	38	2	3	1				90
Total atmospheric and underground tests									
Number of tests	1 103	969	45	205	44	6	6	1	2 379
Yield (Mt)	200	285	10	13	22				530

During fission of uranium or plutonium in a nuclear reactor, thermal (slow) neutrons are used, whereas during a nuclear explosion the fission is induced by fast neutrons. The full fission sequence in a device is finished within a microsecond.

There is little time for complex activation build-up in a nuclear explosion, whereas there is sufficient time for production of many activation products in a nuclear reactor

These differences produce different radionuclide abundances. Since a nuclear blast produces different radionuclide abundances, nuclide ratios may be used for source identification

Fission yield in % for several nuclear explosion relevant nuclides
(Fission yield is a function of the fissioning nuclide and the incident neutron energy)

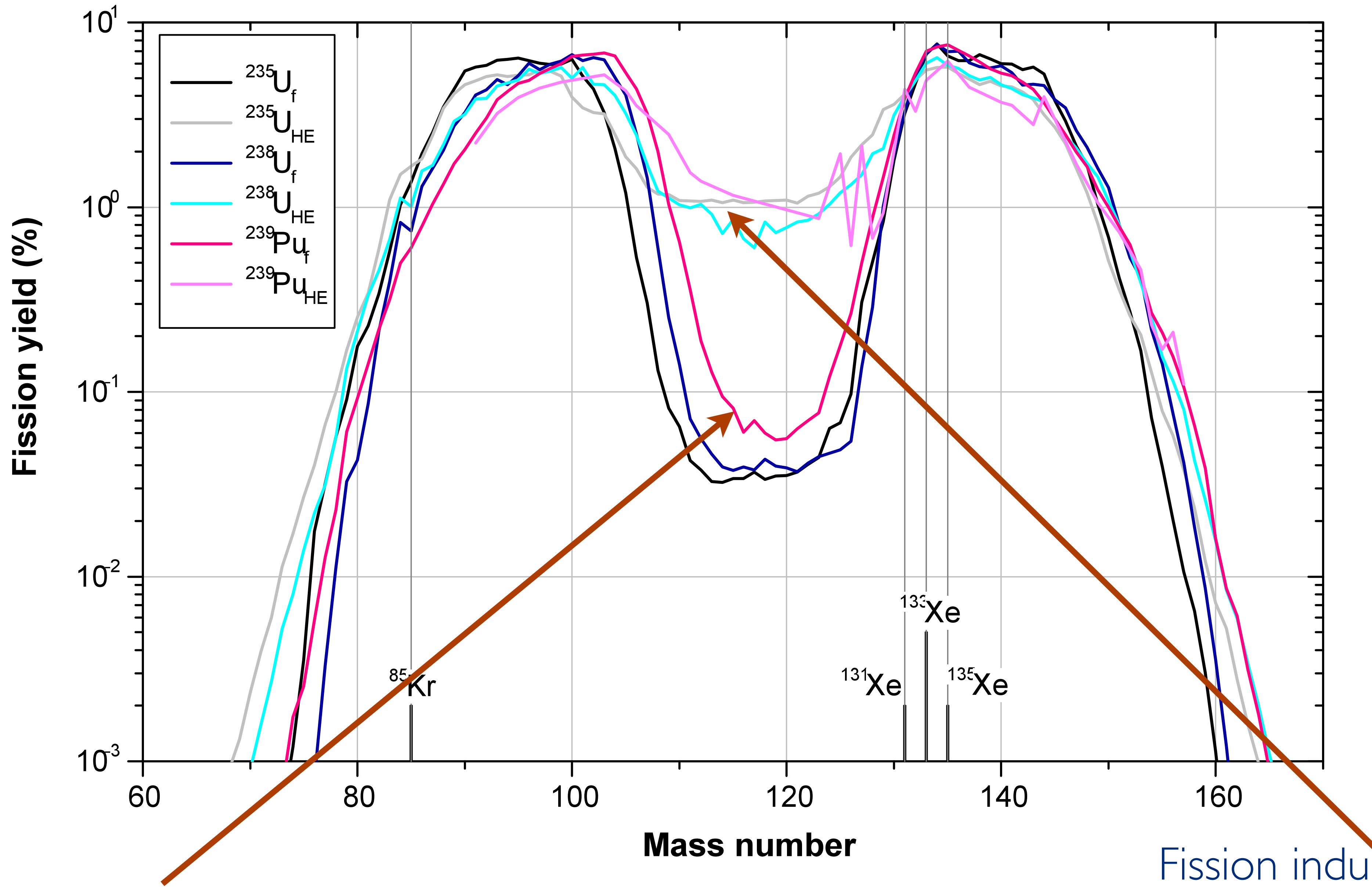

Fission induced by thermal (fission spectrum) neutrons

Fission induced by high energy neutrons (14.7 MeV)

Fission Product	Half-life	Time unit	$^{235}U_f$	$^{235}U_{he}$	$^{238}U_f$	$^{238}U_{he}$	$^{239}Pu_f$	$^{239}Pu_{he}$
^{131m}Xe	11.934	d	0.05	0.06	0.05	0.06	0.05	0.07
^{133m}Xe	2.19	d	0.19	0.29	0.19	0.18	0.24	0.42
^{133}Xe	5.243	d	6.72	5.53	6.76	6.02	6.97	4.86
^{135}Xe	9.14	h	6.6	5.67	6.97	5.84	7.54	6.18

Cumulative fission yields in % for six fission modes relevant to nuclear explosions, induced by fission spectrum neutrons (f) and high energy neutrons (14.7 MeV) (he)

^{133}Xe has high production rates and a not too short half-life. Therefore this xenon isotope is the one most observed in environmental samples

Atmospheric Nuclear Tests

- Infrasonic waves
- Radionuclides: particulates & gases
- Possible seismic/hydro-acoustic coupling
- Noise sources: natural and cultural background, meteors, volcanoes, weather, air/spacecraft

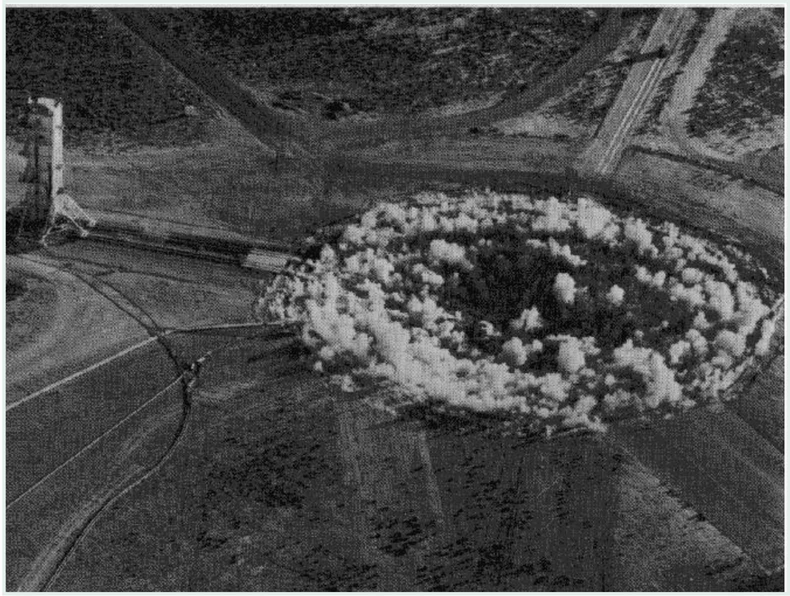

Underground Nuclear Tests

- Seismic waves
- Radionuclides: vented gases
- Possible hydro-acoustic/infra-sound coupling
- Noise sources: natural and cultural background, earthquakes, volcanoes, chemical explosions

Underwater Nuclear Tests

- Hydroacoustic waves
- Radionuclides: vented gases
- Possible seismic/infra-sound coupling
- Noise sources: natural and cultural background, earthquakes, volcanoes, chemical explosions, whales


Suomi Finland
Sverige Sweden
Norge Norway
Iceland
Россия Russia
United Kingdom
Polska Poland
Deutschland Germany
France
Україна Ukraine
España Spain
Italia Italy
Türkiye Turkey
Kazakhstan
Mongolia
Canada
United States
North Atlantic Ocean
North Pacific Ocean
México
Algeria
Libya
مصر Egypt
Saudi Arabia
Iraq
Iran
Afghanistan
Pakistan
China
中国
India
S Korea
Japan
Thailand
Mauritania
Mali
Niger
Chad
Sudan
Nigeria
Ethiopia
Venezuela
Colombia
DR Congo
Kenya
Tanzania
Brasil Brazil
Peru
Bolivia
Angola
Namibia
Botswana
Madagascar
South Africa
Chile
Argentina
South Pacific Ocean
South Atlantic Ocean
Indian Ocean
Indonesia
Papua New Guinea
Australia
New Zealand
Southern Ocean
POWERED BY Google
Map data ©2011 Geocentre Consulting, MapLink, Tele Atlas, Whereis(R), Sensis Pty Ltd – Terms of Use

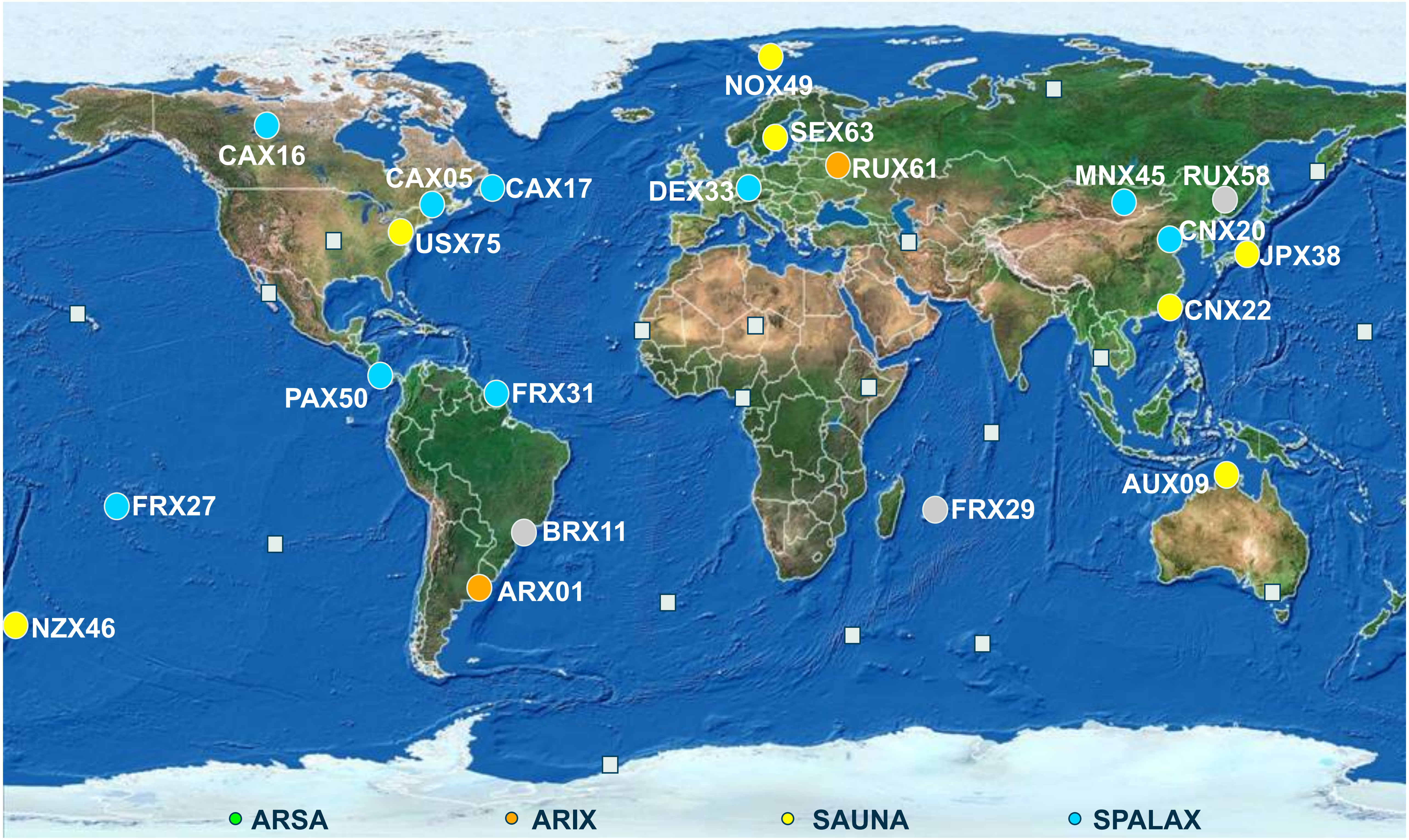
NOX49
SEX63
RUX61
CAX16
CAX05
CAX17
DEX33
MNX45
RUX58
CNX20
JPX38
USX75
CNX22
PAX50
FRX31
AUX09
FRX27
FRX29
BRX11
ARX01
NZX46
ARSA
ARIX
SAUNA
SPALAX

- Backward in time integration
- Release of n particles/h across 24h-sampling period
- Store surface level „retro-plume“ concentration (=SRS) every 3 hours

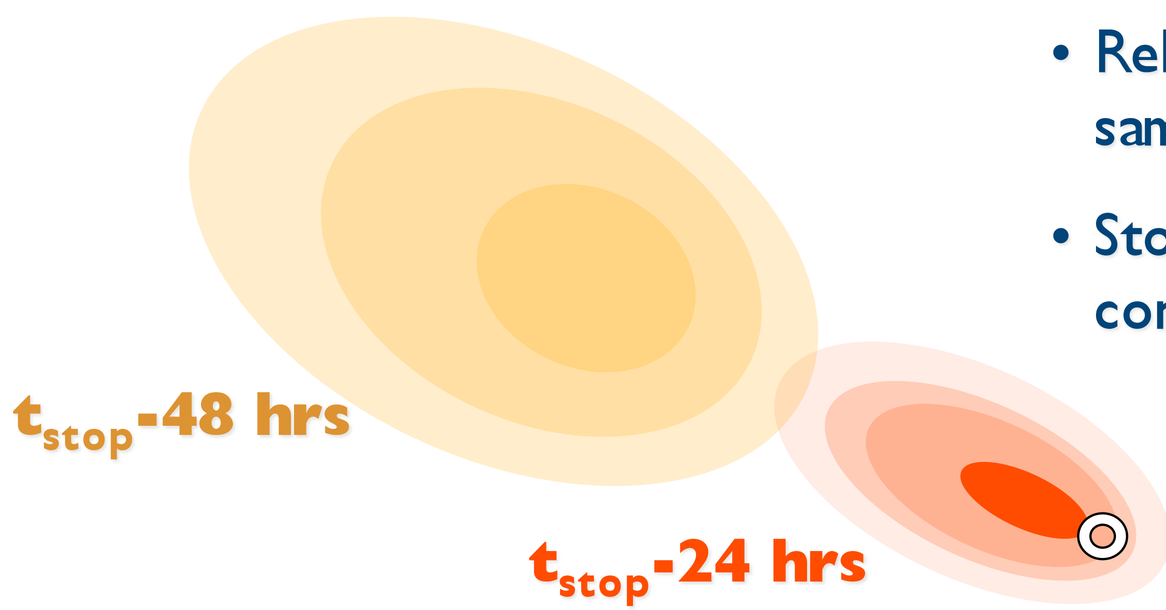

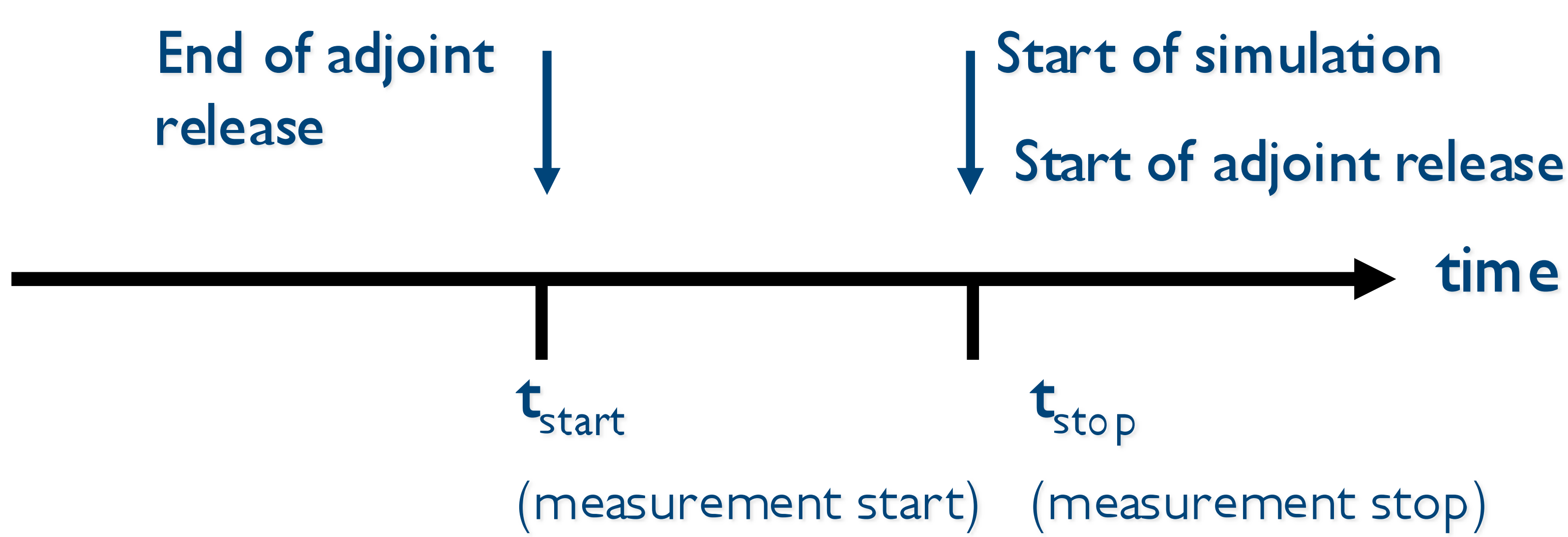

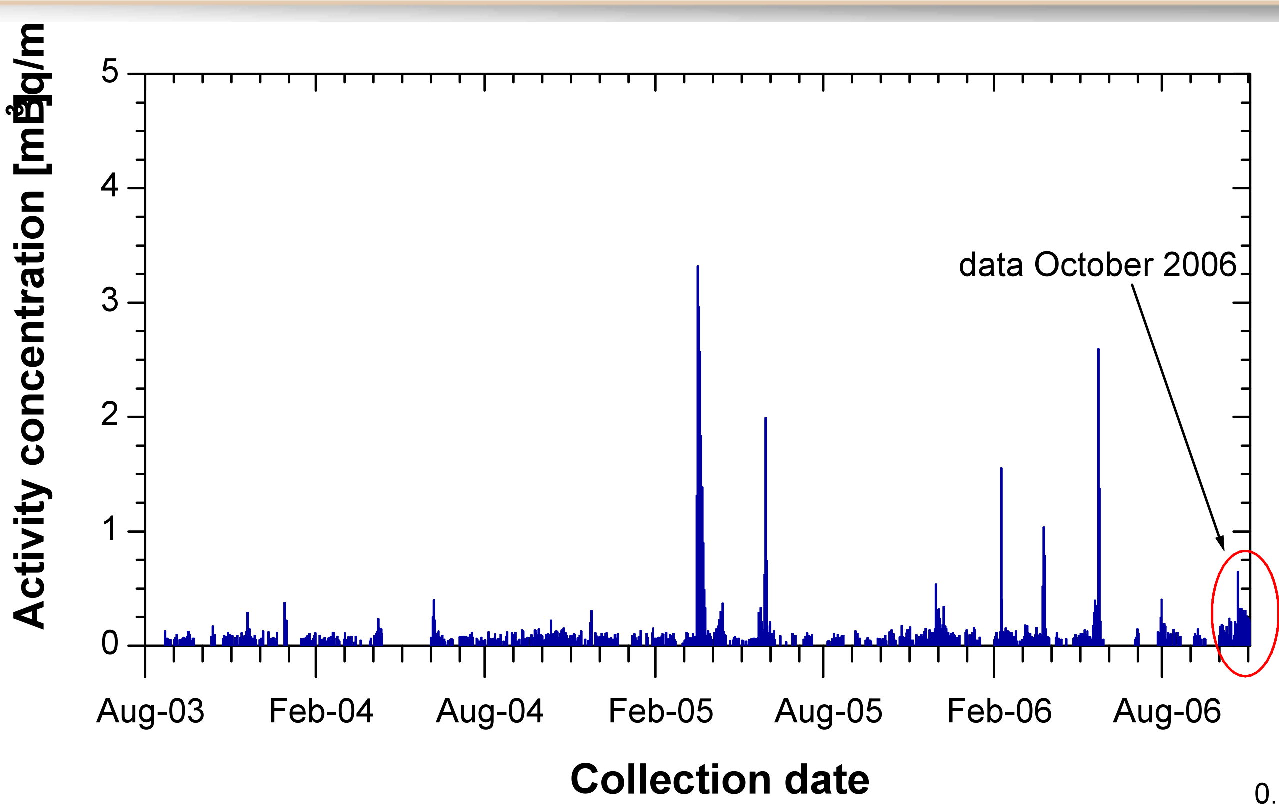
Activity concentration [mBq/m3]
data October 2006
Aug-03
Feb-04
Aug-04
Feb-05
Aug-05
Feb-06
Aug-06
Collection date

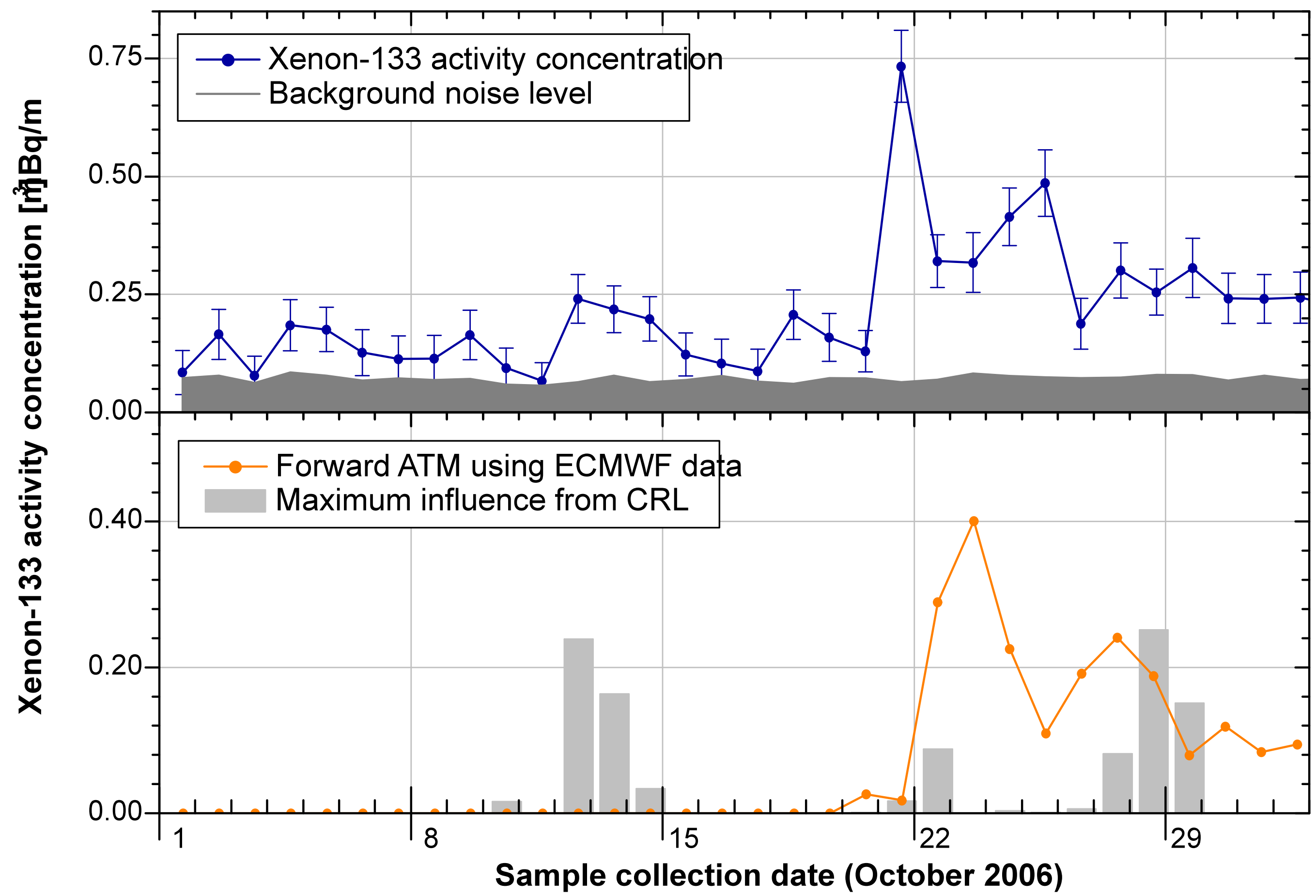
Xenon-133 activity concentration
Background noise level
Forward ATM using ECMWF data
Maximum influence from CRL
Xenon-133 activity concentration [mBq/m3]
Sample collection date (October 2006)

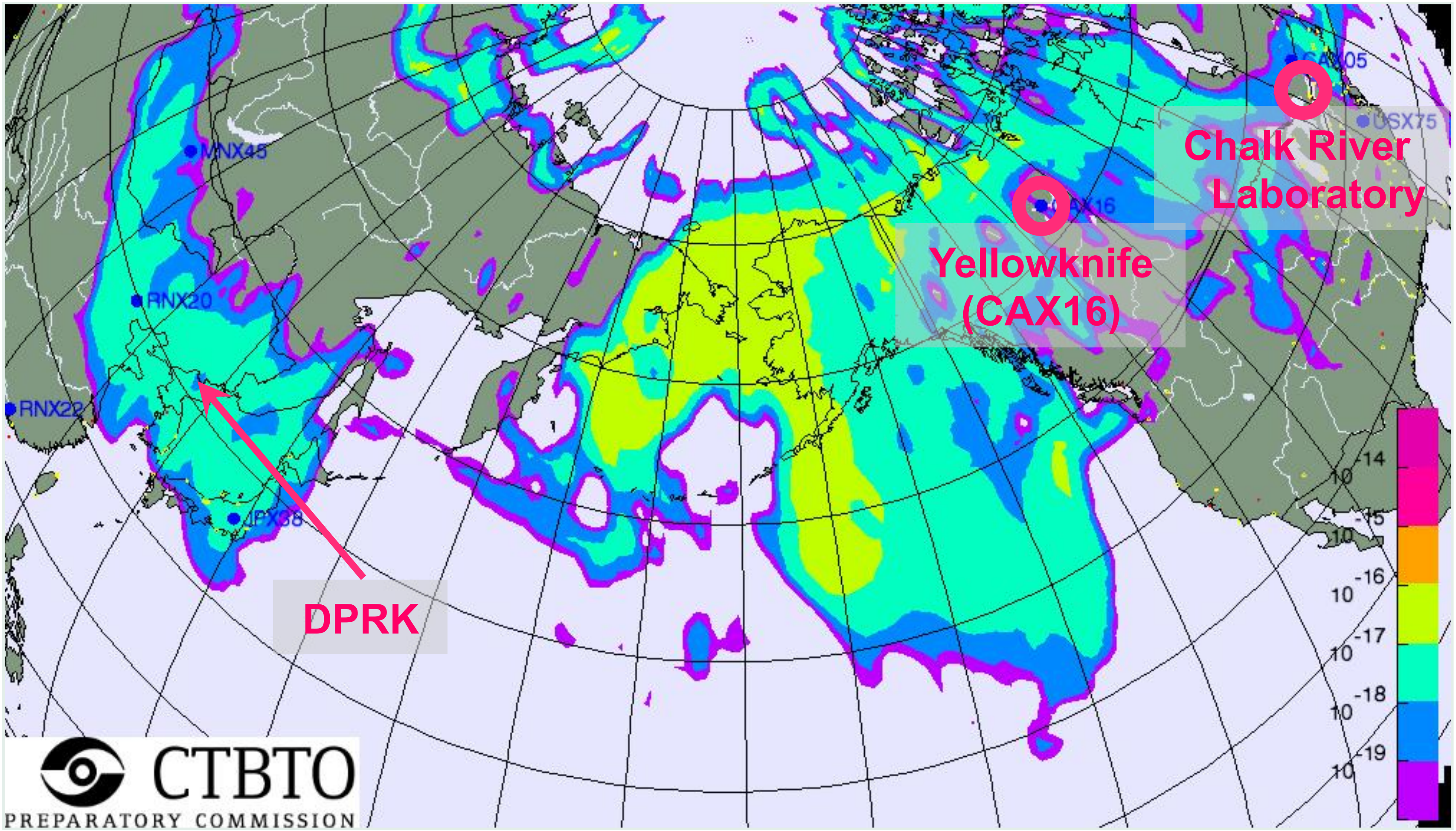

Field of Regard for the 21 October sample in Yellowknife referring to a ground level atmospheric injection of ^{133}Xe between 00 and 03 UTC on 9 October, 2006

The scale gives the dilution factor such that an emission of 10^{15} Bq in for example a green-blue area is consistent with a detection in Yellowknife of 0.1 – 1 mBq/m^3.

This shows that Yellowknife is very sensitive towards East Asia including the DPRK, but not towards a potential alternate ^{133}Xe source, the Chalk River Laboratory in Ontario, Canada

Pure Appl. Geophys.

DOI 10.1007/s00024-009-0030-3

Pure and Applied Geophysics

Radioxenon Time Series and Meteorological Pattern Analysis for CTBT Event Categorisation

Wolfango Plastino,[1,2] Romano Plenteda,[3] George Azzari,[1] Andreas Becker,[3] Paul R. J. Saey,[3] and Gerhard Wotawa[3]

Abstract—Understanding radioxenon time series and being able to distinguish anthropogenic from nuclear explosion signals are fundamental issues for the technical verification of the Comprehensive Nuclear-Test-Ban Treaty. Every radioxenon event categorisation methodology must take into account the background at each monitoring site to uncover anomalies that may be related to nuclear explosions. Feedback induced by local meteorological patterns on the equipment and on the sampling procedures has been included in the analysis to improve a possible event categorisation scheme. The occurrence probability of radioxenon outliers has been estimated with a time series approach characterising and avoiding the influence of local meteorological patterns. A power spectrum estimator for radioxenon and meteorological time series was

and infrasound), two radionuclide technologies: global monitoring of radioactive aerosols and of radioactive noble gases. Atmospheric transport modelling is part of the system to establish a source geolocation capability.

The knowledge of the activity concentration and isotopic composition of radioactive noble gases in the atmosphere indicates the nuclear processes governing their formation. Furthermore, by use of atmospheric transport modelling (ATM), knowledge of possible

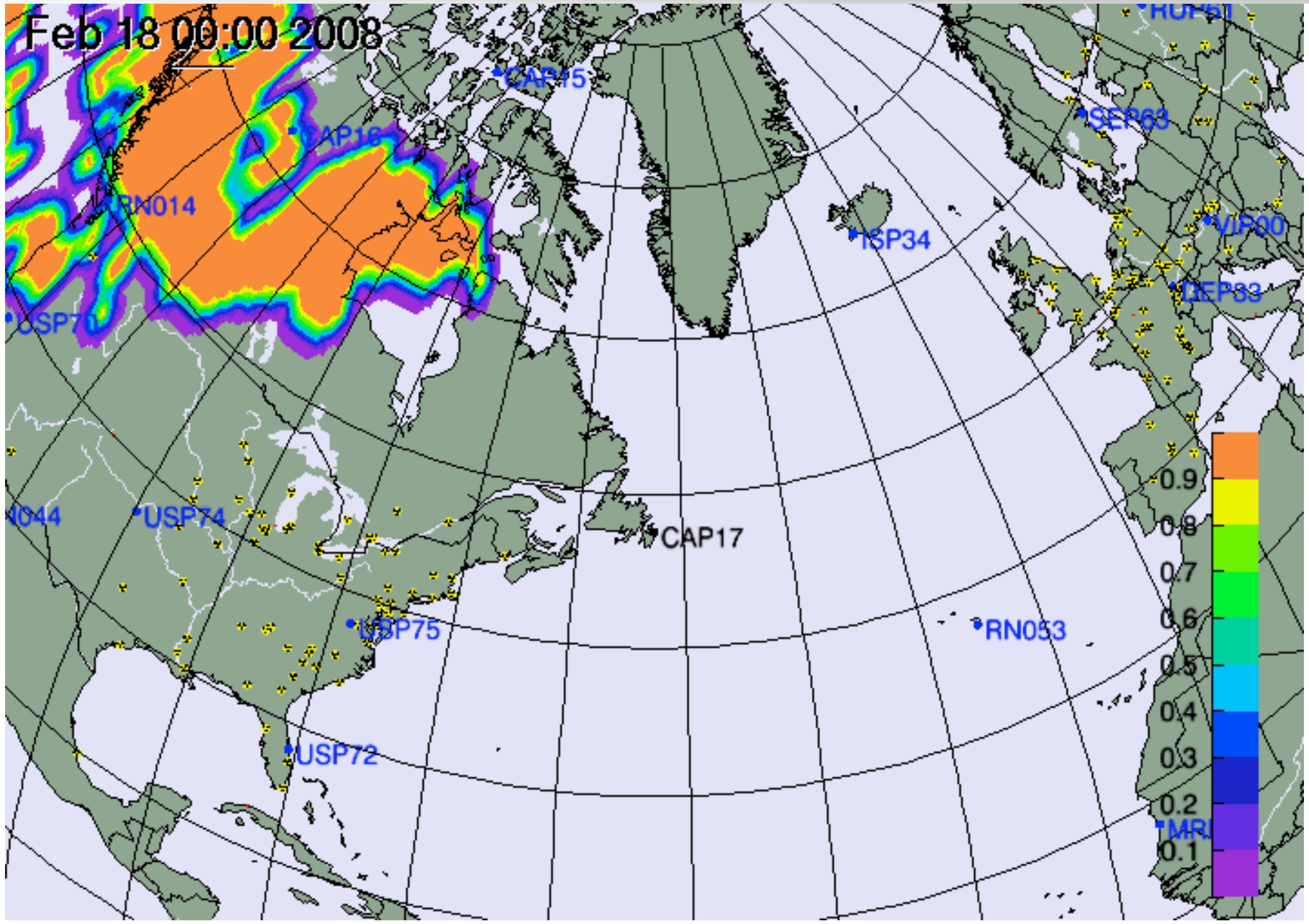
Feb 18 00:00 2008
CAP15
CAP16
RN014
USP70
SEP63
ISP34
VIP00
DEP33
USP74
USP75
USP72
CAP17
RN053
0.9
0.8
0.7
0.6
0.5
0.4
0.3
0.2
0.1

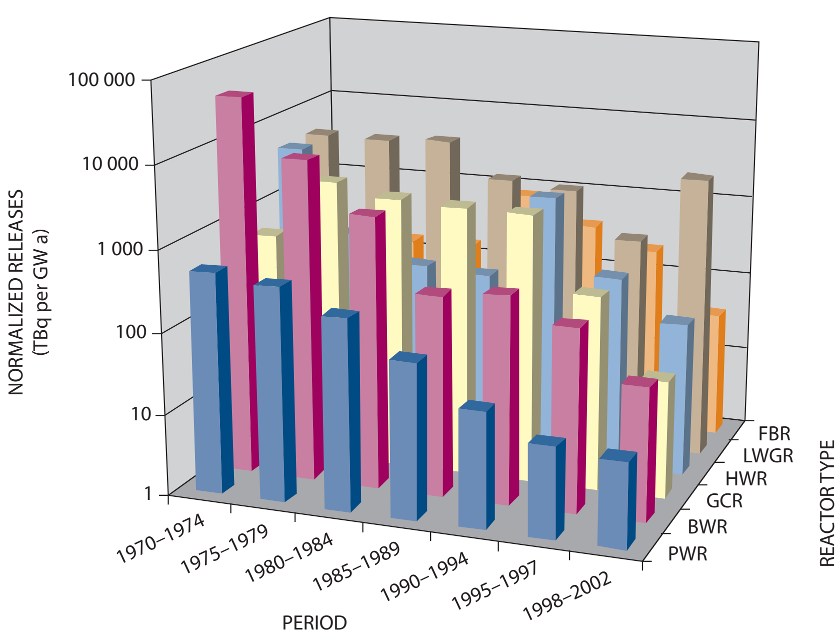
NORMALIZED RELEASES
(TBq per GW a)
100 000
10 000
1 000
100
10
1
1970–1974
1975–1979
1980–1984
1985–1989
1990–1994
1995–1997
1998–2002
PERIOD
FBR
LWGR
HWR
GCR
BWR
PWR
REACTOR TYPE

© UNSCEAR

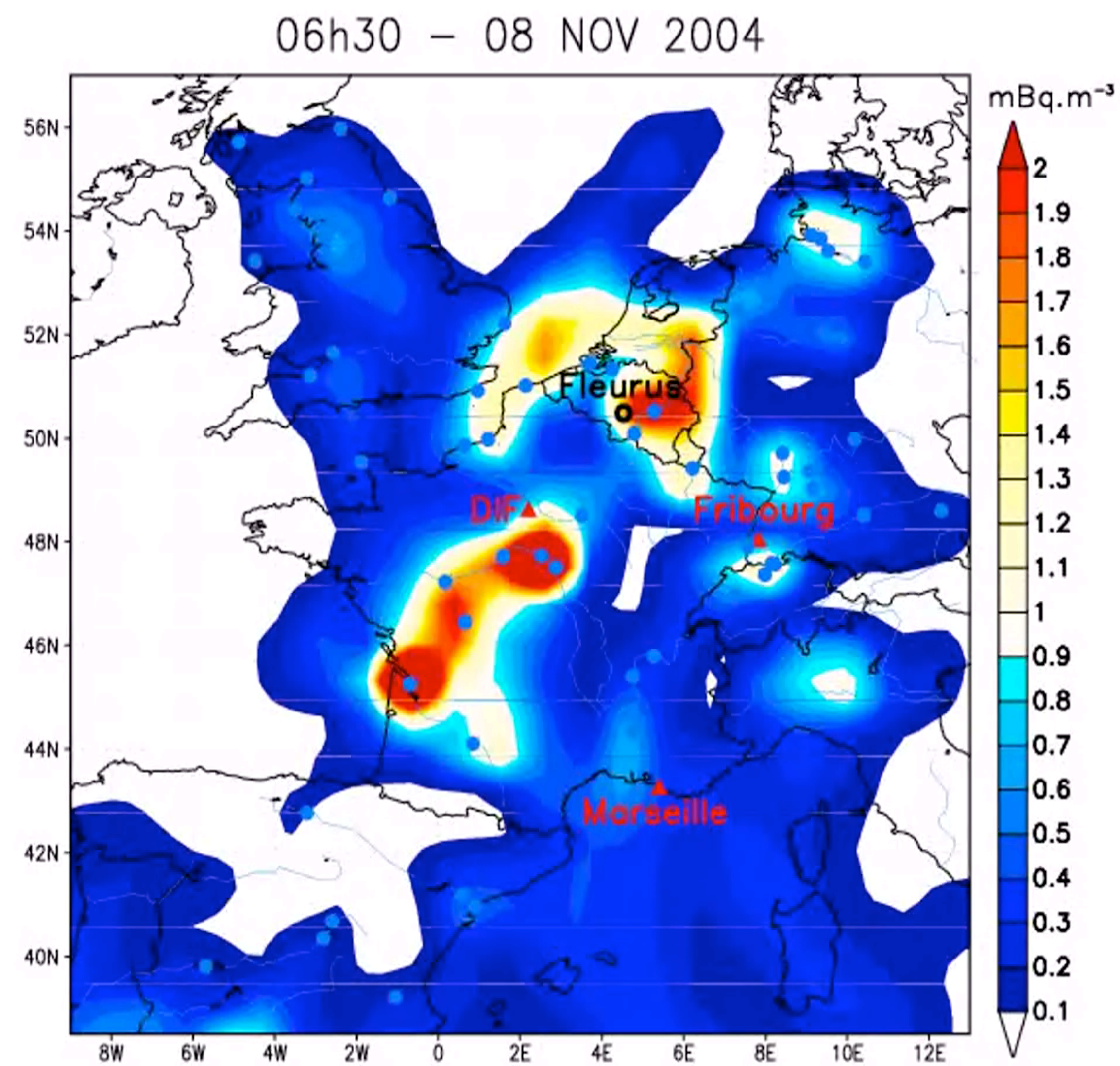
06h30 – 08 NOV 2004
mBq.m⁻³
Fleurus
DIF
Fribourg
Marseille
56N
54N
52N
50N
48N
46N
44N
42N
40N
8W
6W
4W
2W
0
2E
4E
6E
8E
10E
12E
2
1.9
1.8
1.7
1.6
1.5
1.4
1.3
1.2
1.1
1
0.9
0.8
0.7
0.6
0.5
0.4
0.3
0.2
0.1

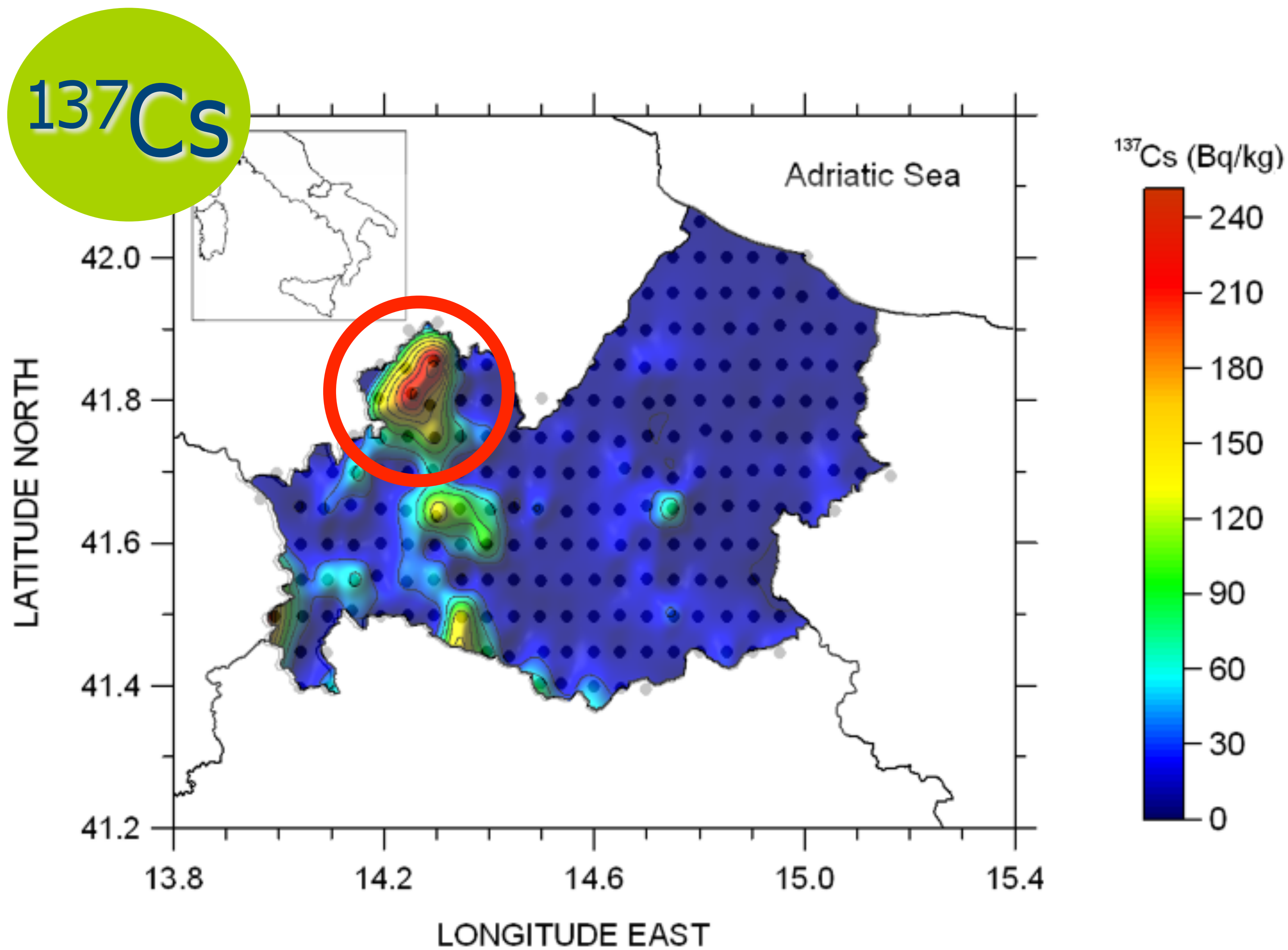
137Cs
Adriatic Sea
137Cs (Bq/kg)
240
210
180
150
120
90
60
30
0
42.0
41.8
41.6
41.4
41.2
LATITUDE NORTH
13.8
14.2
14.6
15.0
15.4
LONGITUDE EAST

Atmospheric Transport Modeling Based Estimation of Radioactive Release from the Fukushima Dai-ichi Nuclear Power Plant Accident

Wolfango Plastino[1,2], Michael Schöppner[1,2], Pavel P. Povinec[3], Gerhard Wotawa[4], Francesco Bella[1], Antonio Budano[2], Mario De Vincenzi[1,2], Federico Ruggieri[2]

[1]University of Roma Tre, Department of Physics, Rome, ITALY
[2]Italian National Institute of Nuclear Physics (INFN), Section of Roma Tre, Rome, ITALY
[3]Comenius University in Bratislava, Department of Nuclear Physics, Bratislava, SLOVAKIA
[4]Central Institute for Meteorology and Geodynamics, Vienna, AUSTRIA

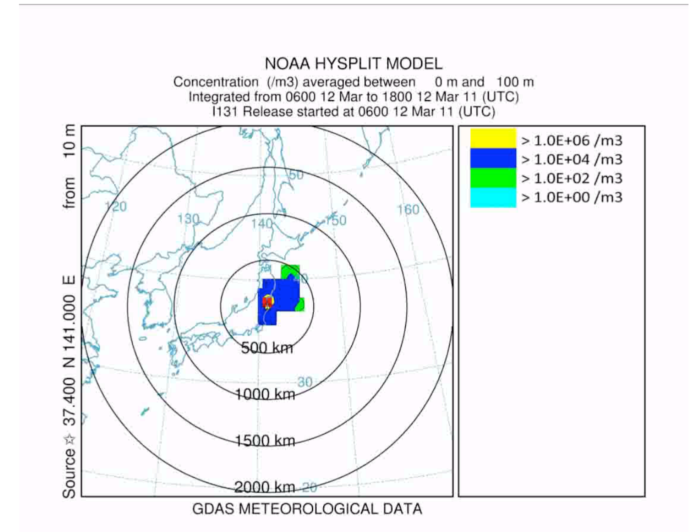

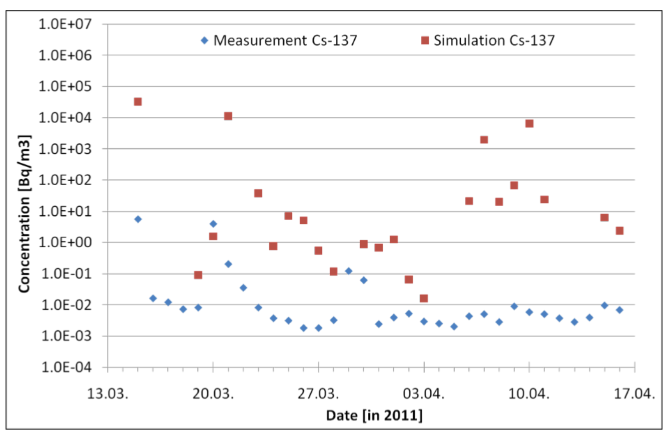

Figure 1: Comparison of concentration measurement and simulation of **caesium-137** at IMS station **JPP38**.

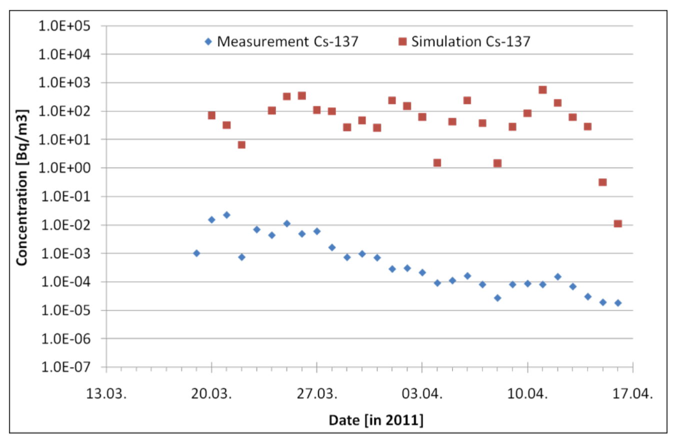

Figure 3: Comparison of concentration measurement and simulation of **caesium-137** at IMS station **USP79**.

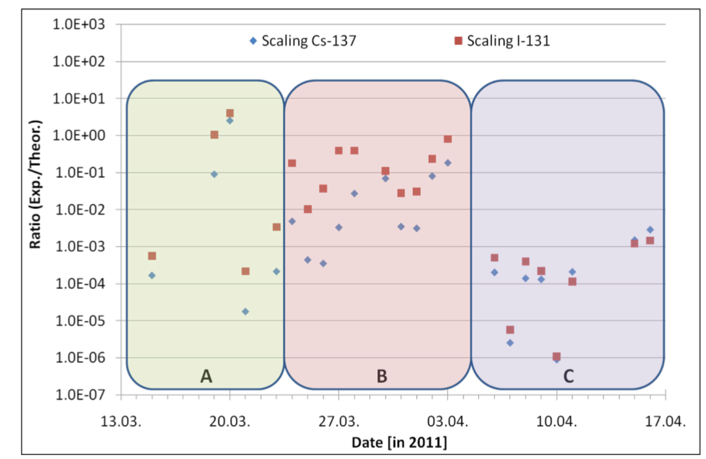

Figure 5: Scaling factors at **JPP38** for **caesium-137** and **iodine-131**, i.e. the ratios of experimental measurement and Flexpart simulation.

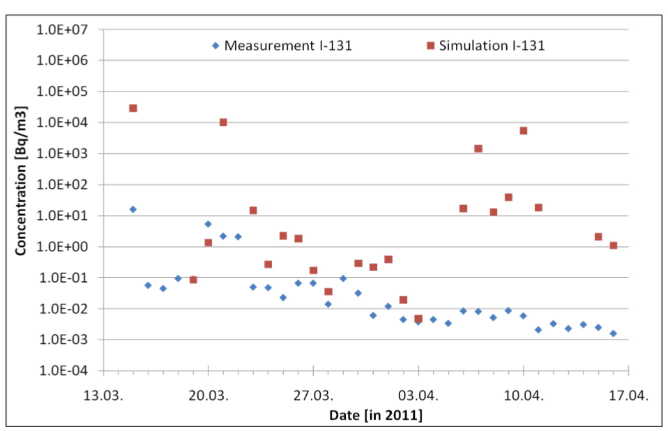

Figure 2: Comparison of concentration measurement and simulation of **iodine-131** at IMS station **JPP38**.

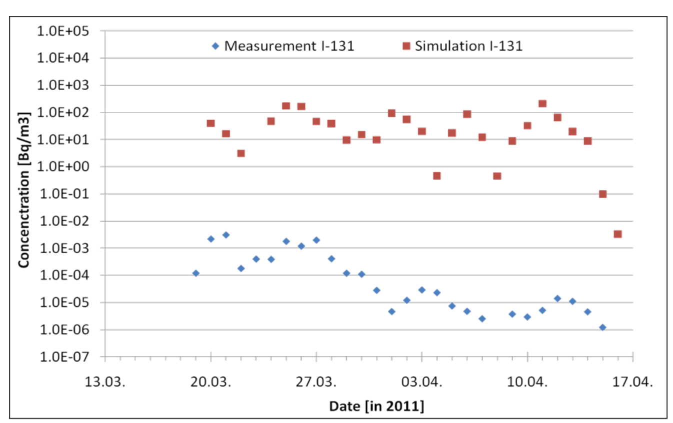

Figure 4: Comparison of concentration measurement and simulation of **iodine-131** at IMS station **USP79**.

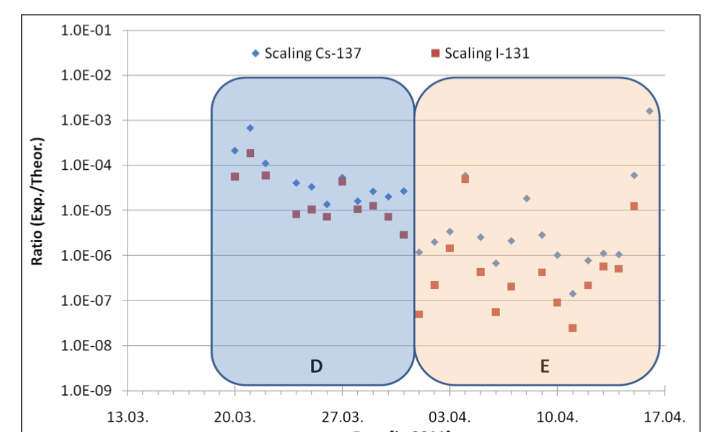

Figure 6: Scaling factors at **USP79** for **caesium-137** and **iodine-131**, i.e. the ratios of experimental measurement and Flexpart simulation.

Conclusions

….. there are a lot of demands impossible to solve using an unilateral approach

The synergy solves a lot of complex problems in theoretical and experimental Physics……although it can produces a lot of more complex numerical problems…..it is a beatiful way to realize a cooperative approach in order to increase communications and cooperations between scientific communities

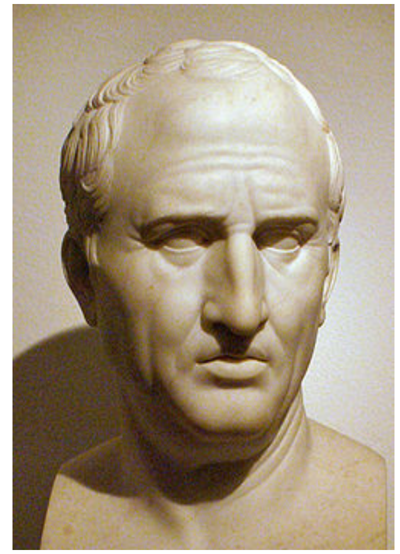

Memoria est thesaurus
omnium rerum et custos

Marcus Tullius Cicero, De oratore (1, 5, 18)

Acknowledgements

Francesco Bella & Michele Caputo
and
Ubaldo Bottigli, Giacomo Maurizio Cuttone, Mario De Vincenzi, Mario Greco, Manfred Gröning, Pavel Povinec, Kazimierz Rozanski, Federico Ruggieri, Ludovico Tortora, . . ., Arthur Schopenhauer, Socrate,......

INFN-ERMES Roma Tre and LNGS

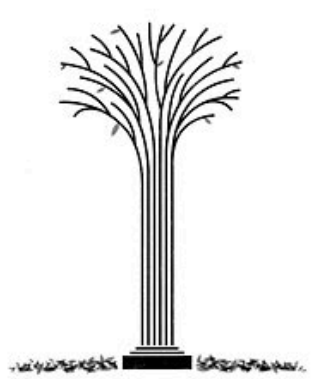

HOME PAGE | MY TIMES | TODAY'S PAPER | VIDEO | MOST POPULAR | TIMES TOPICS

Log In | Register Now | TimesPeople

The New York Times

Opinion

Opinion All NYT Search

WORLD | U.S. | N.Y. / REGION | BUSINESS | TECHNOLOGY | SCIENCE | HEALTH | SPORTS | OPINION | ARTS | STYLE | TRAVEL | JOBS | REAL ESTATE | AUTOS

EDITORIALS | COLUMNISTS | CONTRIBUTORS | LETTERS | N.Y./REGION OPINIONS | THE PUBLIC EDITOR

OP-ED CONTRIBUTOR

Latin Translation: A Vote for Latin

By HARRY MOUNT
Published: December 3, 2007

TWITTER
SIGN IN TO E-MAIL OR SAVE THIS
PRINT
SHARE

Primum, duces nostros linguam Latinam non iam studere triste non videtur.

The Heads of State

Sed reipublicae artem - quae principes iuvenes educationem praeparationem pro curriculo considerare excitat — cum rhetorica exigua, moribus infirmis, grammatica inepta et rationis historicae metu congruissse fors non est; aeterna de quibus Romani nos multum docere possunt. Romani ipsi dicunt,

Roma urbs aeterna; Latina lingua aeterna.*

Nemo principes candidati praefecti Latinae languae periti sunt. Hillaria Clintona scientiae politicae Wellesleiae studuit; Barackus Obamus Columbiae. Rudius Giulianus linguam per quattuor annos theologiae ad Episcopi Loughlin Memorem Scholam Altam Brooklyni attigit, quando se pontificem futurum esse consideravit. Sed tum quod studuit? Scientiae politicae.

Quam res post Patres Fundantes mutaverunt! Ex VII libris in Thomae Jeffersoni bibliotecha in Monticello, soli XXIV domi manent. Posteri alteros vendiderunt, Bibliotecha Concilii emptos. Lectissimus liber, iam in pluteo vitreo in Jeffersoni bibliotecha, Aeneis a Virgilio est.

Related

Op-Ed Contributor: A Vote for Latin (December 3, 2007)

More Articles in Opinion »

MOST POPULAR

E-MAILED | BLOGGED | SEARCHED | VIEWED

1. Is Sugar Toxic?
2. 'Three Cups of Tea' Author Defends Book
3. Op-Ed Columnist : Let's Not Be Civil
4. What's the Single Best Exercise?
5. For Passover, Quinoa Is Popular, but Kosher?
6. Editorial : The New Republican Landscape
7. To Tug Hearts, Music First Must Tickle the Neurons